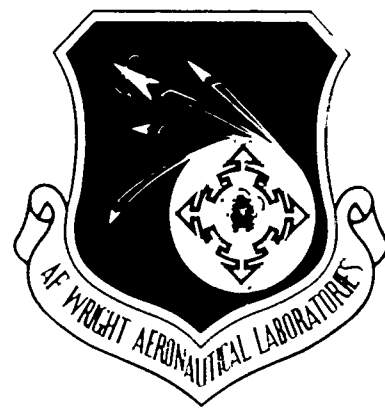


12



AFWAL-TR-85-3042

ROBUST DECENTRALIZED CONTROL

DOUGLAS P. LOOZE
GEORGE C. GOODMAN
JOHN S. ETERNO
MICHAEL ATHANS

ALPHTECH, INC.
2 BURLINGTON EXECUTIVE CENTER
111 MIDDLESEX TURNPIKE
BURLINGTON, MA 01803

AUGUST 1985

**FINAL REPORT FOR PERIOD
JULY 1984 - MAY 1985**

DTIC
STE
NOV 26 1985

D

APPROVED FOR PUBLIC RELEASE: DISTRIBUTION UNLIMITED

FLIGHT DYNAMICS LABORATORY
AIR FORCE WRIGHT AERONAUTICAL LABORATORIES
AIR FORCE SYSTEMS COMMAND
WRIGHT-PATTERSON AIR FORCE BASE, OHIO 45433

11 21-85 009

AD-A161 626

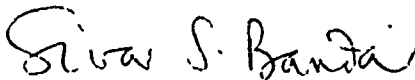
DTIC FILE COPY

NOTICE

When Government drawings, specifications, or other data are used for any purpose other than in connection with a definitely related Government procurement operation, the United States Government thereby incurs no responsibility nor any obligation whatsoever; and the fact that the government may have formulated, furnished, or in any way supplied the said drawings, specifications, or other data, is not to be regarded by implication or otherwise as in any manner licensing the holder or any other person or corporation, or conveying any rights or permission to manufacture use, or sell any patented invention that may in any way be related thereto.

This report has been reviewed by the Office of Public Affairs (ASD/PA) and is releasable to the National Technical Information Service (NTIS). At NTIS, it will be available to the general public, including foreign nations.

This technical report has been reviewed and is approved for publication.



SIVA S. BANDA
Project Engineer
Control Dynamics Branch



VERNON O. HOEHNE, Chief
Control Dynamics Branch
Flight Control Division

FOR THE COMMANDER



FRANK A. SCARPINO
Chief, Flight Control Division
Flight Dynamics Laboratory

"If your address has changed, if you wish to be removed from our mailing list, or if the addressee is no longer employed by your organization please notify AFWAL/FIGC, Wright-Patterson AFB, OH 45433-6553 to help us maintain a current mailing list".

Copies of this report should not be returned unless return is required by security considerations, contractual obligations, or notice on a specific document.

UNCLASSIFIED

SECURITY CLASSIFICATION OF THIS PAGE

AD-A161636

REPORT DOCUMENTATION PAGE

1a. REPORT SECURITY CLASSIFICATION UNCLASSIFIED			1b. RESTRICTIVE MARKINGS N/A		
2a. SECURITY CLASSIFICATION AUTHORITY N/A			3. DISTRIBUTION/AVAILABILITY OF REPORT Approved for public release; distribution unlimited.		
2b. DECLASSIFICATION/DOWNGRADING SCHEDULE N/A					
4. PERFORMING ORGANIZATION REPORT NUMBER(S)			5. MONITORING ORGANIZATION REPORT NUMBER(S) AFWAL-TR-85-3042		
6a. NAME OF PERFORMING ORGANIZATION Alphatech Inc		6b. OFFICE SYMBOL (If applicable) N/A	7a. NAME OF MONITORING ORGANIZATION Air Force Wright Aeronautical Laboratories Flight Dynamics Lab (AFWAL/FIGC)		
6c. ADDRESS (City, State and ZIP Code) 2 Burlington Executive Center 111 Middlesex Turnpike Burlington MA 01803			7b. ADDRESS (City, State and ZIP Code) Wright-Patterson Air Force Base OH 45433		
8a. NAME OF FUNDING/SPONSORING ORGANIZATION Flight Dynamics Lab		8b. OFFICE SYMBOL (If applicable) AFWAL/FIGC	9. PROCUREMENT INSTRUMENT IDENTIFICATION NUMBER F33615-84-C-3618		
8c. ADDRESS (City, State and ZIP Code) Wright-Patterson Air Force Base OH 45433			10. SOURCE OF FUNDING NOS.		
11. TITLE (Include Security Classification) Robust Decentralized Control			PROGRAM ELEMENT NO. 65502F	PROJECT NO. 3005	TASK NO. 30
			WORK UNIT NO. 11		
12. PERSONAL AUTHOR(S) Douglas P. Looze, George C. Goodman, John C. Eterno, and Michael Athans					
13a. TYPE OF REPORT Final Report		13b. TIME COVERED FROM 7/20/84 TO 5-20-85		14. DATE OF REPORT (Yr., Mo., Day) August 1985	
				15. PAGE COUNT 153	
16. SUPPLEMENTARY NOTATION					
17. COSATI CODES			18. SUBJECT TERMS (Continue on reverse if necessary and identify by block number)		
FIELD	GROUP	SUB. GR.	Control Systems Large Space Structures		
2301	1707		Decentralized Control Loop Shaping		
			Robust Control System Analysis		
19. ABSTRACT (Continue on reverse if necessary and identify by block number) This report considers the problem of designing decentralized control systems for Large Space Structures (LSS) to satisfy robustness and performance requirements for multiple system configurations. The problem is motivated by the fact that such structures will have to be assembled in space. A partially assembled structure will need some real-time control so that it maintains its' station, performs partial functions, and damps oscillations during assembly. Completely reprogramming the control computers each time a subassembly is incorporated in the structure is likely to be impractical. A more sound engineering approach would be to require the same control system design to satisfy performance requirements for the partial control system design to satisfy performance requirements for the partial assemblies and to maintain stability for the completely assembled structure. Performance can then be restored for the full assembly by applying an outer loop (hierarchical) control or adjusting the decentralized design parameters. This report approaches this problem by adopting a decentralized control loop shaping methodology. We assume that the performance and robustness requirements for the nominal					
20. DISTRIBUTION/AVAILABILITY OF ABSTRACT UNCLASSIFIED/UNLIMITED <input type="checkbox"/> SAME AS RPT. <input checked="" type="checkbox"/> DTIC USERS <input type="checkbox"/>			21. ABSTRACT SECURITY CLASSIFICATION Unclassified		
22a. NAME OF RESPONSIBLE INDIVIDUAL SIVA S. BANDA			22b. TELEPHONE NUMBER (Include Area Code) (513) 255-8677		22c. OFFICE SYMBOL AFWAL/FIGC

19. (continued)

control design can be expressed in terms of requirements on the closed loop transfer function. The requirement that the closed loop system remain stable following the connection of an additional subassembly is then treated by regarding the modification to the system dynamics as an error source. This error source imposes an additional robustness constraint on the closed loop design model. The report analyzes the constraints and identifies a generic structure that can be exploited to reduce the conservativeness of more traditional unstructured and weighted norm analyses. A result that translates this structure into design constraints compatible with the loop shaping design methodology is developed. This result is combined with existing performance and robustness techniques to specify a complete set of design constraints. The ability of the combined analyses to predict true closed loop system behavior is demonstrated through a simplified application.

FOREWORD

The research described in this report was funded under Contract No. F33615-84-C-3618, from the

Air Force Wright Aeronautical Laboratories
Flight Dynamics Laboratory
Air Force System Command
United States Air Force
Wright Patterson AFB, Ohio 45433

The support of the Air Force, and the personal encouragement of the technical monitor, Dr. Siva S. Banda, is gratefully acknowledged.

In addition, the two appendices contain unpublished papers describing work performed under this contract and at the University of Illinois under Contract No. N00014-79-C-0424 of the Joint Services Electronic Program.

Accession For	
NTIS CRA&I	<input checked="checked" type="checkbox"/>
DTIC TAB	<input type="checkbox"/>
Unannounced	<input type="checkbox"/>
Justification	
By _____	
Distribution / _____	
Availability Codes	
Dist	Avail and/or Special
A-1	



CONTENTS

<u>Section</u>	<u>Page</u>
1 Introduction	1
2 Sequential Assembly Model	7
2.1 Infinite Dimensional Models	7
2.2 Structural Analysis of the Assembled System	12
2.3 Finite Element Approximations for Design and Truth Models	16
3 Error/Structural Analysis and Control Objectives	21
3.1 Methodology	21
3.2 Simplified Control Objectives and Error Sources	23
3.3 Robustness Analysis Tools	26
3.3.1 General Robustness Theorems	26
3.3.2 Unstructured Multiplicative Error	31
3.3.3 Rank One Errors	32
3.3.4 Weak Coupling Errors	39
3.4 Subsystem Errors for the Decoupled System	41
3.5 Subsystem Errors for the Connected System	41
3.6 Interconnection Errors	46
3.7 Summary of the Error Analyses	48
4 Decentralized Control System Design and Analysis	51
4.1 Linear Quadratic Regulator Design	51
4.2 Loop Transfer Function Recovery	56
4.3 Analysis of the Interconnected Decentralized System	59
4.4 Second Level Control Problem	61
5 Summary	63
References	66
Appendix A	A-1
Appendix B	B-1
Appendix C	C-1

LIST OF FIGURES

<u>Number</u>		<u>Page</u>
2-1	Physical Basis for Sequential Assembly Model	9
2-2	Structure of Approximate Models for Three Cases	13
2-3	Example of 5 Element Approximation	17
2-4	Singular Values of the 5 Element Subsystem Truth Model	18
2-5	Singular Values of the 3 Element Subsystem Design Model	19
3-1	Generic Methodology for Control System Design	22
3-2	Graphical Test for Rank One Error Sources	37
3-3	Inverse Multiplicative Error Between the Nominal 3 Element Design Model and the 5 Element Truth Model	42
3-4	Inverse Multiplicative Error Between the 3 Element Subsystem Design Model and the 6 Element Analysis Model	43
3-5	Subsystem Modification Structure	43
3-6	Nyquist Plot of $\sigma_1 \cos \phi e^{j\theta}$	46
3-7	Stability Margin of Coupled Analysis System With Structured Error	47
3-8	Inverse of the Relative Interconnection Error	48
4-1	Linear Quadratic Regulator Transfer Function	54
4-2	Singular Values of the Linear Quadratic Regulator Return Difference	55
4-3	Singular Values of the Closed Loop LQG Design Subsystem	58
4-4	Singular Values of the Closed Loop LQG Truth Subsystem	58
4-5	Singular Values of the Closed Loop Interconnected Truth System	60
4-6	Magnitude of the Second Level Control System Return Difference	62
4-7	Magnitude of the Second Level Transfer Function	62

SECTION 1

INTRODUCTION

Air Force sensor and weapon requirements for Advanced space-based detection, surveillance, and defense will necessitate the construction of large space structures (LSS). These structures will be very large and lightweight, and hence extraordinarily flexible. They will most probably be assembled in space. Their generic characteristics would include the interconnection of several rigid bodies with flexible elements, with the rigid bodies also supporting flexible appendages.

Air Force mission requirements for these structures will impose severe pointing and tracking specifications. Such stringent specifications will necessitate the design of a superior control system that would involve hundreds of sensors and actuators. The space structure dynamics are infinite dimensional, and design models may involve thousands of state variables. Thus, an immense amount of real-time digital computation will have to be carried out by the control system. This massive computation cannot be accomplished by a centralized control computer. Therefore a decentralized control system employing distributed computation is essential.

The need for decentralized control can also be understood by the fact that these very large structures would have to be assembled in a piecemeal manner. A partially assembled space structure will need some real-time control so that it maintains its station, performs partial functions, and does

not bend during further assembly. In addition, certain LSS (e.g., phased array radars) may be capable of functioning with only a partial assembly. The partial assembly will require a complete real-time control system to perform its functions. It would be undesirable to completely reprogram in space a large control computer every time an addition is made to the structure. A more sound engineering approach is to augment a decentralized control system as additional elements of the large space structure (LSS) are brought together. It is obvious that decentralized and hierarchical control architectures are essential if these envisioned large space structures are to accomplish their mission.

Another factor that significantly influences the problem of control system design for large space structures is the inherent uncertainty in modeling the dynamic behavior of flexible structures in space. The combination of large uncertainty, large dimensions, and severe performance specifications creates a difficult control system design problem even were one to use a centralized control architecture. The need for decentralized and hierarchical architectures serves to transform the design problem into one which has received minimal attention and for which few results or design and analysis procedures have been obtained.

The primary objective of this project has been to initiate research to develop a sound engineering approach to the design of decentralized robust control systems for large space structures. The engineering procedure to be developed must, at a minimum, address the following issues:

- (a) The necessary architecture of the control system must be determined from the system structure of the large space structure, the performance requirements of the LSS, hardware implementation considerations, and any sequential assembly requirements for the LSS;

- (b) The procedure must be able to readily handle the large numbers of input, output, and design model state variables that will be present in a realistic design problem;
- (c) The procedure must be able to incorporate the performance specifications for the LSS in the design process;
- (d) The impact of dynamic modeling errors due to the uncertainties of modeling an inherently infinite dimensional system must be incorporated;
- (e) The impact of dynamic modeling errors due to the deliberate model simplifications that will be made to accommodate (a) and (b) must be incorporated.

As discussed in the preceding paragraphs, the required control system architecture will likely require both decentralization and hierarchical control layers to satisfy the requirements listed in (a) and the computational and analytical issues raised in (b). The issues raised in (c) and (d), when taken independently, are standard issues which must be addressed by control system designs for any system. The issue of deliberate modeling error is also of concern in control system design for many systems. However, in the context of LSS, these issues assume special significance when combined with the tight performance specifications, large system models, and non-classical control architecture.

Taken together, the issues raised by (a)-(e) present a formidable control system design and analysis problem which has received very little attention. The combination of robustness and performance with a decentralized architecture has received partial consideration only in [1]-[5]. References [1]-[2] were actually concerned with the development of decentralized synthesis procedures, but the results can also be used to analyze the robustness of weakly coupled systems (as noted in [4]). Reference [3] developed a design procedure that achieved arbitrary performance specifications using a decentralized

architecture for systems that had no bandwidth limitations. The first simultaneous consideration of performance, robustness, and decentralized architectures occurred in [4]-[5]. This work developed a preliminary approach to both qualitative and quantitative analysis of the feedback properties of decentralized systems. Finally, the combination of robustness analysis with a control architecture induced by a system time scale separation structure has been considered in [6]-[7].

This study of decentralized robustness procedures for large space structures attempts to organize the issues discussed in the preceding paragraphs, identify the useful analytical tools that are available [1]-[6], and extend these tools where possible. Clearly this is an ambitious undertaking. Our initial approach limits the scope of the research to the study of a specific simplified problem that retains representative features of the generic decentralized design problem for large space structures with sequential assembly. The limited scope allows us to address the objectives of the study in a well defined context, thereby allowing the development of insights and understanding into the interactions of the numerous system structure and control architecture issues.

Hence, generic system structure assumptions (such as those used in [1]-[7]) can be evaluated for reasonableness and applicability, and the irrelevant structures can be quickly eliminated. The usefulness of the resulting analysis tools can be determined in terms of their ability to produce accurate predictions of system performance and design specifications.

The disadvantage of using a specific system as a basis for such a study is the difficulty of quantitatively asserting that the conclusions of the study can be applied beyond the specific system. This study minimizes this

difficulty by retaining as many generic features of the large space structure problems as possible. Although the quantitative results may be difficult to generalize precisely, the qualitative assessments of available analysis design tools, and the insights into the interactions between system structure, control problem structure, and control system architecture will be valid for many problems.

The specific problem that is considered is the sequential assembly problem for two subassemblies. It is assumed that each subassembly consists of a highly oscillatory system that requires vibrational control to damp the oscillations. The individual control systems must perform their functions on both the decoupled subassemblies and on the interconnected assembled system. A second level controller using a reduced set of controls and measurements can be implemented after the interconnection is effected to augment the decentralized controllers.

This particular problem was chosen for its ability to present the issues (a)-(e) in the context of a simplified problem. The control system architecture (decentralized control with a second level coordinating layer) can be (and is) deduced from the system structure, performance requirements and sequential assembly requirements. The use of decentralized control directly addresses the problems associated with large numbers of variables. The fact that each subassembly is representative of a LSS implies that the LSS control issues must also be addressed and that modeling errors that result from approximating an infinite dimensional system must be considered. Finally, both modeling errors due to low order models of the infinite dimensional system and the decentralized design procedures are incorporated.

Probably the most significant contributions of this research are the identification of issues and problems associated with the decentralized control of large space structure with sequential assembly, and the development of a preliminary design methodology for such systems. At a more technical level, two new multivariable robustness results have been developed. Finally, we have also identified a generic error structure for the sequential assembly problem.

The system that forms the basis for this study is presented in Section 2. Both the subassemblies and the interconnected system are described by partial differential equation models. Decomposition results for such systems (presented in Appendices A and B) are used to analyze the structure of the interconnected system and to deduce necessary features of the control system architecture. Low order design, analysis, and truth models are then derived from the infinite dimensional models using low order finite element approximations.

Section 3 conducts an error analysis of the system with the goal of specifying design constraints for the decentralized control systems. Three generic error sources are identified, and quantitative analyses are performed. The results of these analyses are used to specify the subassembly control systems. The control system designs are presented in Section 4 and the validity of the analyses of Section 3 is verified. Section 5 summarizes the contributions and conclusions obtained from this study.

SECTION 2

SEQUENTIAL ASSEMBLY MODEL

2.1 INFINITE DIMENSIONAL MODELS

The purpose of this section is to present a model that will be used to study the applicability of the various decentralized robustness analysis and design tools [1]-[7] in the context of the sequential assembly of large space structures. The model has been developed to be as simple as possible while retaining the basic features of the sequential assembly problem.

A number qualitative features of large space structures and the sequential assembly problem distinguish the control problems for such systems from other control problems. Large space systems are inherently infinite dimensional with closely spaced, lightly damped modes. This feature implies that any design based on a finite dimensional design model must be able to cope with a (possibly large) number of lightly damped unmodeled modes in the roll-off region of the design. The controls and measurements for the system are typically "point" controls and measurements, with significantly fewer controls than states. The sequential assembly problem imposes a decentralized control architecture on the overall assembly. Each of the decentralized controllers must function with its separate subsystem and must be designed to maintain stability when connected to the overall assembly. Finally, a second level control architecture can be used to minimize the performance degradation caused by the interconnection of the subsystem assemblies.

The model that will be used to represent these features is based on the physical system depicted in Fig. 2-1. Each subsystem consists of three unit masses connected by two uniform beams. The two subsystem controls are the forces on the middle and one end mass, while the two subsystem measurements are the separations of the masses. The generic goal of the subsystem controllers is to maintain the nominal separation of the masses as nearly as possible. The primary contribution to errors in these separations are longitudinal vibrations of the systems. Assuming that the masses can be modeled as point masses on a uniform beam of length L^m , the longitudinal position of an incremented element of a subsystem can be described by the hyperbolic partial differential equation

$$\frac{\partial^2}{\partial t^2} z(x,t) + b \frac{\partial}{\partial t} z(x,t) - c_1^2 \frac{\partial^2}{\partial x^2} z(x,t) = 0 \quad (2-1)$$

where

$z(x,t)$ = longitudinal position of the point x of the beam at time t

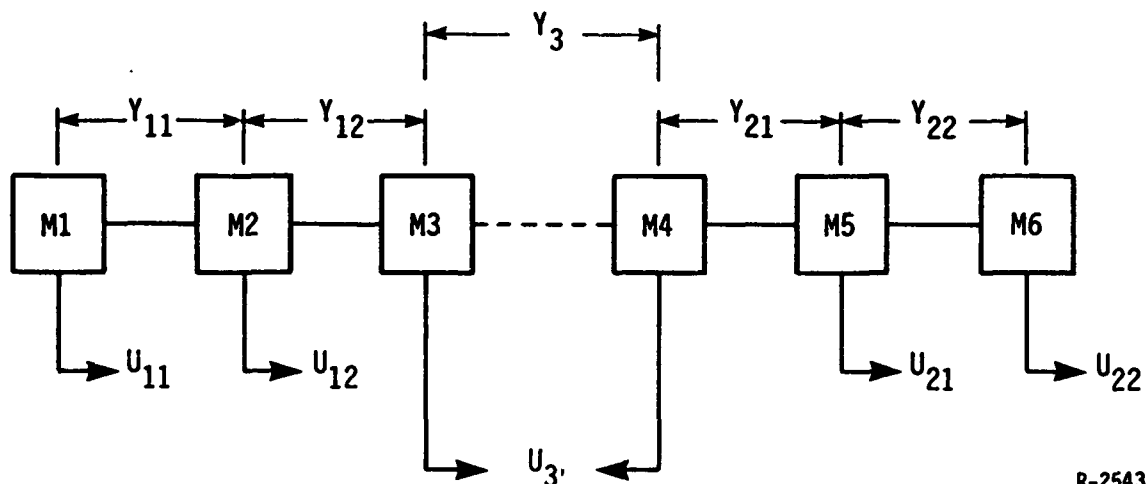
b = coefficient of restoring force

c_1 = velocity of wave propagation

The boundary condition for the first subsystems are

$$\left. \frac{\partial}{\partial x} z(\cdot, t) \right|_{x=0} = -m \frac{\partial^2}{\partial t^2} z(0, t) + u_{11} \quad (2-2)$$

$$\left. \frac{\partial}{\partial x} z(\cdot, t) \right|_{\frac{L^m}{2}} = -m \frac{\partial^2}{\partial t^2} z\left(\frac{L^m}{2}, t\right) + u_{12} \quad (2-3)$$



R-2543

Figure 2-1. Physical Basis for Sequential Assembly Model

$$\left. \frac{\partial}{\partial x} z(\cdot, t) \right|_{x=L^m} = -m \frac{\partial^2}{\partial t^2} z(L^m, t) \quad (2-4)$$

while the boundary conditions for the second subsystem are:

$$\left. \frac{\partial}{\partial x} z(\cdot, t) \right|_{x=0} = -m \frac{\partial^2}{\partial t^2} z(0, t) \quad (2-5)$$

$$\left. \frac{\partial}{\partial x} z(\cdot, t) \right|_{x=\frac{L^m}{2}} = -m \frac{\partial^2}{\partial t^2} z\left(\frac{L^m}{2}, t\right) + u_{21} \quad (2-6)$$

$$\left. \frac{\partial}{\partial x} z(\cdot, t) \right|_{x=L^m} = -m \frac{\partial^2}{\partial t^2} z(L^m, t) + u_{22} \quad (2-7)$$

where m is the mass of the physical masses M1-M6.

The measurements of the subsystems are

$$y_{11}(t) = z_1\left(\frac{L^m}{2}, t\right) - z_1(0, t) \quad (2-8)$$

$$y_{12}(t) = z_1(L^m, t) - z_1\left(\frac{L^m}{2}, t\right) \quad (2-9)$$

$$y_{21}(t) = z_2\left(\frac{L^m}{2}, t\right) - z_2(0, t) \quad (2-10)$$

$$y_{22}(t) = z_2(L^m, t) - z_2\left(\frac{L^m}{2}, t\right) \quad (2-11)$$

For each subsystem, the parameters b , c , L^m and m were chosen as:

$$b = .06 \quad (2-12)$$

$$m = 1 \quad (2-13)$$

$$L^m = 2 \quad (2-14)$$

$$c_1 = 1 \quad (2-15)$$

The subsystems described in the preceding paragraph will define the sub-assemblies for the sequential assembly problem. The connection of the sub-assemblies (with length L) will be made using a beam of length $L^m/2$ whose longitudinal wave propagation velocity is c_2 . The second level input that will be used to maintain the separation between the subassemblies is the differential force applied between the end masses of the two subassemblies, while the second level measurement is the separation of those masses. The overall system is described by the non-uniform hyperbolic partial differential equation

$$\frac{\partial^2}{\partial t^2} z(x, t) + b \frac{\partial}{\partial t} z(x, t) - c^2(x) \frac{\partial^2}{\partial x^2} z(x, t) = 0 \quad (2-16)$$

$$\frac{\partial}{\partial x} z(0, t) = -m \frac{\partial^2}{\partial t^2} z(0, t) + u_{11} \quad (2-17)$$

$$\frac{\partial}{\partial x} z\left(\frac{L}{2}, t\right) = -m \frac{\partial^2}{\partial t^2} z\left(\frac{L}{2}, t\right) + u_{12} \quad (2-18)$$

$$\frac{\partial}{\partial x} z(L, t) = -m \frac{\partial^2}{\partial t^2} z(L, t) + u_3 \quad (2-19)$$

$$\frac{\partial}{\partial x} z\left(-\frac{3}{2}L, t\right) = -m \frac{\partial^2}{\partial t^2} z\left(-\frac{3}{2}L, t\right) - u_3 \quad (2-20)$$

$$\frac{\partial}{\partial x} z(2L, t) = -m \frac{\partial^2}{\partial t^2} z(2L, t) + u_{21} \quad (2-21)$$

$$\frac{\partial}{\partial x} z\left(-\frac{5}{2}L, t\right) = -m \frac{\partial^2}{\partial t^2} z\left(-\frac{5}{2}L, t\right) + u_{22} \quad (2-22)$$

$$y_{11}(t) = z\left(\frac{L}{2}, t\right) - z(0, t) \quad (2-23)$$

$$y_{12}(t) = z(L, t) - z\left(\frac{L}{2}, t\right) \quad (2-24)$$

$$y_{21}(t) = z(2L, t) - z\left(-\frac{3}{2}L, t\right) \quad (2-25)$$

$$y_{22}(t) = z\left(-\frac{5}{2}L, t\right) - z(2L, t) \quad (2-26)$$

where

$$c(x) = \begin{cases} c_1 & 0 < x < L; \quad \frac{3}{2}L < x < \frac{5}{2}L \\ c_2 & L < x < \frac{3}{2}L \end{cases} \quad (2-27)$$

The design and truth models will be derived from the infinite dimensional models (2-1), (2-16) using low order finite element methods. The use of low order finite element models allows the retention of most of the features of the sequential assembly problem and large space structures. However, models derived from low order finite element approximations are typically very inaccurate and vary strongly with the order of the approximation. To minimize the effects of this unrealistic model variation, the length parameter L of the assembled subsystem (2-16) was adjusted to yield the same fundamental mode as the separated subsystem (2-1) when c_2 is taken to be zero. Thus the subsystem models generated by (2-16) when the coupling beam is not present will be the same as the subsystem models generated by (2-1), and any errors between design and truth models can be attributed to physical sources. The values of L that are used will depend on the order of the finite element approximation.

2.2 STRUCTURAL ANALYSIS OF THE ASSEMBLED SYSTEM

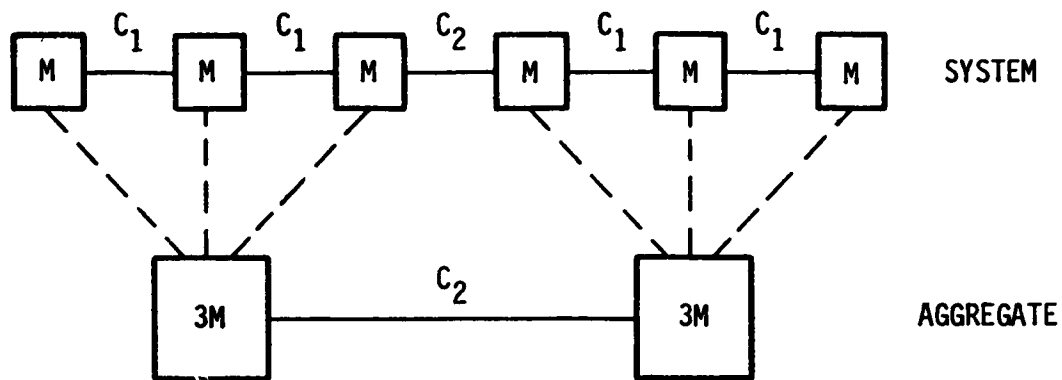
The longitudinal wave velocity c_2 of the coupling beam will determine the system structural properties of the assembled system and, consequently, will affect the decentralized and hierarchical structures that can be utilized. Three cases for the value of c_2 will be qualitatively examined in this subsection (see Fig. 2-2):

$$\text{CASE A: } c_1 \gg c_2 \quad (2-28)$$

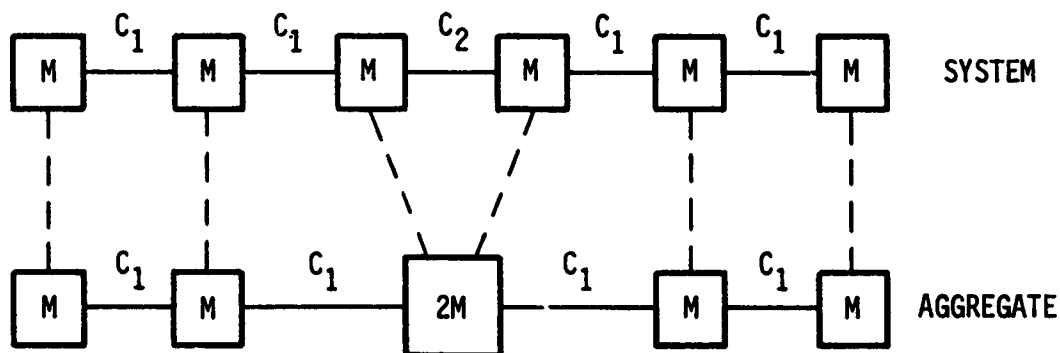
$$\text{CASE B: } c_1 \ll c_2 \quad (2-29)$$

$$\text{CASE C: } c_1 \approx c_2 \quad (2-30)$$

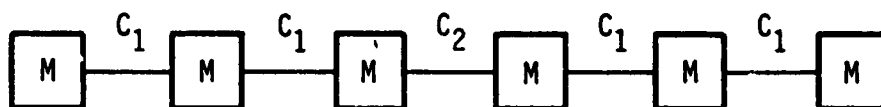
In both cases A and B, the asymptotic eigenanalysis of Appendices A and B and the analyses of [8]-[9] apply. The analysis for case A leads to significant conclusions regarding the control architectures that can be used on the



a) Aggregation for Case A: $C_1 \gg C_2$



b) Aggregation for Case B: $C_1 \ll C_2$



c) No aggregation for Case C: $C_1 \approx C_2$

Figure 2-2. Structure of Approximate Models for Three Cases

R-2993

system. Cases B and C are more difficult to address precisely, but generic conclusions can be drawn from similar system structures.

Appendices A and B address the problem of spectral analysis and solution approximation for a class of stiff systems. This class is defined precisely in the appendices, and includes hyperbolic systems of the form of (2-16) with either (2-28)-(2-29). The basic conclusion of these appendices (and the related works [9]-[10]) applied to (2-16) is that, for the purposes of analysis and control, (2-16) can be decomposed into two independent analysis or control problems (termed the stiff and normal problems). One problem is based on infinite dimensional models of the two subassemblies, while the other problem approximates (2-16) by a single beam connecting two equivalent masses (i.e., the subassemblies are approximated by equivalent point masses). The particular case, A or B, determines the forms of the two problems and hence the control architectures that will be effective.

In case A, (see Fig. 2-2a), the interconnection between the subassemblies is much less stiff than the subassemblies themselves. As noted in the preceding paragraph, the overall problem decomposes into two infinite dimensional problems. The stiff problem approximates (2-16) as two independent systems, each of which is modeled by (2-1)-(2-11). Thus any controller design based on (2-1)-(2-11) will face only a minimal amount of error when applied to the coupled system. The normal problem approximates each subassembly by an equivalent point mass equal to the total subassembly mass. These equivalent point masses are connected by a beam whose longitudinal wave velocity is c_2 . Thus, this structure imposes a natural two level decomposition of (2-16) into two decentralized subassembly controllers and one coordinating controller that

regulates the subassembly separation. This case (2-28) and the corresponding decentralized/hierarchical architecture will be investigated in detail in the remainder of this report.

Case B (see Fig. 2-2b) also decomposes into two problems. The stiff problem in this case is represented by two equivalent point masses connected by a beam whose longitudinal wave velocity is c_2 . However, the equivalent masses are taken as the end masses of the subassembly. The normal problem is based on the subassemblies but does not decompose as in Case A. Rather, the model assumes the form of (2-1) with 5 point masses rather than 3. The middle mass represents the combined mass of the end masses of the subassembly. Thus, the normal problem is an almost uniform system, with the only non-uniformity being the doubled center mass.

Consequently, Cases B and C result in basically the same control problems: a uniform system that must be controlled by a decentralized control architecture. The connection of two uniform subassemblies of the form of (2-1) into a uniform system of the form (2-16) significantly modifies the subassembly transfer function (in particular, the fundamental modes and all harmonics significantly affected) and introduces a strong coupling between the subsystems. Any significant control effects on the subsystems are almost sure to push one or more of the lightly damped modes into the right half plane. Hence a decentralized/hierarchical structure as outlined in the Introduction and in Subsection 2.1 is not feasible.

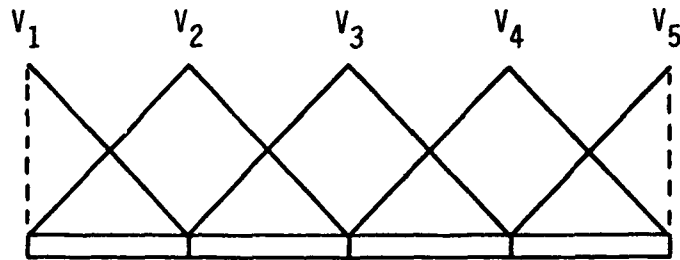
Other combinations of partially decentralized and hierarchical architectures may prove useful for such structures. For example, the use of overlapping local controllers has proven successful in controlling lightly damped systems such as strings of moving vehicles [10] and freeway systems [11].

This architecture would require that a second level controller which overlaps the subassembly controllers be in place and active before the subassemblies are connected. Another promising approach would be to use the local subassembly controllers to induce a system structure that is amenable to decomposition on the assembled structure. Finally, additional mechanisms for natural decompositions of the assembled system exist (e.g., large end masses will impose a decomposition similar to Case A). These mechanisms and their effects can be identified using the results of Appendices A and B. Each of these approaches to Cases B and C warrants further investigation.

2.3 FINITE ELEMENT APPROXIMATIONS FOR DESIGN AND TRUTH MODELS

Low order finite element approximations for systems (2-1) and (2-16) were used to develop design, analysis, and truth models for use in the development and illustration of the decentralized/sequential assembly design procedure. Due to the strong dependence of the system description on the number of elements used in low order approximations, some of the parameters of the design model and the coupled system model were adjusted to reduce the difference between the fundamental modes of the models. These adjustments affect only the errors due to the low order approximations, and not the qualitative properties of the true error sources. The specific adjustments that were made are indicated in the description of the individual models.

The finite element method that was used employs overlapping triangular elements (see Fig. 2-3). The elements on each end of the beam being approximated are right triangles whose base is half the base of the interior elements. The interior elements are isosceles triangles. Each interior element overlaps half the preceding element and half the succeeding element. The



R-2544

Figure 2-3. Example of 5 Element Approximation

elements are normalized with respect to the longitudinal wave velocity, i.e.,

$$\int_0^L c(x) v_1(x)^2 dx = 1$$

Data for each of the models can be found in Appendix C.

The truth models for the unassembled systems were derived from (2-1)-(2-15) using a 5 element approximation. The resulting 10th order system was reduced to an 8th order system by eliminating the unobservable center of mass (CM) position and velocity states. The resulting truth model open loop modes were:

$$-.03 \pm 4.627j$$

$$-.03 \pm 4.62j$$

$$-.03 \pm 1.485j$$

$$-.03 \pm .99j$$

(2-31)

The singular values of the truth subsystem model transfer function are shown in Fig. 2-4.

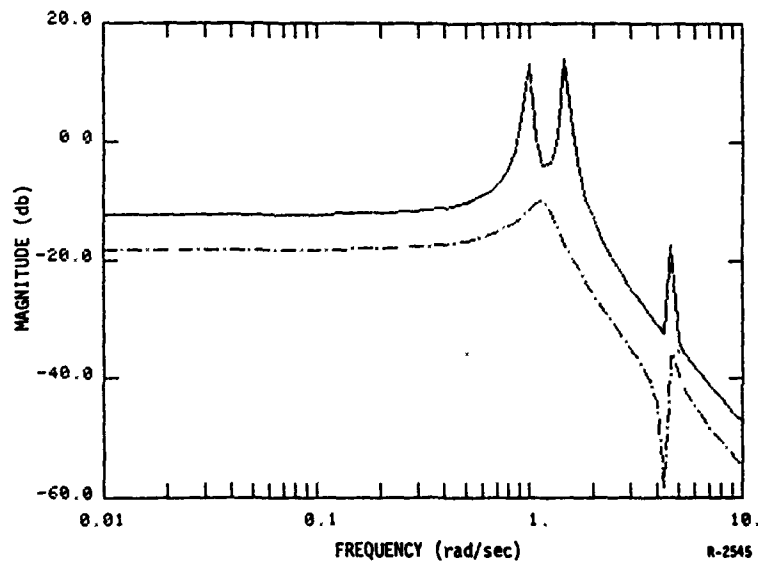


Figure 2-4. Singular Values of the 5 Element Subsystem Truth Model

The design models for the subassemblies were obtained from (2-1)-(2-11) using a 3 element approximation. The longitudinal wave velocity was adjusted to align the fundamental mode of the design model with the truth model. The 0th order unobservable modes were again eliminated. The eigenvalues of the resulting 4th order design systems were:

$$\begin{aligned} &-.03 \pm 1.4685j \\ &-.03 \pm .99j \end{aligned} \quad (2-32)$$

The singular values of the design subsystem model transfer function are shown in Fig. 2-5.

An analysis model was derived from the coupled system (2-12)-(2-27) using a 6 element approximation for the purpose of analyzing the perturbational effects of coupling the two subassemblies. The subassembly lengths were adjusted to be

$$L = 1.6 \quad (2-33)$$

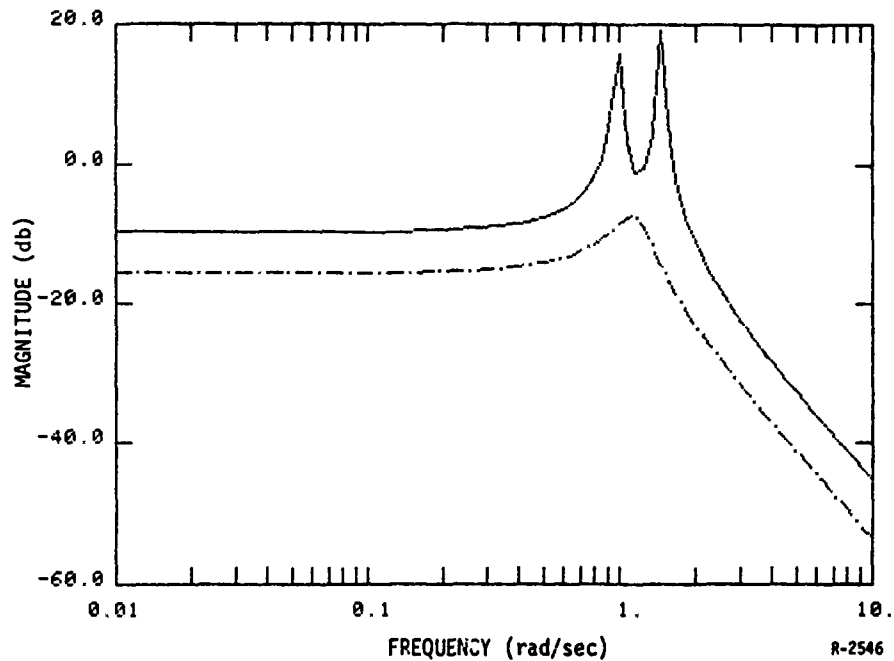


Figure 2-5. Singular Values of the 3 Element Subsystem Design Model

to obtain consistency between the decoupled truth model and the subassembly truth model. The longitudinal wave velocity of the coupling beam was taken to be

$$c_2 = .1$$

(2-34)

The two eigenvalues corresponding to the 0th mode were found to be unobservable and were removed. The resulting 10th order system had the following eigenvalues:

$$\begin{array}{ll}
 \left. \begin{array}{l}
 -.03 \pm 1.468j \\
 -.03 \pm .9913j
 \end{array} \right\} & \text{subsystem 1 modes} \\
 \left. \begin{array}{l}
 -.03 \pm 1.4669j \\
 -.03 \pm .9886j
 \end{array} \right\} & \text{subsystem 2 modes} \\
 \left. \begin{array}{l}
 -.03 \pm .0542j
 \end{array} \right\} & \text{coupling mode}
 \end{array} \quad (2-35)$$

Finally, the truth model for the assembled system was derived from (2-12)-(2-27) and (2-33)-(2-34) using an 11 element approximation. The two eigenvalues corresponding to the 0th order mode were found to be unobservable and were removed. The resulting 20th order system had the following eigenvalues:

$-.03 \pm 4.2572j$	}	coupling mode	
$-.03 \pm 4.7586j$	}	subsystem 1 unmodeled dynamics	
$-.03 \pm 4.5234j$			
$-.03 \pm 4.7586j$	}	subsystem 2 unmodeled dynamics	
$-.03 \pm 4.5234j$			
$-.03 \pm 1.3995j$	}	subsystem 1 modes	
$-.03 \pm .9397j$			
$-.03 \pm 1.3995j$	}	subsystem 2 modes	
$-.03 \pm .9397j$			
$-.03 \pm .0554j$	}	coupling mode	(2-36)

SECTION 3

ERROR/STRUCTURAL ANALYSIS AND CONTROL OBJECTIVES

3.1 METHODOLOGY

The purpose of this section is to describe a methodology for the design of decentralized control systems for large space structures that are to be assembled sequentially, and to develop the necessary analytical tools to implement this methodology. The framework that will be used for the methodology is common to all control system design problems (see Fig. 3-1). The first step is to identify all performance criteria and error sources. These are then mapped (using appropriate analytical tools) into constraints on the control system design. The control system must be designed to satisfy the resulting constraints, and its performance is verified via analysis and simulation. Each transition between steps of this procedure usually requires iterations to guarantee that consistent specifications for the next step are achieved.

Our implementation of the methodology will be based on loop shaping synthesis techniques [12]-[13] that utilize singular value analyses. A decentralized design will be developed by requiring each subsystem to use a local design model. The subsystem design problems will then be determined by specifying control system design constraints in terms of bounds on the singular values of the loop transfer functions of the closed loop subsystem design models.

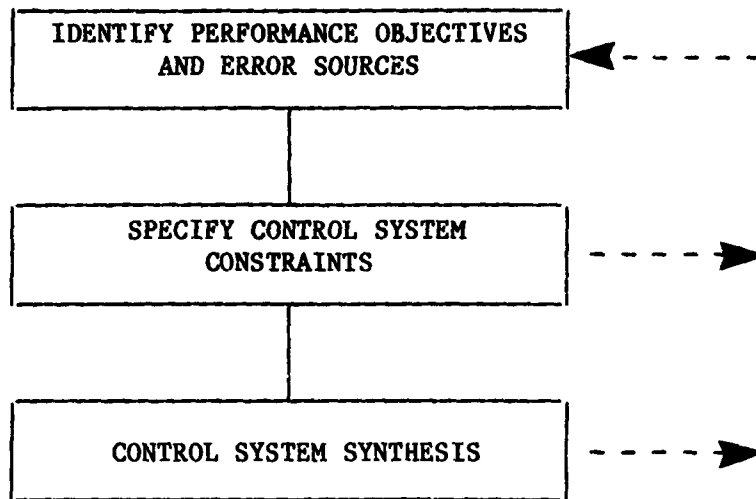


Figure 3-1. Generic Methodology for Control System Design

Once the subsystem design problems are formulated in this manner, the synthesis of a subsystem controller that satisfies the singular value constraints is a standard problem that has been well studied (c.f. [12]-[13]). The unique aspects of this approach for decentralized LSS with sequential assembly are the type of error sources that must be addressed, and the need to develop singular value specifications that are not so conservative that the resulting synthesis problem is unsolvable.

The main emphasis of this section will be the development and evaluation of analysis tools that map the unique large space structure/sequential assembly decentralized control problem error sources into specifications on the singular values of the subsystem design problems. There are three dominant error sources for this problem: the usual system modeling errors, a modification of the subsystem transfer function model due to the neglected coupling, and interactions between the subsystems due to the neglected couplings. An

appropriate analysis tool is developed or identified for each error source to guarantee that the resulting control system design problems are feasible.

The appropriateness of an analysis tool for a particular error source depends largely on the presence of an underlying system structure for the LSS and error source. The presence of such a structure presents an opportunity to exploit that structure to reduce the conservativeness of the corresponding design specification. In fact, large error sources can make exploitation of structure essential. One of the significant contributions of this section is to identify a generic structure for a dominant error source and to develop an analysis tool that exploits this structure.

3.2 SIMPLIFIED CONTROL OBJECTIVES AND ERROR SOURCES

As noted in the preceding subsection, the purpose of this section is to develop or identify analytical tools that can be used to implement the decentralized design methodology illustrated in Fig. 3-1. To concentrate on this objective, the methodology will be applied to system models derived from the system described in Section 2 with simplified performance goals and error analyses. The simplifications serve to concentrate our effort on the methodology development and analysis by minimizing the conceptually unimportant details which result from the full problem. Meanwhile, the use of a system such as that of Section 2 allows us to retain the generic structure of the models and error sources.

The primary objective of a feedback control system is to maximize performance in an appropriate sense within the constraints imposed by the actuator and sensor limitations and plant modeling errors. In general, the performance goals will be quantified in a number of ways. Examples include reduction in

the system response due to classes of external disturbances, percent accuracy in following classes of commands, and maintenance of such goals in the presence of parameter variations. All these are compatible goals and serve primarily to quantify the system properties that are required. Since our goal is to focus on a systematic procedure for handling the multiple sources of modeling error in the sequential assembly problem, we will use a simplified performance goal: maximize the system bandwidth while maintaining stability and zero steady state errors in the mass separations. We will view this goal in a loose sense in that we will also attempt to evaluate the conservativeness of the specifications that result from the error analysis. The latter will be achieved by synthesizing a control system that "nearly" violates the design specifications.

The error sources that will be considered are those that can be directly attributed to the special features of the LSS/sequential assembly decentralized control problem. These error sources can be represented by differences between the design, analysis and truth models. The errors can be associated with three sources, each of which must be addressed differently due to the structure of the error source.

The first error source is the mismatch between the local design model for a subassembly and the actual subassembly dynamics. For purposes of simplicity, this error source will be specified as the error between the subassembly design and truth models described in Section 2. In practice, this error source would have to be quantified to account for all possible subsystem parameter variations and for all the high frequency unmodeled dynamics. However, the general character of this source can be represented by our approach

as long as the limitations of the quantitative error analysis based on this simplified model are recognized.

The connection of the subassemblies leads to the remaining two error sources. The interconnection causes the subsystem transfer functions (i.e., the transfer function from the inputs to outputs of a single subsystem) to change, and introduces a coupling transfer function between subsystems. Although the control system design is based on the subsystem design models, it must also stabilize the interconnected system. This means that the nominal design must be robust to the two error sources (subsystem modification and neglected coupling interactions).

The error source due to subsystem modification will be specified as the difference between the subassembly design model and the subassembly transfer function that results from the analysis model. The general approach to characterizing this error source would use an analysis model of the coupled system that is at least as detailed as the design models for the subsystem. The structure and magnitude of the error source would be determined from the difference between the analysis subsystem models and the design models. The errors would then be characterized in terms of specifications on the singular values and singular subspaces of the closed loop design. We will follow this approach with the only difference being the level of detail of the design and analysis models. It should be emphasized that the analysis model is only used to characterize the error source for robustness analysis, and impacts the control system synthesis only through this characterization. Hence the additional complexity of this model does not automatically translate into comparable controller complexity, and the decentralized control architecture will be retained.

The third error source, the neglected subsystem interactions of the interconnected system, will also be specified by the intersubsystem coupling transfer functions of the analysis model. Again, one would generally use a more detailed analysis model to characterize the structure and magnitude of this error source. However, the level of detail of the analysis model does not conceptually effect this approach. As with the subsystem modification error, this error characterization will be used to determine specifications for the subsystem designs. Since the designs will still be based on the uncoupled design models, the resulting control system will retain the desired decentralized architecture.

3.3 ROBUSTNESS ANALYSIS TOOLS

3.3.1 General Robustness Theorems

The purpose of this subsection is to present and, when necessary, develop the analysis tools that are required to implement the methodology outlined in the preceding subsections. The results are presented in a uniform framework based on a restatement of a singular value robustness result by Lehtomaki et. al. [14] and a new result, Theorem 3.2, that allows the combination of different robustness tests. A series of tests which fit this category and are applicable to the problem described in Section 2 are then presented in Subsections 3.3.2-3.3.4.

Let $P_0(s)$ be the nominal model of the plant transfer function, and let $P_t(s)$ be the true plant transfer function. Let $\Delta(s)$ denote the input multiplicative error between $P_0(s)$ and $P_t(s)$:

$$P_t(s) = P_0(s) [I + \Delta(s)] \quad (3-1)$$

We will assume that $P_t(s)$ is only known to be in a convex set P . The class of allowable perturbations \mathcal{D} is then defined as the convex set:

$$\mathcal{D} = \{\Delta(s): \Delta(s) = P_0^{-1}(s) [P_t(s) - P_0(s)], P_t(s) \in P\} \quad (3-2)$$

Note that in practice \mathcal{D} may be either specified directly or derived from the specification of P .

Let $K(s)$ denote the feedback compensation. Then, the loop transfer function of the nominal feedback system at the plant input will be defined by:

$$L_0(s) = K(s) P_0(s) \quad (3-3)$$

and the loop transfer function of the true feedback system will be defined by:

$$L_t(s) = K(s) P_t(s) \quad (3-4)$$

It will be assumed that the feedback compensator is square and invertible. Hence the relationship (3-2) between the error class \mathcal{D} and plant class P remains valid.

We will assume that the nominal plant model $P_0(s)$ and each plant $P_t(s) \in P$ satisfy the following assumptions:

- (A1) $P_0(s)$ has a finite dimensional realization.
- (A2) $P_t(s)$ is a matrix of functions, each analytic in the closed right half plane except for a finite number of poles.
- (A3) $P_t(s)$ and $P_0(s)$ have the same number of closed right half plane poles.
- (A4) $[I + P_0(s)]^{-1}$ is analytic and bounded in the closed right half plane (i.e., stable).

(A5) If $P_t(s)$ has a pole at $s=j\omega_0$, then $P_0(s)$ has a pole at $s=j\omega_0$.

(A6) $P_0^{-1}(s)$ exist except at a finite number of points in the complex plane.

Finally, let D_R denote the Nyquist contour which closes in the right half plane with a circle of radius R and indents into the left half plane around each $j\omega$ axis pole of $L_0(s)$ with a circle of radius $1/R$.

With this background we can state the following fundamental robustness theorem.

Theorem 3.1: Assume that (A1)-(A6) hold and that there exists an R_0 such that for all $R > R_0$, for each $s \in D_R$ and for each $\Delta(s) \in \mathcal{D}$

$$\underline{\sigma} [I + L_0^{-1}(s) + \alpha \Delta(s)] > 0 \quad 0 < \alpha < 1 \quad (3-5)$$

Then the true closed loop system sensitivity matrix $[I + L_t(s)]^{-1}$ and transfer function matrix $[I + L_t(s)]^{-1} L_t(s)$ are analytic and bounded in the closed right half plane (i.e., the closed loop system is stable).

Proof: This theorem is a slightly generalized restatement of Theorem 2.2 in [14]. First, ([14], Theorem 2.2) can be extended to distributed systems by invoking the generalized Nyquist criterion [15] in the proof of ([14], Theorem 2.2). Assumptions (A1)-(A5) imply that assumptions a)-c) of ([14], Theorem 2.2) are satisfied. Assumption (A2) implies that $L_t(s)$ is a member of the class of distributed systems for which the generalized Nyquist criterion [15] holds (i.e., $L_t(s) \in \mathcal{B}(\sigma)$; see [15] for details). Finally, (3-5) is simply a restatement of assumption d) of ([14], Theorem 2.2), as the following argument shows.

The condition

$$\det [I + (I-\alpha) L_0(s) + \alpha L_t(s)] = 0 \quad L_t(s) \in KP \quad (3-6)$$

holds for some value $s \in D_R$, some $L_t(s) \in P$ and some $\alpha \in [0,1]$ if and only if

$$\det [I + L_0(s)^{-1} + \epsilon \Delta(s)] = 0 \quad (3-7)$$

for the same $s \in D_R$, $\alpha \in [0,1]$ and for some $\Delta(s) \in \mathcal{D}$. But condition (3-7) holds if and only if*

$$\underline{\sigma} [I + L_0(s)^{-1} + \alpha \Delta(s)] = 0 \quad (3-8)$$

Hence (3-3) holds if and only if d) of ([14], Theorem 2.2) holds. ■

This Theorem (and its parent [14]) are the basis for most of the guaranteed robustness tests to date. The results for multiplicative perturbations, [12], [6] additive perturbations, [12], divisive perturbations [14], phase information [16], and weak coupling [1]-[2] can all be shown to guarantee that (3-5) (or a minor variant) holds for each frequency on the Nyquist contour D_R . Two of these results, multiplicative perturbations and weak coupling, will be used in subsequent subsections, and a third result for perturbations with a specific structure will be derived directly from Theorem 3.1.

*Note that the use of the smallest singular value in (3-8) can be replaced by any inverse norm function, i.e., any function τ defined as:

$$\tau[A] = \|A^{-1}\|^{-1}$$

where $\|\cdot\|$ is any induced norm.

A difficulty that arises when using a number of diverse stability tests that are satisfied only on part of the Nyquist contour is that Theorem 3.1 and the results [6], [12], [14], [16] do not apply directly. The following Theorem allows the integration of tests to guarantee that Theorem 3.1 holds and that the resulting true closed loop system will be stable.

Theorem 3.2: Let $T_i(\Omega_i)$ denote a test that is true if and only if condition (3-5) is satisfied for each $s \in \Omega_i \subset D_R$, and each $\Delta(s) \in \mathcal{D}$. Assume that assumptions (A1)-(A6) hold, that $\{T_i(\Omega_i)\}_{i=1}^N$ are a set of tests that are all true, and that $\bigcup_{i=1}^N \Omega_i = D_R$. Then the closed loop system is stable.

Proof: Given any $s \in D_R$, there is a set Ω_j such that $s \in \Omega_j$. Then the assumption that $T_j(\Omega_j)$ is true implies that (3-5) holds. Hence Theorem 3.1 implies the closed loop system is stable. ■

The power of this theorem lies in its ability to combine different types of robustness tests over different frequency ranges into a comprehensive analysis which guarantees stability of the closed loop system. For example, the general multiplicative modeling error test [12] may be a tight constraint at high frequencies, but conservative at low frequencies. If a structured analysis test can be developed for the low frequency error, then it can be combined with the high frequency multiplicative error analysis to yield a complete robustness result.

For the system described in Section 2, three error sources dominate. As will be seen in subsection 3.4, the local modeling error is predominantly a high frequency error for which the unstructured modeling error analysis is appropriate. The subsystem model error that results from connecting the sub-assemblies dominates at low frequencies as subsection 3.5 demonstrates. This error requires a structural error analysis to avoid being overly conservative.

Finally, the neglected subsystem interaction that results from connecting the subassemblies is examined in subsection 3.6. This error source is largest in the mid-frequency range, and can be analyzed using a weak coupling analysis analogous to that developed by Bennett and Baras [1].

Each of these three robustness tests that will be used subsequently in this report will be presented in the remainder of this section. In each case, we will use the identity

$$T_0(s) = [I + L_0(s)^{-1}]^{-1} \quad (3-9)$$

3.3.2 Unstructured Multiplicative Error

The general multiplicative error robustness test has been developed in [12] and has been used in a variety of contexts. The unstructured multiplicative error $\Delta_m(s) \in \mathcal{D}_m$ characterized by the bound $\ell_m(j\omega)$:

$$\mathcal{D}_m = \{\Delta_m(s) : \overline{\sigma}[\Delta(j\omega)]^{-1} > \ell_m(j\omega)\} \quad (3-10)$$

Stated in the form of Theorems 3.1 and 3.2 the unstructured multiplicative error robustness test for a frequency range Ω_m is:

Theorem 3.3: (Unstructured Multiplicative Error Robustness Test) If

$$\overline{\sigma}[T_0(j\omega)] < \ell_m(j\omega) \quad \forall \omega \in \Omega_m \quad (3-11)$$

then condition (3-5) holds for all $\omega \in \Omega_m$.

Proof: Condition (3-5) can be written as

$$\underline{\sigma}[I + L_0(j\omega)^{-1}] - \alpha \overline{\sigma}[\Delta_m(j\omega)] > 0 \quad \alpha \in [0,1] \quad (3-12)$$

Condition (3-11) is obtained by moving the second term to the right side of the inequality, maximizing over α ($\alpha=1$), inverting both sides of the inequality, and using (3-9).

3.3.3 Rank One Errors

The subsystem model error that results from connecting the subassemblies is highly structured. The principal structural features of the error source $\Delta_g(s)$ are that $\Delta_g(s)$ has rank one and that $\Delta_g(s)$ is dominant over low frequencies (see subsection 3.5 for a more complete discussion). The first feature implies that only one of the singular values of $\Delta_g(s)$ is non-zero. Hence we can write the singular value decomposition of $\Delta_g(s)$ as (where the explicit dependence on s has been suppressed for notational clarity):

$$\Delta_g = U \Sigma V^H \quad (3-13)$$

where

$$\Sigma = \begin{bmatrix} \sigma_1 & 0 \\ 0 & 0 \end{bmatrix} \quad (3-14)$$

$$U = [u_1 \ u_2]$$

$$V = [v_1 \ v_2]$$

Quantities that will be useful in the statement and proof of Theorem 3.4 are the angle ϕ between the left and right singular subspaces corresponding to σ_1 and the relative complex angle θ between the left and right singular vectors (see [17]-[18] for details). These angles are defined uniquely whenever u_1 is not orthogonal to v_1 by:

$$v_1^H u_1 = \cos \phi e^{j\theta} \quad 0 < \phi < \frac{\pi}{2}, \quad -\pi < \theta < \pi \quad (3-15)$$

when u_1 is orthogonal to V_1 , θ is undefined and $\phi = \frac{\pi}{2}$.

The second structural feature of $\Delta_g(s)$ implies that the nominal closed loop function can be approximated by the identity matrix over the dominant frequency range Ω_g of the structural error

$$\overline{\sigma} [T_0(j\omega) - I] < \epsilon \quad \omega \in \Omega_g \quad (3-16)$$

with $\epsilon < 1$. Theorem 3.4 is a guarantee that (3-5) holds for error sources with this structure and a given value of ϵ in (3-16).

Theorem 3.4: (Rank One Error Robustness Test). Assume that the nominal closed loop transfer function $T_0(s)$ satisfies (3-16). Define

$$r = \frac{\epsilon}{1-\epsilon} + \sup_{\substack{\omega \in \Omega_g \\ \Delta_g \in \mathcal{D}_g}} [\sigma_1 \sin \phi] \quad (3-17)$$

If for each $\Delta_g \in \mathcal{D}$

$$|1 + \sigma_1 \cos \phi e^{j\theta}| > r \quad \forall \omega \in \Omega_g \quad (3-18)$$

then condition (3-5) holds for each $\omega \in \Omega_g$.

Proof: Let $\omega \in \Omega_g$ and $D_g \in \mathcal{D}_g$. Since $T_0(j\omega)$ satisfies (3-14), $T_0^{-1}(j\omega)$ satisfies

$$\underline{\sigma}_0 [T_0^{-1}(j\omega) - I] < \frac{\epsilon}{1-\epsilon} \quad (3-19)$$

Condition (3-5) can be rewritten as:

$$\underline{\sigma}_0 \{ [T_0^{-1}(j\omega) - I] + I + \alpha \Delta_g(j\omega) \} > 0 \quad \forall \alpha \in [0,1] \quad (3-20)$$

Inequality (3-20) will be satisfied if

$$\underline{\sigma} [I + \alpha \Delta_g(j\omega)] > \overline{\sigma} [T_0^{-1}(j\omega) - I] \quad \forall \alpha \in [0,1] \quad (3-21)$$

which in turn will be satisfied if (using (3-19)):

$$\underline{\sigma} [I + \alpha \Delta_g(j\omega)] > \frac{\epsilon}{1-\epsilon} \quad \forall \alpha \in [0,1] \quad (3-22)$$

After multiplying the bracketed term on the left by (the unitary matrix) U^H and on the right by U , condition (3-22) becomes:

$$\sigma [I + \alpha \Sigma v^H U] > \frac{\epsilon}{1-\epsilon} \quad \forall \alpha \in [0,1] \quad (3-23)$$

Using (3-12) - (3-13) in (3-23) gives:

$$\underline{\sigma} \left\{ \begin{bmatrix} 1 + \alpha \sigma_1 \cos \phi e^{j\theta} & 0 \\ 0 & I \end{bmatrix} + \begin{bmatrix} 0 & \alpha \sigma_1 v_1^H U_2 \\ 0 & 0 \end{bmatrix} \right\} > \frac{\epsilon}{1-\epsilon} \quad \forall \alpha \in [0,1] \quad (3-24)$$

Condition (3-24) will be satisfied if

$$\underline{\sigma} \left\{ \begin{bmatrix} 1 + \alpha \sigma_1 \cos \phi e^{j\theta} & 0 \\ 0 & I \end{bmatrix} \right\} > \frac{\epsilon}{\epsilon-1} + \alpha \sigma_1 \overline{\sigma} [v_1^H U_2] \quad \forall \alpha \in [0,1] \quad (3-25)$$

Since U is a unitary matrix and v_1 has unit magnitude, the maximum singular value on the right of (3-25) satisfies:

$$\overline{\sigma} [v_1^H U_2] = \sin \phi \quad (3-26)$$

Substituting (3-26) into (3-25) and maximizing the right side over $\alpha \in [0,1]$, $w \in \Omega_S$, and $\Delta_S \in \mathcal{D}_S$ implies that (3-25) will be satisfied if

$$\underline{\sigma} \left\{ \begin{bmatrix} 1 + \alpha \sigma_1 \cos \phi e^{j\theta} & 0 \\ 0 & 1 \end{bmatrix} \right\} > \frac{\epsilon}{\epsilon-1} + \sup_{\substack{w \in \Omega_S \\ \Delta_S \in \mathcal{D}_S}} [\sigma_1 \sin \phi] = r \quad \forall \alpha \in [0,1] \quad (3-27)$$

Condition (3-27) will be satisfied if

$$|1 + \alpha \sigma_1 \cos \phi e^{j\theta}| > r \quad \forall \alpha \in [0,1] \quad (3-28)$$

Assume there exists and $\alpha_0 \in [0,1]$ such that (3-28) does not hold. Then, since \mathcal{D}_S is convex and $0 \in \mathcal{D}_S$,

$$\Delta_{S0} = \alpha_0 \Delta_S \quad (3-29)$$

is an element of \mathcal{D}_S with

$$\begin{aligned} u_1^H \Delta_{S0} u_1 & \stackrel{\Delta}{=} \sigma_{10} \cos \phi_0 e^{j\theta_0} \\ & = \alpha_0 \sigma_1 \cos \phi e^{j\theta} \end{aligned} \quad (3-30)$$

Hence

$$|1 + \sigma_{10} \cos \phi_0 e^{j\theta_0}| \leq r$$

which contradicts (3-18). Thus condition (3-28) must hold. Since (3-28) is sufficient for (3-5) the proof is complete. ■

Theorem 3.4 provides a simple graphical test for the robustness of systems with rank one error sources. The test is a Nyquist-like test on the (non-analytic) function

$$\begin{aligned} f(s) & = \sigma_1 \cos \phi e^{j\theta} \\ & = u_1^H(s) \Delta_S(s) u_1(s) \quad \Delta_S \in \mathcal{D}_S \end{aligned} \quad (3-31)$$

where $u_1(s)$ is the first column of U . Condition (3-18) requires the Nyquist locus of each $f(s)$ to avoid a circle in the complex plane of radius r and centered at the point $(-1,0)$ (see Fig. 3-2). Specifically, the circle F_r is defined as

$$F_r = \{x \in \mathbb{C}: |x - (-1,0)| < r\} \quad (3-32)$$

Since \mathcal{D}_s is a convex set, any point inside a locus for a particular $\Delta_s \in \mathcal{D}_s$ (i.e., any point on a line segment from the origin to the locus) will lie on a locus for some other $\Delta_s \in \mathcal{D}_s$. This means that the set of all points on a locus for some $\Delta_s \in \mathcal{D}_s$

$$L = \{x \in \mathbb{C}: x = f(j\omega) \text{ for some } \Delta_s \in \mathcal{D}_s, \omega \in \Omega_s\} \quad (3-33)$$

is a solid region in the complex plane (as illustrated by the shaded region in Fig. 3-2). Hence, the region can be completely characterized by its boundary.

Thus, the test for stability can be conducted by the following steps:

1. Determine r (from (3-17))
2. Draw the circle F_r (see (3-32))
3. Plot the boundary of L (see (3-33))
4. Check that $F_r \cap L = \emptyset$.

Theorem 3.4 is reminiscent of the various circle theorems [19]-[21] that are available for nonlinear, time varying and multivariable systems. However, this result incorporates the error source phase and directionality structure, as well as the usual magnitude variation of the error source. The ability to incorporate phase structure is also more general than the structures that can be analyzed using the structural singular value [22]-[23].

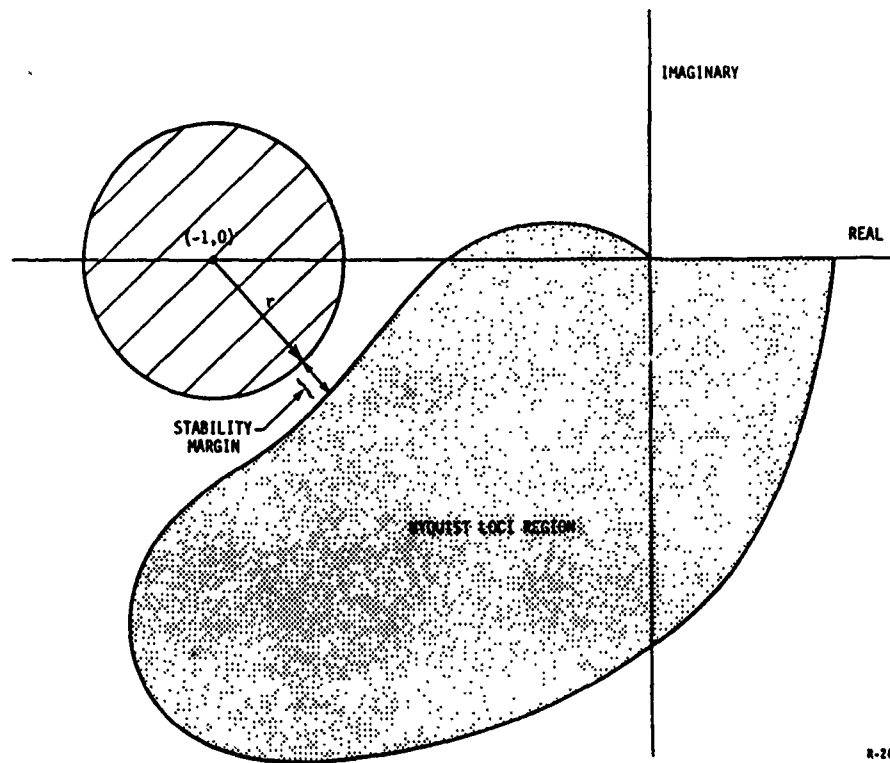


Figure 3-2. Graphical Test for Rank One Error Sources

The set \mathcal{D}_s defines the structural information about the error source that is required by Theorem 3.4. While the rank one structure is imbedded in the theorem statement, \mathcal{D}_s must still define the phase and directionality information. This information can be specified either by the complex boundary function $f(j\omega)$ and the second term of (3-17), or by the real functions $\sigma_1(j\omega)$, $\phi(j\omega)$ and $\theta(j\omega)$.

Directionality information is incorporated through the second term on the right side of (3-17). This term is a bound on the how much the loop coupling can be modified in the nominal system. If the relative change between the nominal and true system input-output directions is large in a frequency range that also has a significant magnitude variation then this term will be large. This bound can be very conservative (a result of (3-27)). However, the

conservativeness can be removed, if necessary, at the expense of a more complex test and a more complex characterization of the set \mathcal{D}_s .

Finally, it should be noted that Theorem 3.4 can be used to determine how tight the approximation (3-16) must be for a given error source set \mathcal{D}_s , and how much stability margin is guaranteed for the true system. Given a set \mathcal{D}_s , define

$$l_1 = \sup_{\substack{\omega \in \Omega_s \\ \Delta_s \in \mathcal{D}_s}} |\sigma_1 \sin \phi| \quad (3-34)$$

and

$$l_2 = \inf_{\substack{\omega \in \Omega_s \\ \Delta_s \in \mathcal{D}_s}} |1 + \sigma_1 \cos \phi e^{j\theta}| \quad (3-35)$$

Then if

$$l_1 + l_2 < 1 \quad (3-36)$$

there is a value of ϵ such that Theorem 3.4 holds. In particular, any value ϵ that satisfies

$$\epsilon < \frac{1 - l_1 - l_2}{2 - l_1 - l_2} \quad (3-37)$$

will work. This value in turn determines how tight the control loop must be over the frequency range Ω_s . The controller can be chosen to satisfy (3-17) and thus guarantee stability (assuming, of course, that such a controller choice does not violate any other robustness or performance constraints).

Once a value for ϵ has been determined, the graphical test can be used to determine the guaranteed stability margin m of the closed loop system with the rank one perturbation included. In this context, the guaranteed stability margin is magnitude of the largest allowable unstructured error in either the inverse of the nominal closed loop transfer function $T_0^{-1}(s)$ or in the error source characterization \mathcal{D}_s that can be tolerated. The value m is given by:

$$m = \inf_{\substack{x \in F_r \\ y \in L}} |x - y| \quad (3-38)$$

That is, m is the minimum distance from F_r to L (see Fig. 3-2).

3.3.4 Weak Coupling Errors

The third principal error source is the interconnection dynamics that result from connecting the subassemblies. This error source will be characterized by the set of interconnection matrices \mathcal{D}_w . Let $\{P_{i10}\}_{i=1}^N$ denote the nominal subsystem models of the decoupled plant. Then the nominal model is

$$P_0 = \text{diag} [P_{i10}] \quad (3-39)$$

and the error between P_0 and any true model P is:

$$\Delta_w = \begin{bmatrix} 0 & P_{11}^{-1} P_{12} & \cdots & P_{11}^{-1} P_{1N} \\ P_{22}^{-1} P_{21} & 0 & & P_{22}^{-1} P_{2N} \\ \vdots & & & \vdots \\ P_{NN}^{-1} P_{N1} & P_{NN}^{-1} P_{N2} & \cdots & 0 \end{bmatrix} \quad (3-40)$$

Hence, the interconnection error set is:

$$\mathcal{D}_w = \{\Delta = [\Delta_{ij}]: \Delta_{ii} = 0, i=1, \dots, N\} \quad (3-41)$$

A number of systems analyses have been developed to handle the interconnected systems problem (see [24] for a detailed survey). Most have assumed that the set \mathcal{D}_w has some form of weak interconnecting structure. The most relevant results are those of Bennett and Baras [1], and Limebeer [2]. Both utilize the concept of block diagonal dominance [25] to prove stability of an interconnected system given a nominally stable block diagonal system. The following Theorem presents a similar result cast in the framework of Theorems 3.1-3.2.

Theorem 3.5: (Weak Interconnection Error Robustness Test). Assume that assumptions (A1)-(A6) hold. Let $\{T_{oii}\}_{i=1}^N$ denote the closed loop transfer function of the nominal uncoupled subsystem. If for each $\Delta \in \mathcal{D}_w$

$$\bar{\sigma}[T_{oii}] < \left[\sum_{j=1}^N \bar{\sigma}(\Delta_{ij}) \right]^{-1} \quad \forall i=1, \dots, N \quad \forall \omega \in \Omega_w \quad (3-42)$$

then condition 3.5 holds for each $\omega \in \Omega_w$.

Proof: Condition (3.42) can be rewritten as:

$$\underline{\sigma}[T_{oii}^{-1}] > \sum_{j=1}^N \bar{\sigma}(\Delta_{ij}) \quad \forall i=1, \dots, N \quad \forall \omega \in \Omega_w \quad (3-43)$$

inequality (3-43) implies that $(T_0^{-1} + \Delta)$ is block diagonally dominant (see [25]), which in turn implies that $(T_0^{-1} + \Delta)$ is nonsingular for each $\Delta \in \mathcal{D}_w$ [25]. Thus

$$\underline{\sigma}_0(T_0^{-1} + \Delta) > 0 \quad \forall \Delta \in \mathcal{D}_w \quad \forall \omega \in \Omega_w \quad (3-44)$$

Let $\alpha \in [0,1]$. Then, for any $\Delta \in \mathcal{D}_w$, $\alpha\Delta \in \mathcal{D}_w$. By (3-44),

$$\underline{\sigma} \begin{pmatrix} T^{-1} + \alpha\Delta \\ 0 \end{pmatrix} > 0 \quad \forall \omega \in \Omega_w \quad (3-45)$$

Since $\alpha \in [0,1]$ is arbitrary, (3-45) is identical to (3-5). ■

3.4 SUBSYSTEM ERRORS FOR THE DECOUPLED SYSTEM

The first error source results from the unmodeled higher frequency dynamics due to the reduced order design model. Since such neglected dynamics are almost invariably harmful, it is appropriate to treat them as unstructured multiplicative perturbations to the plant as represented by (3-1) with $\Delta(s) \in \mathcal{D}_m$ and \mathcal{D}_m defined as in (3-10). Theorem 3.3 and condition (3-11) give the appropriate robustness test for errors in the class \mathcal{D}_m .

The multiplicative error between the 5 element truth model ($P_t(s)$) and the 3 element design model ($P_0(s)$) defined in Section 2 is given by (3-2). A plot of the inverse of the largest and smallest singular values is shown in Fig. 3-3. The bound function $\ell_m(j\omega)$ can be taken to be

$$\ell_m(j\omega) = \left[\frac{4}{1.76s + 1} \right]_{s=j\omega} = \frac{4}{\sqrt{3.1\omega^2 + 1}} \quad (3-46)$$

Note that if this were the sole error source a bandwidth of approximately 1-2 rad/sec could be achieved.

3.5 SUBSYSTEM ERRORS FOR THE CONNECTED SYSTEM

The second error source results from the dynamic modification of the subsystem transfer function caused by the connection of the two subsystems. Let $P_t(s)$ denote the subsystem transfer function obtained from the 6 element analysis model of the coupled system, and let $P_0(s)$ denote the 3 element

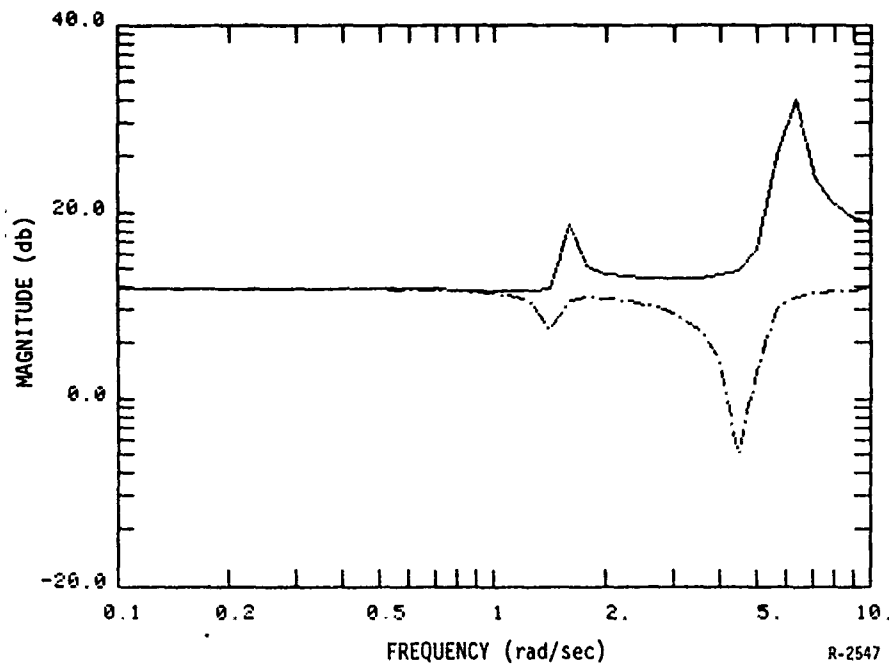


Figure 3-3. Inverse Multiplicative Error Between the Nominal 3 Element Design Model and the 5 Element Truth Model

design model of the subsystem. The inverse of the largest singular value of the relative error (3-2) is shown in Fig. 3-4. Note that the most significant modification to the model is for frequencies less than .1 radians/second. In fact, if this error were completely unstructured condition (3-2) would require the closed loop transfer function to have a magnitude less than .2, and the control objectives would not be attainable within this control architecture.

Fortunately, the error depicted in Fig. 3-4 is highly structured. A more detailed and accurate analysis can be performed by applying the rank one analysis tool developed in Subsection 3.3.3.

The interconnection of two subsystems by a single beam can be viewed as a single-input single-output loop closure. Figure 3-5 depicts a single

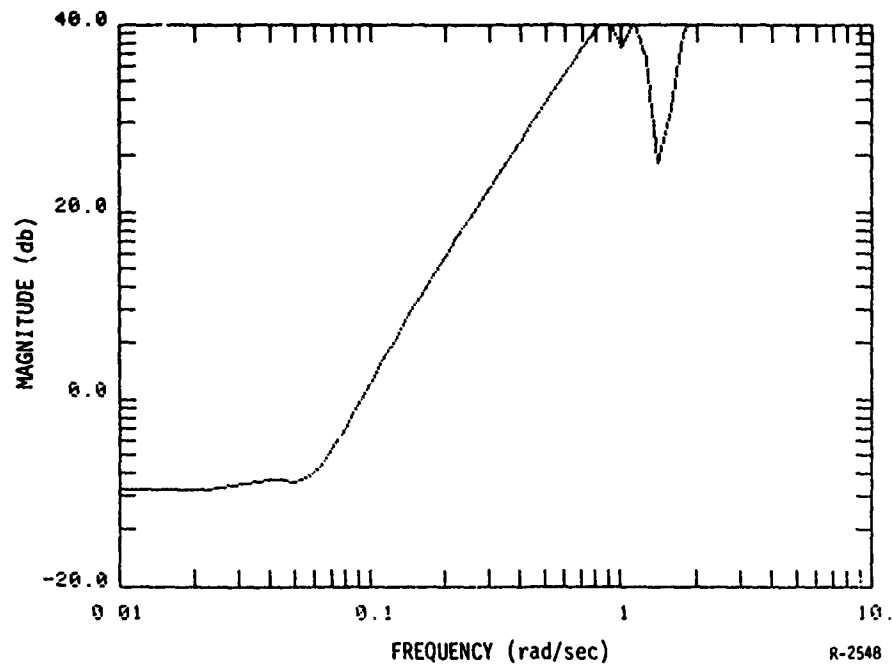


Figure 3-4. Inverse Multiplicative Error Between the 3 Element Subsystem Design Model and the 6 Element Analysis Model

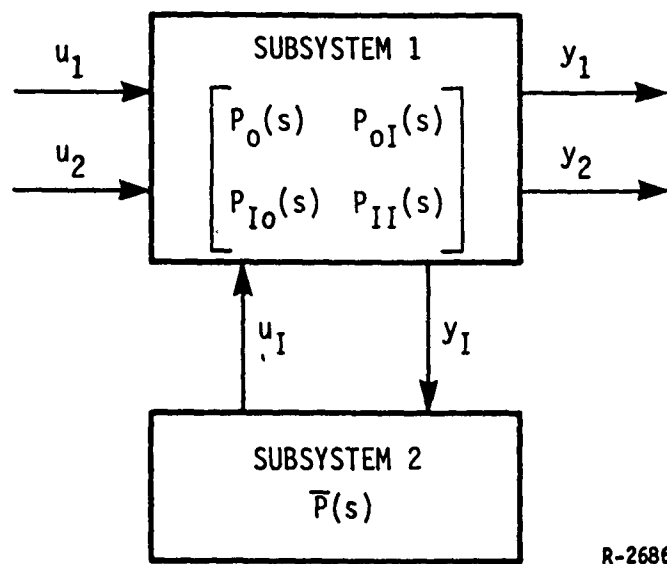


Figure 3-5. Subsystem Modification Structure

subsystem described by:

$$\begin{bmatrix} y \\ y_I \end{bmatrix} = \begin{bmatrix} P_0 & P_{0I} \\ P_{I0} & P_{II} \end{bmatrix} \begin{bmatrix} u \\ u_I \end{bmatrix} \quad (3-47)$$

where u is the 2 dimensional subsystem input vector, y is the 2 dimensional subsystem output vector, u_I is the 1 dimensional interconnection input, and y_I is the 1 dimensional interconnection output. The second subsystem is assumed to have the interconnection transfer function

$$u_I = \bar{P} y_I \quad (3-48)$$

Following the interconnection, the subsystem transfer function from u to y becomes:

$$\begin{aligned} y &= [P_0 + P_{0I} (1 - \bar{P} P_{II})^{-1} \bar{P} P_{I0}] u \\ &\triangleq P_t u \end{aligned} \quad (3-49)$$

The relative error between P_t and P_0 is given by (3-2)

$$\Delta_s = P_0^{-1} [P_{0I} (1 - \bar{P} P_{II})^{-1} \bar{P} P_{I0}] \quad (3-50)$$

Since the bracketted term on the right side of (3-50) has rank one for all values of s (P_{0I} and P_{I0} are 2×1 and 1×2 matrices, respectively) the perturbation has the rank one structure examined in subsection 3.3.3.

The set \mathcal{D}_g of all subsystem interconnection errors can be characterized by a boundary function $f(j\omega)$ whose Nyquist locus is the boundary of the set of

all Nyquist loci of $\Delta_s \in \mathcal{D}_s$. For the purposes of this report, we will use the relative error between the nominal 3 element subsystem design model and the subsystem transfer function generated by the 6 element interconnected analysis model to define the function $f(j\omega)$. Thus, $f(j\omega)$ will be defined as:

$$f(j\omega) = \sigma_1 \cos \phi e^{j\theta} \quad (3-51)$$

where σ_1 , ϕ and θ are defined by (3-13)-(3-15) applied to the relative error.

The Nyquist plot of $f(j\omega)$ is shown in Fig. 3-6. This locus will avoid any circle centered at the point $(-1,0)$ with a radius less than 0.6. Hence, if r (as defined by (3-17)) satisfies

$$r < .6 \quad (3-52)$$

then the rank one robustness test (Theorem 3-4) will be satisfied. For this relative error

$$\sup_{\omega \in R} [\sigma_1 \sin \phi] < 10^{-4} \quad (3-53)$$

and its contribution to r is negligible. As long as the control system design satisfies (3-16) with

$$\epsilon < .38$$

over the frequency range for which the error source is dominant

$$\Omega_s = \{\omega < .2\} \quad (3-54)$$

the test will still be satisfied.

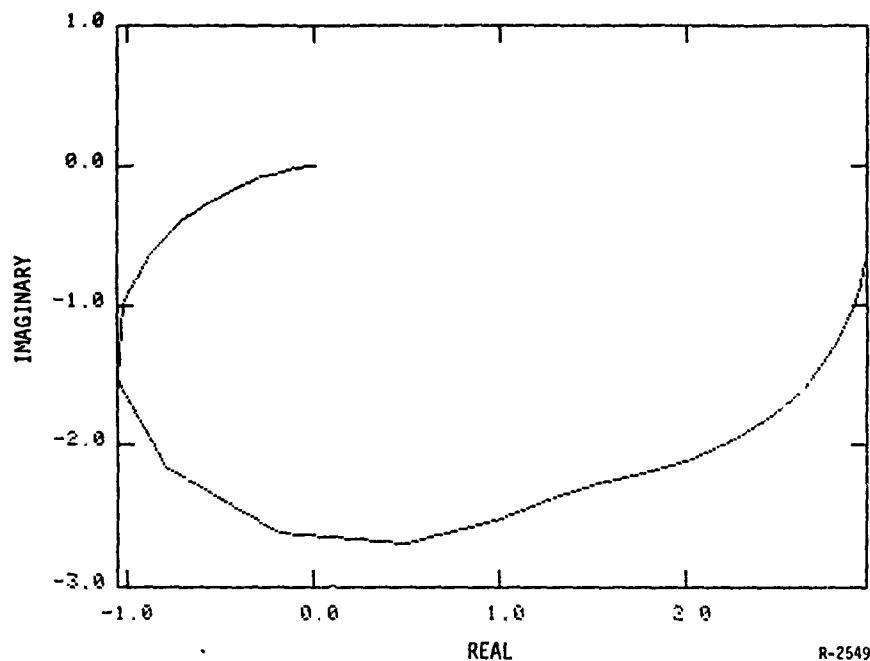


Figure 3-6. Nyquist Plot of $\sigma_1 \cos \phi e^{j\theta}$

Additional information regarding the behavior of the coupled decentralized system can be readily obtained from (3.39) once a value for ϵ has been specified. For $\epsilon=0$, the guaranteed margin is plotted in Fig. 3-7 versus frequency. Based on this margin, we would expect the coupled system using decentralized control system designs to have a mode with a natural frequency of .1 rad/sec and a peak amplitude of approximately 6 db. Since the actual design will require a nonzero value for ϵ , the peak will be somewhat higher. For $\epsilon = .25$ (i.e., $T_0(s)$ within -2.5 db of the identity over the frequency range Ω_s), the peak would be 9db.

3.6 INTERCONNECTION ERRORS

The final error source is the interconnection transfer function between the subsystems. This error class, \mathcal{D}_w , is characterized by the largest

SUBSYSTEM COUPLING ERROR

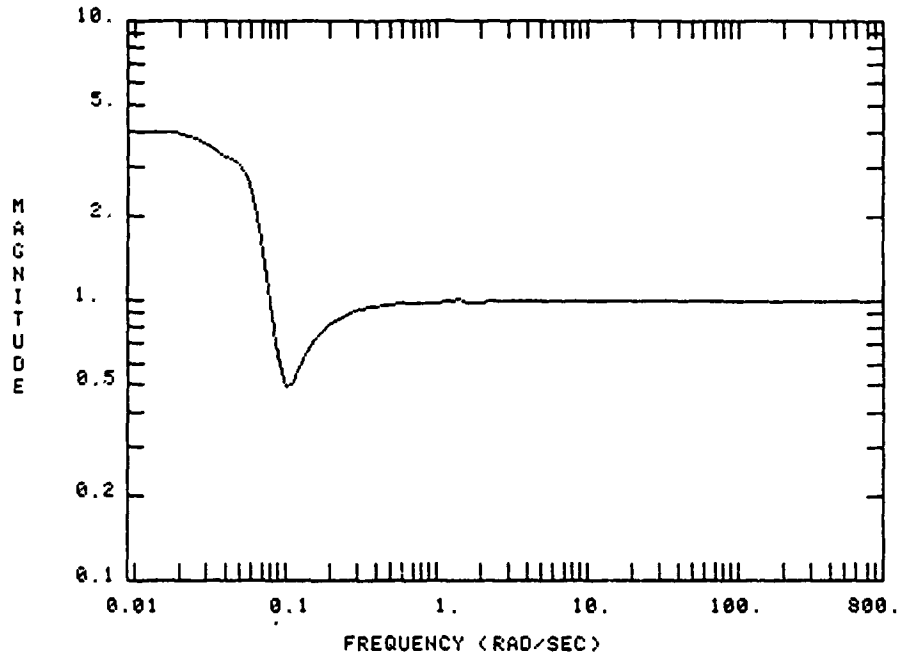


Figure 3-7. Stability Margin of Coupled Analysis System With Structured Error

relative norms of the interconnection transfer functions $\{\ell_{wi}(\omega)\}_{i=1}^N$. The class \mathcal{D}_w for the two subassembly problem of Section 2 is defined as:

$$\mathcal{D}_w = \{\Delta(s) = \begin{bmatrix} 0 & \Delta_{12}(s) \\ \Delta_{21}(s) & 0 \end{bmatrix} : \bar{\sigma}\{\Delta_{ij}(j\omega)\} < \ell_{wi}(\omega), i=1, 2; j \neq i\} \quad (3-55)$$

The relative interconnection error will be determined from the 3 element design model ($P_0(s)$) and the 6 element analysis model ($P_t(s)$). A plot of the inverse error $\bar{\sigma} \begin{bmatrix} P^{-1} & P \\ 0_{11} & 12 \end{bmatrix}^{-1}$ is shown in Fig. 3-8 for subsystem 1. Due to the symmetry of the problem, the plot of the error $\bar{\sigma} \begin{bmatrix} P^{-1} & P \\ 0_{22} & 21 \end{bmatrix}^{-1}$ for subsystem 2 is identical. As can be seen from Fig. 3-8, the bounds $\{\ell_{wi}\}_{i=1,2}$ can be chosen to be:

$$\ell_{wi}(\omega) = -20 \text{ dB} \quad i=1,2, \omega \in \Omega_w \quad (3-56)$$

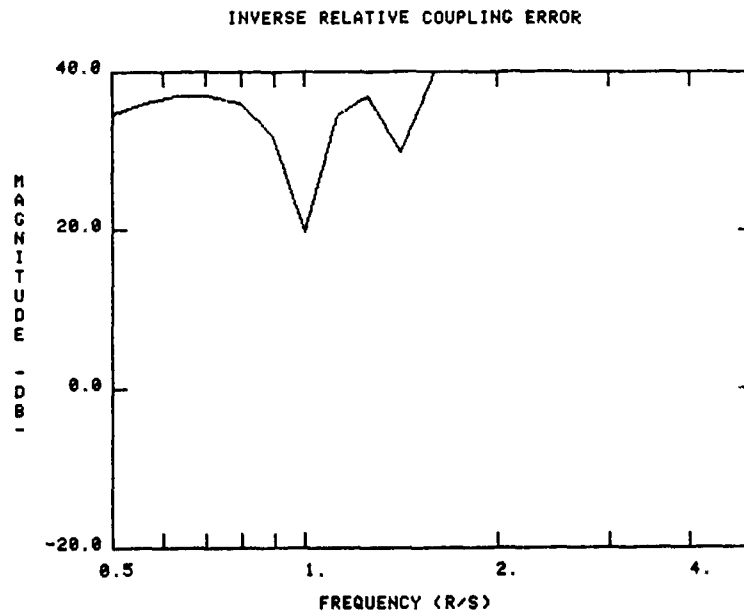


Figure 3-8. Inverse of the Relative Interconnection Error

where Ω_w is the frequency range:

$$\Omega_w = \{\omega: .5 < \omega < 2\} \quad (3-57)$$

Theorem 3.5 indicates that this error will not be significant as long as the nominal subsystem closed loop transfer functions are small ($\ll 20\text{db}$) in the frequency range Ω_w .

3.7 SUMMARY OF THE ERROR ANALYSES

The analyses of the error sources in subsections 3.4-3.6 can be combined to provide specifications for the decentralized control system designs. The total error Δ can be written in terms of the three principal errors:

$$\Delta(s) = \Delta_m(s) + \Delta_g(s) + \Delta_w(s) \quad (3-58)$$

Each of the three error sources is dominant in a different frequency region. The latter two (Δ_s and Δ_w) possess significant structure (rank one error and weak interconnection, respectively) over the frequency region in which they are dominant. Each of these error sources (Δ_s and Δ_w) is relatively small outside the frequency region. They can be regarded as unstructured errors outside the dominant regions, and can be combined with the error source Δ_m with insignificant effects.

Thus we can decompose our stability analysis and design specification into three frequency regions:

$$\Omega_s = \{\omega: \omega < .2\}$$

$$\Omega_w = \{\omega: .5 < \omega < 2\}$$

$$\Omega_m = \mathbb{R}$$

The design specifications can then be derived from the analyses of subsections 3.4-3.6 and Theorems 3.3-3.5. Theorem 3.4 implies that the transfer function $T_0(s)$ for each subsystem must be nearly unity in the frequency range Ω_s . That is,

$$T_0(j\omega) \approx 1 \quad \omega \in \Omega_s \quad (3-59)$$

The weak coupling Theorem (Theorem 3.5) implies that nominal transfer function design must be less than 20dB to avoid the interconnection error in the frequency range Ω_w . There is actually a more severe constraint in this region resulting from the multiplicative error source Δ_m . This source consists of the nominal subsystem modeling error (Fig. 3-3), and the subsystem connection error (Fig. 3-4). If these are assumed to combine in the most harmful manner,

the total inverse error would be bounded by

$$\overline{\sigma} (\Delta(j\omega))^{-1} > 1.9 \quad \omega \in \Omega_w \quad (3-60)$$

Hence, by Theorem 3.5 the nominal subsystem transfer function designs must satisfy

$$\overline{\sigma} [T_0(j\omega)] < 1.9 \quad \omega \in \Omega_w \quad (3-61)$$

Finally, the unstructured multiplicative error source becomes significant at frequencies greater than 2 radians/sec. From Fig. 3-3, the bound $\ell_m(j\omega)$ (Eq. (3-46)), and Theorem 3-3, the nominal subsystem transfer function must satisfy.

$$\sigma [T_0(j\omega)] < \frac{4}{\sqrt{3.1 \omega^2 + 1}} \quad \forall \omega \quad (3-62)$$

Conditions (3.61), (3.63) and (3.64) provide specifications for the subsystem designs that will guarantee that the closed loop system will be stable, both while decoupled and while connected.

SECTION 4

DECENTRALIZED CONTROL SYSTEM DESIGN AND ANALYSIS

4.1 LINEAR QUADRATIC REGULATOR DESIGN

A control system was designed for each of the subassemblies to satisfy the decentralized design requirements developed in Section 3. To recapitulate, these requirements were:

$$T_0(j\omega) \approx 1 \quad \omega < .2 \quad (4-1)$$

$$\|T_0(j\omega)\| < 1.9 \quad 1 < \omega < 2 \quad (4-2)$$

$$\|T_0(j\omega)\| < \frac{4}{\sqrt{3.1\omega^2 + 1}} \quad \forall \omega \quad (4-3)$$

The design goal is to obtain the largest bandwidth possible (in the sense described in subsection 3.1) with zero steady state errors in the mass separation.

The subassembly control system designs were developed using the Linear Quadratic-Gaussian/Loop Transfer Function Recovery (LQG/LTR) procedure [13]. Integral states were appended to produce the desired zero steady state errors. The subassembly design models can be represented in state space form as:

$$\dot{x}_m = A_m x_m + B_m u \quad (4-4)$$

Define the integral states:

$$\dot{e} = y \quad (4-6)$$

Then the regulator design system becomes:

$$\dot{z} = A_D z + B_D u \quad (4-7)$$

where

$$z = \begin{bmatrix} e \\ x_m \end{bmatrix} \quad (4-8)$$

$$A_D = \begin{bmatrix} 0 & C_m \\ 0 & A_m \end{bmatrix} \quad (4-9)$$

$$B_D = \begin{bmatrix} 0 \\ B_m \end{bmatrix} \quad (4-10)$$

Define the regulator cost

$$J = \int_0^{\infty} z^T Q_D z + u^T R u \, dt \quad (4-11)$$

where

$$Q_D = C_D^T C_D \quad (4-12)$$

$$C_D = \begin{bmatrix} C_I & C_P \end{bmatrix} \quad (4-13)$$

$$R = \rho I \quad (4-14)$$

The the LQ regulator solution is given by

$$u = - G_m z_m = - [G_I \, G_P] \begin{bmatrix} e \\ x_m \end{bmatrix} \quad (4-15)$$

$$G_m = R^{-1} B_D^T K \quad (4-16)$$

where K is the solution of the regulator Riccati equation

$$A_D^T K + K A_D + Q_D - K B_D R^{-1} B_D^T K = 0 \quad (4-17)$$

The loop transfer function $L(s)$ of the LQ regulator can be approximated by

$$L_0(s) = \left[\frac{1}{s} C_I C_m (sI - A_m)^{-1} B_m + C_p (sI - A_m)^{-1} B_m \right] \quad (4-18)$$

Equation (4-18) was used to specify C_I and C_p to satisfy the basic design goals summarized at the beginning of this section. The integral weight C_I was chosen to satisfy

$$L_0(s) \approx \frac{1}{s} I \quad |s| \ll 1 \quad (4-19)$$

This was achieved by specifying

$$C_I = [C_m A_m^{-1} B_m]^{-1} \quad (4-20)$$

The state weighting matrix C_p was chosen to penalize only the outputs:

$$C_p = X C_m \quad (4-12)$$

The remaining degrees of freedom (i.e., the choice of X) were used to match the high frequency singular values of (4-18):

$$X = [C_m A_m^{-1} B_m]^{-1} \quad (4-22)$$

Finally, the scale factor ρ of the input penalty matrix was chosen to maximize the bandwidth of the LQ regulator by choosing its value as small as possible while still satisfying (4-2). The resulting value of ρ was:

$$\rho = .1 \quad (4-23)$$

The resulting LQ regulator design has closed loop eigenvalues:

$$\left. \begin{array}{l} -.301 \pm 1.53j \\ -.223 \pm 1.01j \end{array} \right\} \text{ subsystem modes}$$

$$\left. \begin{array}{l} -.280 \\ -.292 \end{array} \right\} \text{ integrator poles} \quad (4-24)$$

The singular values of the closed loop system transfer function from system input to controller output is shown in Fig. 4-1. The singular values of the return difference at the system input is shown in Fig. 4-2.

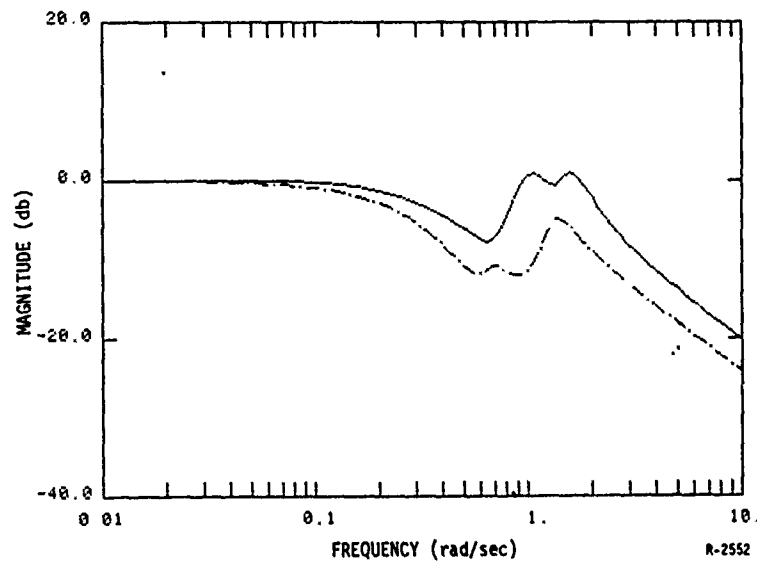


Figure 4-1. Linear Quadratic Regulator Transfer Function

The primary features of note with respect to the LQ designs are that the design constraints (4-1)-(4-3) imposed by the error analysis of Section 3 are satisfied. However, both condition (4-1) and (4-3) are barely satisfied by this design. Consequently, we will expect that the unmodeled mode that determined (4-3) is likely to be very oscillatory when this controller is

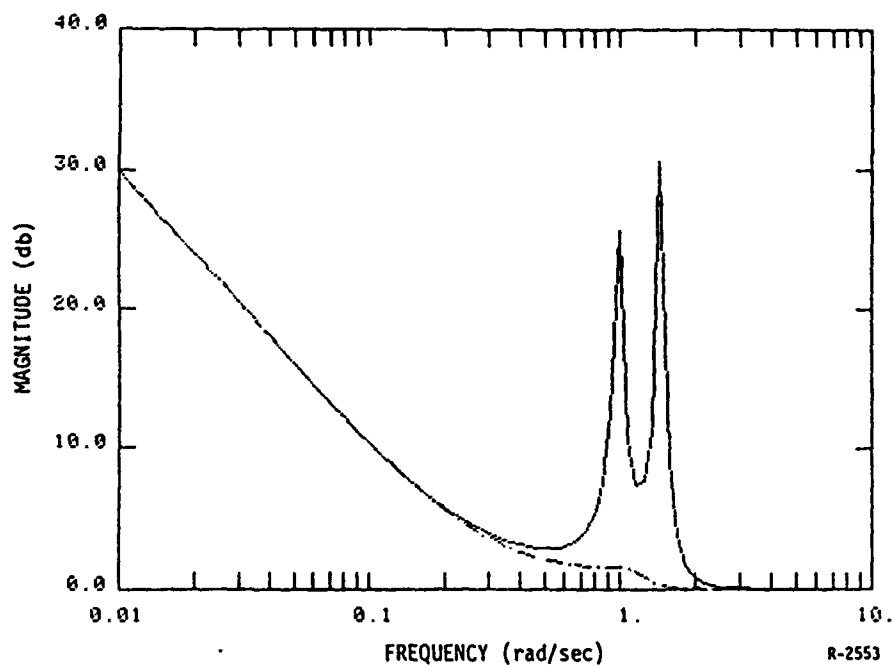


Figure 4-2. Singular Values of the Linear Quadratic Regulator Return Difference

applied to the truth system. Also, the coupling pole that is expected to occur at $s \approx \pm .1j$ will be somewhat more lightly damped than the analysis based on the approximation (4-1) would indicate. In fact, the amount by which (4-1) is violated results in a value for ϵ (see (3-14)) of .25. As subsection 3-5 indicates, we should expect an approximately 9db peak in the closed loop transfer function of the true system.

Finally, we should emphasize that this design was developed specifically to test the a priori analysis procedures used in Section 3. There are numerous features of the preceding design that could prove undesirable for a true system. However, this design will serve the purpose of pushing the design to the limits of design specifications.

4.2 LOOP TRANSFER FUNCTION RECOVERY

The loop transfer function recovery procedure developed by Stein and Doyle [12] and Kwakernaak [26] was applied to the model system (4-4)-(4-5) to produce an output feedback compensator. The Kalman-Bucy filter design used the spectral density matrices

$$\Xi_m = B_m B_m^T \quad (4-25)$$

$$\Theta = \delta I \quad (4-26)$$

to produce a filter design:

$$\dot{\hat{x}}_m = A_m \hat{x}_m + B_m u + H_m (y - C_m \hat{x}_m) \quad (4-27)$$

where

$$H_m = \Sigma C_m^T \Theta^{-1} \quad (4-28)$$

and Σ is the solution of the filter Riccati equation:

$$A_m \Sigma + \Sigma A_m^T + \Xi_m - \Sigma C_m^T \Theta^{-1} C_m \Sigma = 0 \quad (4-29)$$

The LQG feedback compensator that results from the Kalman-Bucy filter (4-27) and the LQ regulator design (4-7), (4-15) is described by the equations:

$$\dot{\hat{x}}_m = (A_m - B_m G_p - H_m C_m) \hat{x}_m - B_m G_I e + H_m y \quad (4-30)$$

$$\dot{e} = y \quad (4-31)$$

$$u = -G_p \hat{x}_m - G_I e \quad (4-32)$$

As $\delta \rightarrow 0$, the loop transfer function of the overall closed loop system (evaluated at the plan input) approaches the loop transfer function of the LQ

regulator. For the LQ design of subsection 4.1 and the design constraints (4-1)-(4-3), the choice

$$\delta = 10^{-5} \quad (4-33)$$

resulted in a satisfactory approximation to the LQ loop transfer function (accurate for frequencies less than 8 radians/second). The KBF eigenvalues for this value of δ are

$$\begin{aligned} -9.25 \pm 9.36j \\ -5.73 \pm 5.83j \end{aligned} \quad (4-34)$$

The singular values of the closed loop transfer function for the design model (4-4)-(4-5) and controller defined by (4-30)-(4-32) are shown in Fig. 4-3. The same controller was applied to the subsystem truth model. The singular values of the resulting closed loop transfer functions are shown in Fig. 4-4. As expected, the mode corresponding to the unmodeled dynamics is highly oscillatory and produces a small gain margin. The eigenvalues of the closed loop system for the 5 element truth model are:

$$\begin{aligned} & \begin{aligned} & -9.38 \pm 9.48j \\ & -5.81 \pm 5.88j \end{aligned} \left. \vphantom{\begin{aligned} & -9.38 \pm 9.48j \\ & -5.81 \pm 5.88j \end{aligned}} \right\} \text{filter eigenvalues} \\ & \begin{aligned} & -.03 \pm 4.89j \\ & -.048 \pm 4.65j \end{aligned} \left. \vphantom{\begin{aligned} & -.03 \pm 4.89j \\ & -.048 \pm 4.65j \end{aligned}} \right\} \text{unmodeled dynamics} \\ & \begin{aligned} & -.236 \pm 1.55j \\ & -.172 \pm 1.01j \end{aligned} \left. \vphantom{\begin{aligned} & -.236 \pm 1.55j \\ & -.172 \pm 1.01j \end{aligned}} \right\} \text{subsystem modes} \\ & -0.209 \pm .0053j \left. \vphantom{-0.209 \pm .0053j} \right\} \text{integrators} \end{aligned} \quad (4-35)$$

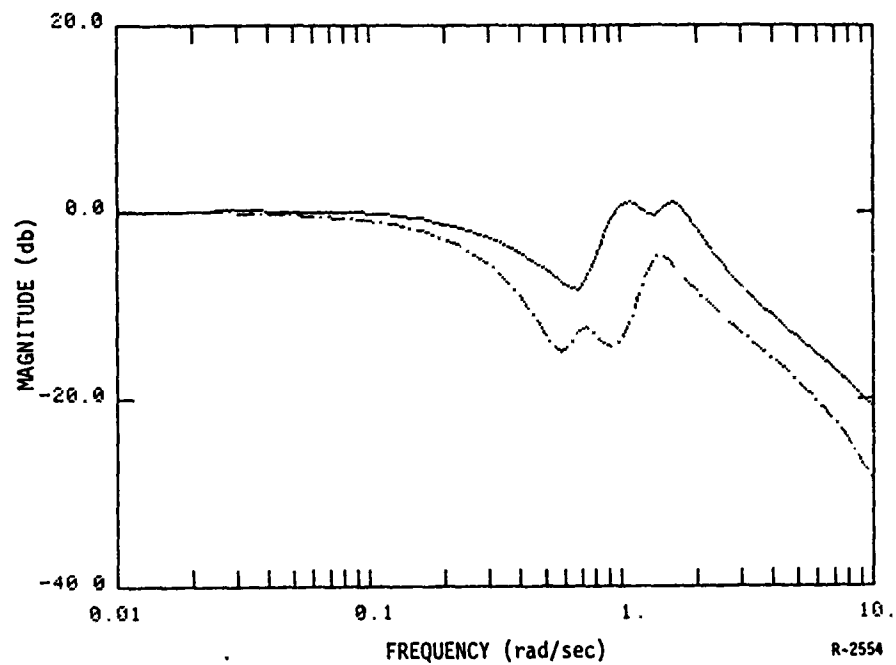


Figure 4-3. Singular Values of the Closed Loop LQG Design Subsystem

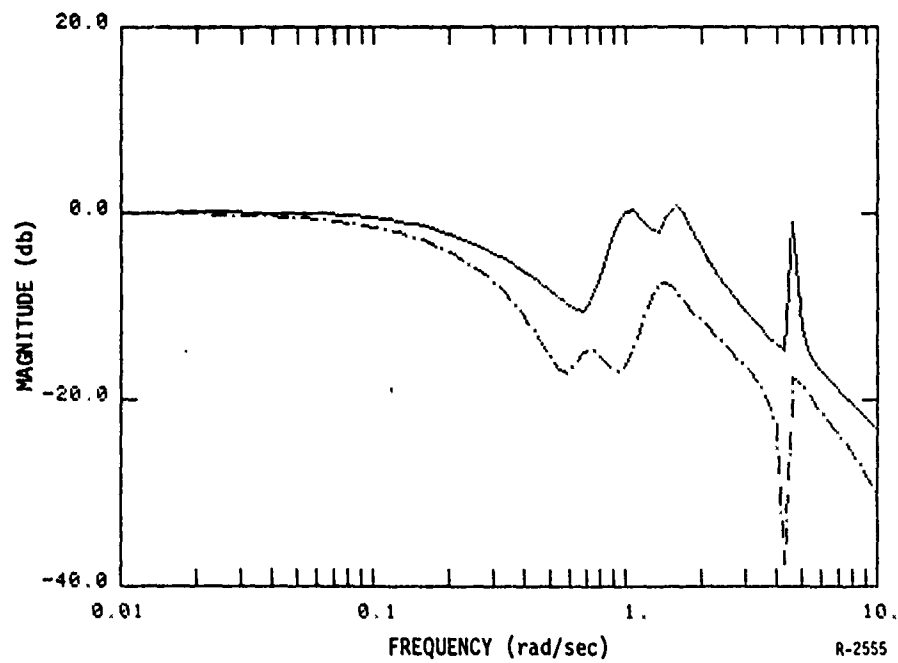


Figure 4-4. Singular Values of the Closed Loop LQG Truth Subsystem

4.3 ANALYSIS OF THE INTERCONNECTED DECENTRALIZED SYSTEM

The decentralized subsystem compensators (one for each subsystem) developed in subsection 4.2 were applied to the 20th order truth model of the coupled system. The singular values of the transfer function of the closed loop system are shown in Fig. 4-5, and the closed loop eigenvalues of the resulting 32nd order system are:

$$\begin{array}{ll}
 \begin{array}{l} -9.38 \pm 9.48j \\ -5.80 \pm 5.88j \end{array} \left. \vphantom{\begin{array}{l} -9.38 \pm 9.48j \\ -5.80 \pm 5.88j \end{array}} \right\} & \text{subsystem 1 filter} \\
 \begin{array}{l} -9.38 \pm 9.48j \\ -5.80 \pm 5.88j \end{array} \left. \vphantom{\begin{array}{l} -9.38 \pm 9.48j \\ -5.80 \pm 5.88j \end{array}} \right\} & \text{subsystem 2 filter} \\
 \begin{array}{l} -.03 \pm 4.76j \\ -.05 \pm 4.54j \end{array} \left. \vphantom{\begin{array}{l} -.03 \pm 4.76j \\ -.05 \pm 4.54j \end{array}} \right\} & \text{subsystem 1 unmodeled} \\
 & \text{dynamics} \\
 \begin{array}{l} -.03 \pm 4.76j \\ -.05 \pm 4.54j \end{array} \left. \vphantom{\begin{array}{l} -.03 \pm 4.76j \\ -.05 \pm 4.54j \end{array}} \right\} & \text{subsystem 2 unmodeled} \\
 & \text{dynamics} \\
 -.03 \pm 4.26 \left. \vphantom{-.03 \pm 4.26} \right\} & \text{coupling dynamics} \qquad (4-36) \\
 \\
 \begin{array}{l} -.226 \pm 1.46j \\ -.167 \pm .953j \end{array} \left. \vphantom{\begin{array}{l} -.226 \pm 1.46j \\ -.167 \pm .953j \end{array}} \right\} & \text{subsystem 1 modes} \\
 \begin{array}{l} -.225 \pm 1.46j \\ -.166 \pm .953j \end{array} \left. \vphantom{\begin{array}{l} -.225 \pm 1.46j \\ -.166 \pm .953j \end{array}} \right\} & \text{subsystem 2 modes} \\
 -.0083 \pm .115j \left. \vphantom{-.0083 \pm .115j} \right\} & \text{coupling mode} \\
 \begin{array}{l} -.272 \\ -.228 \end{array} \left. \vphantom{\begin{array}{l} -.272 \\ -.228 \end{array}} \right\} & \text{subsystem 1} \\
 & \text{integrators} \\
 \begin{array}{l} -.272 \\ -.228 \end{array} \left. \vphantom{\begin{array}{l} -.272 \\ -.228 \end{array}} \right\} & \text{subsystem 2} \\
 & \text{integrators}
 \end{array}$$

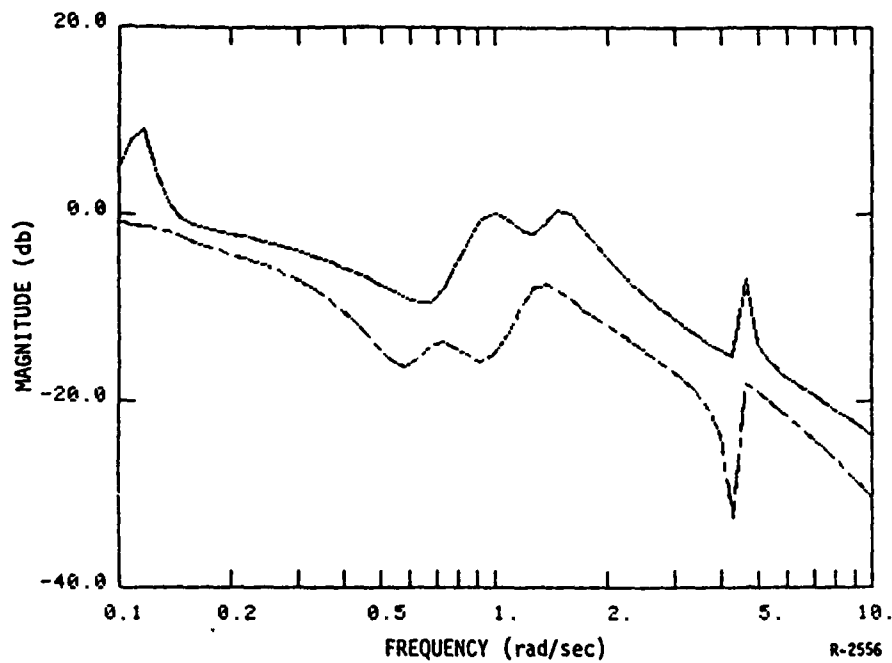


Figure 4-5. Singular Values of the Closed Loop Interconnected Truth System

The qualitative and quantitative features of Fig. 4-5 and the closed loop eigenvalues (4-36) illustrate the validity of a priori analysis of Section 3 and the resulting design specifications (4-1)-(4-3). The closed loop system is stable, although only marginally as a consequence of the deliberate attempt to push the design specifications. The higher frequency unmodeled dynamics produce a small gain margin at approximately 4 radians/second. The low frequency oscillation between the subsystems has a natural frequency of .11 radians/second as compared to the predicted value of .1 radians/second from subsection 3.2. Also, the peak magnitude of the transfer function due to this mode is about 9db, which is precisely the prediction of subsection 3.5.

4.4 SECOND LEVEL CONTROL PROBLEM

The asymptotic analysis of Appendices A and B indicate that the second level control problem can be approximated by a system of two masses (each with an equivalent value of the total mass of one subsystem) connected by a beam with a longitudinal wave velocity of c_2 . For the system described in Section 2 (Eq. 2-16), a 2 element finite element approximation yields a system with an oscillatory mode of approximately .15 radians/second. This figure agrees nicely with the observed mode from subsection 4.4. However, an analysis of the zeroes of the truth system and decentralized controller from the second level input to the second level output indicates a non minimum phase zero pair at

$$.049 \pm .63j$$

This zero pair is a manifestation of the fact that the low frequency approximation that results from Appendices A and B are only valid for a limited frequency range. The pair limits the ability to extend the bandwidth of the closed loop system without more extensive modeling of the overall system.

In recognition of this limitation a simple low gain controller was designed to slightly increase the damping ratio of the lightly damped low frequency coupling mode. The controller consists of a simple lead-lag filter with a lead break at .1 radians/second and a lag break at 1 radian/second. The magnitude of the return difference of the second level closed loop system is shown in Fig. 4-6, and indicates a 30 db reduction in sensitivity at .11 radians/second. The magnitude of the transfer function of the second level closed loop system is shown in Fig. 4-7. This figure illustrates the reduction in the peak of the coupling mode. The closed loop eigenvalues corresponding to this coupling mode are:

$$-.063 \pm .318j$$

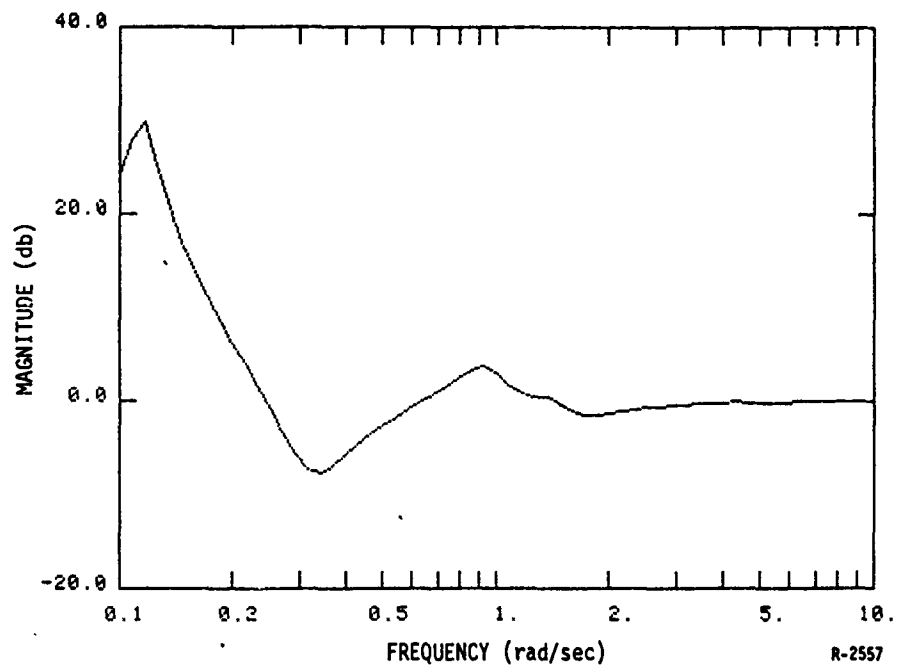


Figure 4-6. Magnitude of the Second Level Control System Return Difference

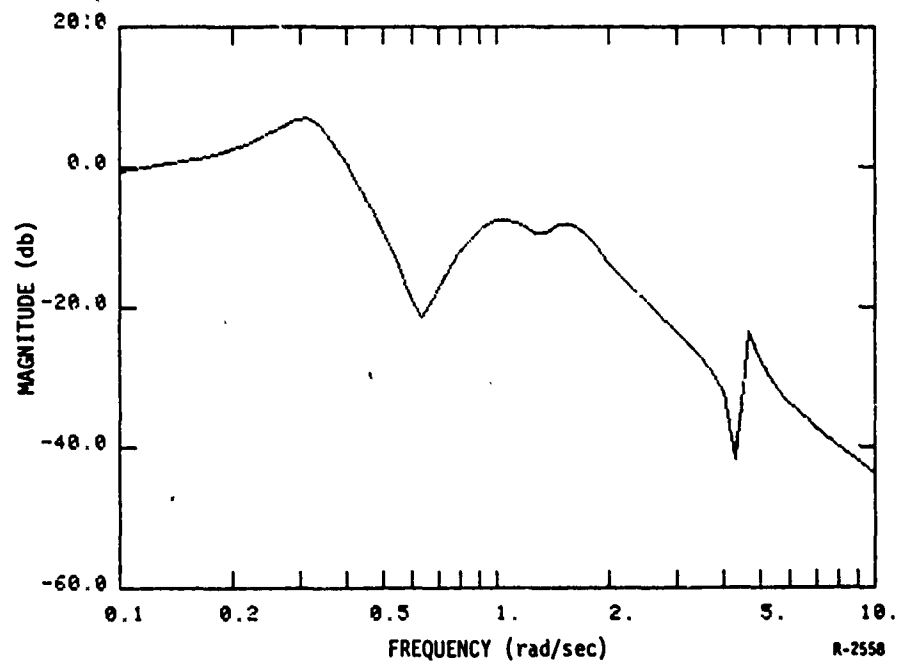


Figure 4-7. Magnitude of the Second Level Transfer Function

SECTION 5

SUMMARY

This report has initiated a study of the problem of robust decentralized control system design for large space structures that will be assembled sequentially. The salient features of this problem are the general system characteristics of a LSS, the requirement that the control system be completely decentralized, and the requirement that the decentralized control system must stabilize the total structure as well as a partially assembled structure.

All of the relatively few studies of robust decentralized control have concentrated on theoretical studies of generic decentralized systems, with only mild assumptions about the structure of the underlying system. While such results are important (and have been used in this report), they can be conservative when a problem possesses more specific system structures. The research presented in this report has identified and used system and error structures that will be generically present in the problem of decentralized control system design for sequentially assembled large space structure. The system structural analysis was conducted qualitatively using the infinite dimensional singular perturbation analysis of the Appendices and [8]-[9]. The system structures were evaluated for their ability to support a completely decentralized control architecture and one such structure was chosen for detailed analysis and design.

The conceptual methodology for robust decentralized design that was proposed in this report requires the identification of all significant error sources and performance measures, the quantification of the possible detrimental effects of the errors on the decentralized design, and the decentralized synthesis of a control system that minimizes the detrimental effects. These dominant error sources were identified: unstructured modeling error, subsystem modeling error induced by the interconnection of the subsystems, and the neglected interconnection dynamics. Appropriate analysis tools were identified or developed for each error source. Both the unstructured error and neglected interconnection dynamics were quantified using existing results. The subsystem errors induced by the interconnection were sufficiently large that the structure of the error had to be exploited. This structure was identified and a new robustness analysis technique was developed to produce a less conservative quantification. The three separate analyses were then combined using the integration theorem that was derived in Section 3.

These analysis procedures were applied to a specific example. The analysis results were used to specify design constraints for the decentralized synthesis problems. A decentralized design was then developed with the specific objective of testing the ability of the analysis results to predict the properties of the true closed loop system. The properties predicted by each of the individual analyses and the integrated analysis were accurate.

Several extensions to this work should be pursued. First, the design methodology and analysis tools have only been applied to a single, simplified problem. A more complete problem which incorporates more realistic models, error sources, and control objectives should be addressed. Secondly, only the completely decentralized control architecture has been studied in this report.

As noted in Section 2, this architecture requires a specific system structure. Other control architectures, such as a partially overlapping control system, may be useful for other system structures and for relatively homogeneous systems. The issues raised by the interaction of such system structures and control architectures need to be examined. Finally, the possibility of using hierarchical designs for enhancing the control system performance following the subsystem assembly is promising and warrants further study.

REFERENCES

1. W.H. Bennett and J.S. Baras, "Block Diagonal Dominance and Design of Decentralized Compensators," Proceedings Large Scale Systems: Theory and Applications, Toulouse, France, June 1980, pp. 93-102.
2. Y.S. Hung and D.J.N. Limebeer, "Robust Stability of Additively Perturbed Interconnected Systems," IEEE Trans. A.C., Vol. AC-29, No. 12, pp. 1069-1075, December 1984.
3. G. Zames and D. Bensoussan, "Multivariable Feedback, Sensitivity, and Decentralized Control," IEEE Trans. A.C., AC-28 No. 11, November 1983, pp. 1030-1035.
4. D.P. Looze and J.S. Freudenberg, "Analysis of Global Feedback Properties in Large Scale Systems," Topical Report, U.S. Department of Energy, Contract DE-AC01-81RA50658, September 1983.
5. J.S. Freudenberg, D.P. Looze, and J.B. Cruz, Jr., "Conditions for Simultaneous Achievement of Local and Global Feedback Objectives with Multiple Controllers," 21st IEEE Conference on Decision and Control, pp. 611-615, Orlando, FL, December 1982.
6. N.R. Sandell, Jr., "Robust Stability of Linear Dynamic Systems with Application to Singular Perturbation Theory", Automatica, Vol. 15, No. 4, July 1979, pp. 467-470.
7. K. Haiges, "Multivariable Flight Control with Time-Scale Separation," S.M. Thesis, MIT, Cambridge, MA, May 1984.
8. Lions, J.L., Perturbations Singulieres dans les Problemes aux Limites et en Controle Optimal, Springer-Verlag, New York, 1973.
9. P.P.N. de Croer, "Singular Perturbations of Spectra," in Asymptotic Analysis, F. Verhulst (ed.), Lecture Notes in Mathematics, Springer-Verlag, New York, 1979.
10. W.S. Levine and M. Athans, "On the Optimal Error Regulation of a String of Moving Vehicles," IEEE Trans. Automat. Contr., Vol. AC-11, pp. 355-361, July 1966.
11. L. Isaksen and H.J. Payne, "Suboptimal Control of Linear Systems by Augmentation with Application to Freeway Traffic Regulation," IEEE Trans. A.C., AC-18, No. 3, June 1973, pp. 210-219.

12. J.C. Doyle and G. Stein, "Multivariable Feedback Design: Concepts for Classical/Modern Synthesis", IEEE Trans. on Auto. Control, Vol. AC-26, No. 1, February 1981, pp. 4-16.
13. G. Stein and M. Athans, "The LQG/LTR Procedure for Multivariable Feedback Control Design," IEEE Trans. A.C., (to appear; also paper LIDS-P-1384, Laboratory for Information and Decision Systems, M.I.T., Cambridge, MA).
14. Lehtomaki, N.A., N.R. Sandell, Jr., and M. Athans, "Robustness Results in Linear-Quadratic Gaussian Based Multivariable Control Designs," IEEE Trans. A.C., Vol. AC-26, No. 1, pp. 75-92, February 1981.
15. Desoer, C.A., and Y.-T. Wang, "On the Generalized Nyquist Stability Criterion," IEEE Trans. A.C., Vol. AC-25, No. 2, pp. 187-196, April 1980.
16. Postlethwaite, I., J.M. Edmunds, and A.G.J. MacFarlane, "Principal Gains and Principal Phases in the Analysis of Linear Multivariable Feedback Systems," IEEE Trans. A.C., Vol. AC-26, No. 1, pp. 32-46, February 1981.
17. D.P. Looze and J.S. Freudenberg, "On the Relation of Open Loop to Closed Loop Properties in Multivariable Feedback Systems," 1983 American Control Conference, San Francisco, CA, June 1983.
18. J.S. Freudenberg, Ph.D. Thesis, University of Illinois, February 1985.
19. Zames G., "On the Input-Output Stability of Time-Varying Nonlinear Feedback Systems - Part I: Conditions Using Concepts of Loop Gain, Conicity and Positivity," IEEE Trans. A.C., Vol. AC-11, pp. 228-238, 1966.
20. Sandberg, I.W., "A Frequency-Domain Condition for the Stability of Feedback Systems Containing a Single Time-Varying Nonlinear Element," Bell System Tech. J., Vol. 43, pp. 1601-1608, 1964.
21. Safonov, M.G., and M. Athans, "A Multiloop Generalization of the Circle Criterion for Stability Margin Analysis," IEEE Trans. A.C., Vol AC-26, pp. 415-422, 1981.
22. Doyle, J.C., "Analysis of Feedback Systems with Structural Uncertainties," Proc. IEEE, November 1982.
23. Doyle, J.C., J.E. Wall, and G. Stein, "Performance and Robustness Analysis for Structural Uncertainty," Proc. 21st IEEE Conf. on Dec. and Control, Orlando, FL, pp. 629-636, 1982.
24. Sandell, N.R., Jr., P. Varaiya, M. Athans, and M.G. Safonov, "Survey of Decentralized Control Methods for Large Scale Systems," IEEE Trans. A.C., Vol. AC-23, pp. 108-128, 1978.

25. Feingold, D.G., and R.S. Varga, "Block Diagonally Dominant Matrices and Generalizations of the Gerschgorin Circle Theorems," Pac. J. Math., Vol 12, pp. 1241-1250, 1962.
26. H. Kwakernaak and R. Sivan, Linear Optimal Control Systems, Wiley-Interscience, 1972.

APPENDIX A

TP-220

SPECTRAL ANALYSIS OF A CLASS OF
STIFF OPERATORS

By:

Hassan Salhi
Douglas P. Looze

May 1985

ALPHATECH, Inc.
2 Burlington Executive Center
111 Middlesex Turnpike
Burlington, MA 01803
617-273-3388

*This work was supported at the University of Illinois by the Joint Services Electronics Program under Contract N00014-79-C-0424, and at ALPHATECH by Contract No. F33615-84-C-3618.

ABSTRACT

This paper examines the spectral decomposition of a class of operators that depend on a small parameter ϵ . The convergence of the eigenvalue-eigenvector pairs as $\epsilon \rightarrow 0$ of these "stiff" operators, using the terminology of [7]*, is investigated with the objective of shedding light on the singular behavior.

*References are indicated by numbers in square brackets, the list appears at the end of this Appendix.

SECTION 1

INTRODUCTION

This paper considers the eigenvalue problem of the so-called "stiff" operators using the terminology of [7]. Their dependence on a small parameter ϵ suggests some spectral "separation". This last intuitive idea is fully investigated in the sequel.

Many physical problems can be described by models containing stiff operators. Examples of such problems in distributed parameter systems are numerous. Without being exhaustive, the examples include the following:

1. Interfaced media having very different properties from one region to another, such as diffusivity in heat conduction or permittivity in electromagnetic wave propagation [3].
2. Continuous stochastic problems when the noise intensity level is different from one part to another of a medium [2].

There are several motivations for studying the present eigenvalue problem. First, the "singular" behavior of stiff operators can be better understood by investigating their spectral decomposition as a function of ϵ . Second, it is well-known that the solution of a boundary value problem can be expanded, at least theoretically, in infinite series of the eigenvectors. The presence of a small parameter may be advantageous because the aforementioned solution may also be expanded in fractional powers of ϵ , depending on its convergence as $\epsilon \rightarrow 0$. Therefore, it is important to analyze the convergence as $\epsilon \rightarrow 0$ of the eigenvalue-eigenvector pairs of stiff operators.

The eigenvalue problems involving several perturbed operators has been studied in the literature [4]-[6], [8] and the references therein. However, the spectral analysis of stiff operators seems to be new. In the sequel, a general formulation of the eigenvalue problem of stiff operators is presented, using bilinear forms to avoid cumbersome and complex boundary and interface conditions. The properties of the eigenvalue-eigenvector pairs as functions of ϵ are analyzed.

This paper is organized as follows. The eigenvalue problem formulation of a class of stiff operators involving two bilinear forms is presented in Section 2. In Section 3, the convergence of the eigenvalues and their corresponding eigenvectors as $\epsilon \rightarrow 0$ is investigated. In Section 4, a numerical analysis of the operator of Example 3-2 is undertaken to illustrate some of the properties discussed in Section 3. Finally, the last section contains some concluding remarks.

SECTION 2

EIGENVALUE PROBLEM FORMULATION

In this section, the eigenvalue problem of class of stiff operators is formulated. Let V, H be two given real Hilbert spaces such that V is dense in H and

A1) the injection of V into H is compact.

Let V^* denote the dual space of V . After identifying H with H^* , one has

A2) $V \subset H \subset V^*$.

Let $a_i(\phi, \psi)$, $i = 0, 1$ be two forms on V such that the following assumptions hold:

A3) $a_1(\phi, \psi)$ is bilinear, symmetric on V

A4) $a_1(\phi, \psi)$ is continuous on V , i.e., there exists β_1 such that

$$a_1(\phi, \psi) \leq \beta_1 \|\phi\|_V \|\psi\|_V, \quad \forall \phi \in V, \quad \forall \psi \in V$$

A5) $a_1(\phi, \phi) \geq a_1 p_1(\phi)^2$, where $a_1 > 0$ and $p_1(\cdot)$ is a continuous semi-norm on V

A6) $p_0(\phi) + p_1(\phi)$ is a norm equivalent to $\|\phi\|_V$

A7) $a_1(\phi, \phi) = 0$ on $V_i \subset V$, where V_i is an infinite-dimensional subspace of V , $i=0, 1$.

A8) If $\psi \mapsto L_0(\psi)$ is a continuous linear form on V , null on V_0 , there exists $\phi \in V$ (modulo V_0) such that

$$a_0(\phi, \psi) = L_0(\psi), \quad \forall \psi \in V$$

Let $a_\varepsilon(\phi, \psi)$, $a(\phi, \psi)$ be defined as

$$a_\varepsilon(\phi, \psi) = a_0(\phi, \psi) + \varepsilon a_1(\phi, \psi) \quad (2-1)$$

$$a(\phi, \psi) = a_0(\phi, \psi) + a_1(\phi, \psi) \quad (2-2)$$

Now some important remarks clarifying the above assumptions and definitions are in order:

Remark 2.1:

It can be easily seen from (A3-A6) that $a_\varepsilon(\phi, \psi)$, $a(\phi, \psi)$ are bilinear, symmetric, coercive and bounded on V . In particular, for sufficiently small ε , they satisfy

$$\alpha \|\phi\|_V^2 < a_\varepsilon(\phi, \phi) < \nu \|\phi\|_V^2, \quad \forall \phi \in V \quad (2-3)$$

$$\alpha \|\phi\|_V^2 < a(\phi, \phi) < \nu \|\phi\|_V^2, \quad \forall \phi \in V$$

where α (resp. ν) is independent of ε and depends solely on α_0 , α_1 (resp. ν_0 , ν_1) and the semi-norms $p_i(\cdot)$, $i = 0, 1$.

Remark 2.2:

The bilinear forms $a_\varepsilon(\phi, \psi)$, $a(\phi, \psi)$ define selfadjoint operators [1]

$$A_\varepsilon, A \in \mathcal{L}(V; V^*),$$

i.e.,

$$a_\varepsilon(\phi, \psi) = (A_\varepsilon \phi, \psi), \quad \forall \phi, \psi \in V$$

$$a(\phi, \psi) = (A \phi, \psi), \quad \forall \phi, \psi \in V$$

where (\cdot, \cdot) denotes the duality pairing between V and its dual V^* . From the preceding remarks, one concludes that the spectra of A_ε , A are subsets of \mathbb{R}^+ ,

consisting only of the point spectrum [1], [5], [12]. The eigenvalue problem for A_ϵ is, then, to seek $\{\gamma_\epsilon^k, \chi_\epsilon^k\} \in \mathbb{R}^+ \times V$ such that

$$A_\epsilon \chi_\epsilon^k = \gamma_\epsilon^k \chi_\epsilon^k \quad . \quad (2-4)$$

The equivalent variational formulation is

$$a_\epsilon(\chi_\epsilon^k, \phi) = \gamma_\epsilon^k (\chi_\epsilon^k, \phi) \quad \forall \phi \in V \quad (2-5)$$

Now, some well-known facts are summarized in:

Proposition 2.1:

If (A1-A6) hold, then there exist unique sequences $\{\gamma_\epsilon^k\}_{k=1}^\infty \in \mathbb{R}^+$, $\{\chi_\epsilon^k\}_{k=1}^\infty \in V$ such that (2-4) (or, equivalently, (2-5)) is satisfied.

Furthermore,

$$1) \quad 0 < \gamma_\epsilon^1 < \gamma_\epsilon^2 < \dots, \quad \lim_{k \rightarrow +\infty} \gamma_\epsilon^k = +\infty$$

$$2) \quad \{\chi_\epsilon^k\}_{k=1}^\infty \text{ is a complete orthonormal set in } H, \text{ i.e., in particular}$$

$$(\chi_\epsilon^k, \chi_\epsilon^\ell) = \delta^{k\ell} \quad (\text{Kronecker delta})$$

$$3) \quad \text{The multiplicity of each eigenvalue is finite}$$

$$4) \quad \text{The eigenvalues satisfy the following minimax formula:}$$

$$\gamma_\epsilon^k = \min_{W \subset V, \dim W = k} \max_{\substack{X \in V, \|X\|_H = 1}} a_\epsilon(X, X) \quad (2-6)$$

Proof: See [1], [5], [12]

Remark 2.3:

It is noteworthy to mention that Prop. 2.1 is valid for any positive value of ϵ , e.g., $\epsilon=1$. In this case, the eigenvalue-eigenvector pair of A is obtained.

SECTION 3

SPECTRAL ANALYSIS OF THE OPERATOR A_ϵ

This section starts with a series of lemmas which characterize the various properties of the spectrum of A_ϵ . Then the convergence of the eigenvalues and their corresponding eigenvectors as $\epsilon \rightarrow 0$ is stated and proved in Theorem 3.1. Some typical examples are given at the end of this section to illustrate the ideas advanced in the course of the present analysis.

One way to gather information about the behavior of a single eigenvalue as $\epsilon \rightarrow 0$, is to bound it from below and from above by known functions of ϵ . This task is accomplished in:

Lemma 3.1:

For sufficiently small positive ϵ , the following estimate holds:

$$\epsilon \gamma^k \leq \gamma_\epsilon^k \leq \gamma^k \quad (3-1)$$

for $k = 1, 2, \dots$, where $\{\gamma^k\}_{k=1}^\infty$ are the eigenvalues of the operator A , i.e., they satisfy

$$a_0(\rho^k, \phi) + a_1(\rho^k, \phi) = \gamma^k(\rho^k, \phi), \quad \forall \phi \in V$$

Proof: For sufficiently small ϵ , one has

$$\epsilon a(\phi, \phi) \leq a_\epsilon(\phi, \phi) \leq a(\phi, \phi), \quad \forall \phi \in V \quad (3-2)$$

Using the minimax characterization of eigenvalues (2-6), one readily deduces (3-1) from (3-2).

Now an upper bound for the eigenvector norm in V is derived:

Lemma 3.2:

If χ_{ϵ}^k is any normalized eigenvector of A_{ϵ} , corresponding to γ_{ϵ}^k , i.e., $\|\chi_{\epsilon}^k\|_H = 1$, then

$$\alpha \epsilon \|\chi_{\epsilon}^k\|_V^2 < \gamma_{\epsilon}^k < \gamma^k \quad (3-3)$$

for $k = 1, 2, \dots$.

Proof: For each k , the sequence γ_{ϵ}^k is bounded by Lemma 3.1. Let $\phi = \chi_{\epsilon}^k$ in (2.5) to get

$$\begin{aligned} a_{\epsilon}(\chi_{\epsilon}^k, \chi_{\epsilon}^k) &= \gamma_{\epsilon}^k(\chi_{\epsilon}^k, \chi_{\epsilon}^k) \\ &= \gamma_{\epsilon}^k < \gamma^k \end{aligned}$$

Now one easily gets (3-3) by using (2-3).

At this point, the tools necessary for finding the limits of the eigenvalues are available.

Lemma 3.3:

The sequence $\{\gamma_{\epsilon}^k\}_{k=1}^{\infty}$ is decomposable into two subsequences $\{\gamma_{\epsilon}^k\}_{k=1}^{\infty}$, $\{\mu_{\epsilon}^k\}_{k=1}^{\infty}$ such that, for each k ,

$$\lim_{\epsilon \rightarrow 0} \lambda_{\epsilon}^k = 0 \quad (3-4)$$

$$\lim_{\epsilon \rightarrow 0} \mu_{\epsilon}^k = \mu_0^k > 0 \quad (3-5)$$

$k = 1, 2, \dots$.

Proof: The following three-step contradiction argument is used to ascertain the above lemma.

1) Suppose $\lim_{\epsilon \rightarrow 0} \gamma_{\epsilon}^k = 0$, $k = 1, 2, \dots$. Let $V = V_0 \oplus V_0^{\perp}$, where the orthogonality is that of V . Take $v \in V_0^{\perp}$ and write it as

$$v = \sum_{k=1}^{\infty} (v, \chi_{\epsilon}^k) \chi_{\epsilon}^k \quad (3-6)$$

with this choice of v , the following inequality holds:

$$a_{\epsilon}(v, v) = a_0(v, v) + \epsilon a_1(v, v) > C \quad (3-7)$$

for some strictly positive constant C , which is independent of ϵ .

Using (3-6), $a_{\epsilon}(v, v) = \sum_{k=1}^{\infty} \gamma_{\epsilon}^k (v, \chi_{\epsilon}^k)^2$, which converges to zero as $\epsilon \rightarrow 0$, contradicting (3-7).

2) Suppose $\lim_{\epsilon \rightarrow 0} \gamma_{\epsilon}^k = \gamma^k > 0$, $k = 1, 2, \dots$. Select $v \in V_0$ and write it as in (3-6). It is clear that the following inequality holds:

$$a_{\epsilon}(v, v) = \sum_{k=1}^{\infty} \gamma_{\epsilon}^k (v, \chi_{\epsilon}^k)^2 > C \quad (3-8)$$

for some strictly positive constant C , which is independent of ϵ . However $a_{\epsilon}(v, v) = \epsilon a_1(v, v)$, which converges to zero as $\epsilon \rightarrow 0$, contradicting (3-8).

3) Suppose $\lim_{\epsilon \rightarrow 0} \gamma_{\epsilon}^k = 0$, for $k = 1, 2, \dots, \ell$, without loss of generality.

Let

$$V_{\ell} = \text{span}\{\chi_{\epsilon}^1, \chi_{\epsilon}^2, \dots, \chi_{\epsilon}^{\ell}\}.$$

Select $v \in V_0^{\perp} \cap V_{\ell}^{\perp}$ and repeat step 2, to conclude that V_{ℓ} is infinite dimensional, unless V_0 is degenerate (i.e., finite-dimensional). An identical argument can be advanced to contradict the possibility that (3-5) is true for $k=1, 2, \dots, \ell$ (ℓ finite).

Now decompose $\{\gamma_{\epsilon}^k, \chi_{\epsilon}^k\}_{k=1}^{\infty}$ into $\{\lambda^k, \phi^k\}_{k=1}^{\infty}$ if $\lim_{\epsilon} \gamma_{\epsilon}^k = 0$ and into $\{\mu^k, \psi^k\}_{k=1}^{\infty}$, otherwise.

Some attention must be focused on how λ_{ϵ}^k converges to zero, $k = 1, 2, \dots$.

Lemma 3.4

The sequence λ_{ϵ}^k converges to zero with a linear rate λ_1^k , i.e.,

$$\lambda_{\epsilon}^k = \lambda_1^k \epsilon + o(\epsilon), \quad k = 1, 2, \dots$$

Proof: By Lemma 3.1, one may assume, without loss of generality, that

$$\lambda_{\epsilon}^k = \lambda_1^k \epsilon^{\nu} + o(\epsilon) \quad (3-9)$$

with $\nu \in (0, 1)$. In order to complete the proof, it suffices to show that $\nu=1$.

If ϕ_{ϵ}^k is a normalized eigenvector, i.e., $(\phi_{\epsilon}^k, \phi_{\epsilon}^k)_H = 1$, corresponding to λ_{ϵ}^k , then

$$\lambda_{\epsilon}^k = a_0(\phi_{\epsilon}^k, \phi_{\epsilon}^k) + \epsilon a_1(\phi_{\epsilon}^k, \phi_{\epsilon}^k) \quad (3-10)$$

from which one observes that

$$a_0(\phi_{\epsilon}^k, \phi_{\epsilon}^k) < O(\epsilon^{\nu}) \quad (3-11)$$

Therefore, $a_0(\phi_{\epsilon}^k, \phi_{\epsilon}^k) \rightarrow 0$ as $\epsilon \rightarrow 0$, which implies

$$p_0(\phi_{\epsilon}^k) \rightarrow 0, \text{ as } \epsilon \rightarrow 0$$

by (A5). Using (A6), one has

$$p_1(\phi_{\epsilon}^k) > C \quad (3-12)$$

for some strictly positive constant C , which is independent of ϵ .

Suppose that $\nu < 1$. Then, from (3-9)-(3-12) one concludes that

$$\begin{aligned}\lambda_{\varepsilon}^k &= \lambda_l^k \varepsilon^{\nu} + o(\varepsilon) \\ &= a_0(\phi_{\varepsilon}^k, \phi_{\varepsilon}^k) + o(\varepsilon)\end{aligned}\quad (3-13)$$

From this, there exists an element of V , $\phi_{\varepsilon}^{-k} = \frac{\phi_{\varepsilon}^k}{\varepsilon^{\nu/2}}$ such that

$$\lambda_l^k = a_0(\phi_{\varepsilon}^{-k}, \phi_{\varepsilon}^{-k}) + o(\varepsilon^{1-\nu}) .$$

However, such a claim is false because

$$(\phi_{\varepsilon}^{-k}, \phi_{\varepsilon}^{-k})_H = \frac{1}{\varepsilon^{\nu}} \rightarrow +\infty \text{ as } \varepsilon \rightarrow 0.$$

Since the injection of V into H is continuous, $\|\phi_{\varepsilon}^{-k}\|_V \rightarrow +\infty$ as $\varepsilon \rightarrow 0$. In conclusion, there is no element of V such that (3-12) is satisfied.

Remark 3.1:

For $\nu < 1$, the major contribution to λ_{ε}^k is supplied from V_0^1 (c.f. (3-13)), but the norm of the contribution is concentrated on V_0 (c.f. (3-12)), which is the paradox.

Hereafter, the focus will be on the asymptotic behavior of the eigenvectors. The following lemma summarizes the norm bounds of the eigenvectors:

Lemma 3.5:

Let $\{\lambda_{\varepsilon}^k, \phi_{\varepsilon}^k\}_{k=1}^{\infty}$, $\{\mu_{\varepsilon}^k, \psi_{\varepsilon}^k\}_{k=1}^{\infty}$ be as in the proof of Lemma 3.3, with the eigenvectors normalized in H . Then, for sufficiently small ε , the following estimates hold:

$$1) \quad \|\phi_{\varepsilon}^k\|_V \leq C_1 \quad (3-14)$$

$$2) \sqrt{\epsilon} \|\psi_{\epsilon}^k\|_V < C_2 \quad (3-15)$$

$$k = 1, 2, \dots$$

where C_1, C_2 denote constant independent of ϵ .

Proof: Use Lemmas 3.2-3.4.

The forthcoming theorem is the main result of this section. It states the convergence of the eigenvalues and their corresponding eigenvectors as $\epsilon \rightarrow 0$.

Theorem 3.1

Let $\{\gamma_{\epsilon}^k\}_{k=1}^{\infty}$ be the eigenvalues of A_{ϵ} and $\{\chi_{\epsilon}^k\}_{k=1}^{\infty}$ the corresponding normalized system of eigenvectors. Then, given a sequence of ϵ converging to zero, $\{\gamma_{\epsilon}^k, \chi_{\epsilon}^k\}_{k=1}^{\infty}$ can be decomposed into two subsequences $\{\lambda_{\epsilon}^k, \phi_{\epsilon}^k\}_{k=1}^{\infty}$ and $\{\mu_{\epsilon}^k, \psi_{\epsilon}^k\}_{k=1}^{\infty}$ which have the following asymptotic properties, for each k :

$$1) \lambda_{\epsilon}^k \rightarrow 0 \text{ linearly in } \epsilon, \phi_{\epsilon}^k \rightarrow \phi^k \text{ weakly in } V$$

$$2) \mu_{\epsilon}^k \rightarrow \mu_0^k > 0, \psi_{\epsilon}^k \rightarrow \psi^k \text{ weakly in } H$$

where $\{\phi^k\}_{k=1}^{\infty}$ and $\{\psi^k\}_{k=1}^{\infty}$ satisfy

$$a_1(\phi^k, \chi) = \lambda_1^k(\phi^k, \chi), \phi^k \in V_0 \subset V, \quad \forall \chi \in V_0 \quad (3-16)$$

$$a_0(\psi^k, \chi) = \mu_0^k(\psi^k, \chi), \psi^k \in H_1 \subset H, \quad \forall \chi \in V. \quad (3-17)$$

Proof: Using the fact that $\|\phi_{\epsilon}^k\|_H = 1$, and the estimates (3-11), (3-14), one concludes, that, given a sequence of ϵ converging to zero, $\phi_{\epsilon}^k \rightarrow \phi^k$ weakly in V

(hence strongly in H by compactness). From (3-11), it results that $\phi^k \in V_0$. By Lemma 3.4, λ_ϵ^k is asymptotically equal to λ_1^k . Hence (2-5) degenerates into (3-16) in the limit. Now,

$$\mu_\epsilon^k = a_0(\psi_\epsilon^k, \psi_\epsilon^k) + \epsilon a_1(\psi_\epsilon^k, \psi_\epsilon^k) \quad (3-18)$$

for ψ_ϵ^k normalized to 1 in H . Since μ_ϵ^k is $O(1)$, using (3-18) and the minimax characterization of eigenvalues, i.e., (2.6), it results that $a_0(\psi_\epsilon^k, \psi_\epsilon^k)$ is $O(1)$ and $a_1(\psi_\epsilon^k, \psi_\epsilon^k)$ is $O(\frac{1}{\epsilon})$ or equivalently

$$p_0(\psi_\epsilon^k) = O(1) \quad (3-19)$$

$$p_1(\psi_\epsilon^k) = O(\frac{1}{\sqrt{\epsilon}}). \quad (3-20)$$

Hence, the estimate (3-15) is right. Therefore

$$\|\psi_\epsilon^k\|_V \rightarrow +\infty \quad \epsilon \rightarrow 0. \quad (3-21)$$

Note that ψ_ϵ^k also satisfies

$$a_0(\psi_\epsilon^k, \chi) + \epsilon a_1(\psi_\epsilon^k, \chi) = \mu_\epsilon^k(\psi_\epsilon^k, \chi), \quad \forall \chi \in V. \quad (3-22)$$

From (3-19)-(3-20), one deduces that $a_0(\psi_\epsilon^k, \chi)$ is bounded as $\epsilon \rightarrow 0$ and $a_1(\psi_\epsilon^k, \chi)$ is $O(\frac{1}{\sqrt{\epsilon}})$. Since $\|\psi_\epsilon^k\|_H = 1$, taking formally the limit as $\epsilon \rightarrow 0$ in (3-22) yields:

$$a_0(\psi^k, \chi) = \mu_0^k(\psi^k, \chi), \quad \forall \chi \in V \quad (3-23)$$

where $\psi^k \in H_1$ (a subspace of H).

Now consider the following boundary value problem

$$a_0(v_\epsilon^k, \chi) + \epsilon a_1(v_\epsilon^k, \chi) = \mu_0^k(\psi^k, \chi), \quad \forall \chi \in V$$

which admits a unique solution $v_\epsilon^k \in V$ for positive values of ϵ . As $\epsilon \rightarrow 0$,

$v_\epsilon^k \rightarrow \psi^k$ strongly in H .

Let $w_\epsilon^k = \psi_\epsilon^k - v_\epsilon^k$, which satisfies

$$a_0(w_\epsilon^k, \chi) + \epsilon a_1(w_\epsilon^k, \chi) = \mu_\epsilon^k(\psi_\epsilon^k - \psi^k, \chi)$$

$$+ (\mu_\epsilon^k - \mu_0^k)(\psi^k, \chi), \quad \forall \chi \in V.$$

The left-hand side of this equation goes to zero as $\epsilon \rightarrow 0$, implying

$$(\psi_\epsilon^k - \psi^k, \chi) \rightarrow 0 \text{ as } \epsilon \rightarrow 0.$$

Therefore

$$\psi_\epsilon^k \rightarrow \psi^k \text{ weakly in } H.$$

The results of Theorem 3.1 hold for negative powers of ϵ as well. To illustrate this claim, let

$$b_\epsilon(\phi, \chi) = \frac{1}{\epsilon} b_{-1}(\phi, \chi) + b_0(\phi, \psi)$$

where $b_i(\phi, \chi)$, $i=-1, 0$ satisfy (A3-A7). Then, one has:

Corollary 3.1

Let $\{\nu^k\}_{k=1}^\infty$ be the eigenvalues and $\{\chi^k\}_{k=1}^\infty$ the corresponding normalized eigenvectors, derived from

$$b_\epsilon(\chi_\epsilon^k, \phi) = \nu_\epsilon^k(\chi_\epsilon^k, \phi), \quad \forall \phi \in V$$

then, given a sequence of ε converging to zero, $\{v_{\varepsilon}^k, \chi_{\varepsilon}^k\}_{k=1}^{\infty}$ can be decomposed into $\{\lambda_{\varepsilon}^k, \phi_{\varepsilon}^k\}_{k=1}^{\infty}$ and $\{\phi_{\varepsilon}^k, \chi_{\varepsilon}^k\}_{k=1}^{\infty}$, with the following properties:

- 1) $\lambda_{\varepsilon}^k \rightarrow \lambda_0^k > 0$, $\phi_{\varepsilon}^k \rightarrow \phi$ weakly in V
- 2) $\mu_{\varepsilon}^k = \frac{\mu_{-1}^k}{\varepsilon} + o(1)$, $\chi_{\varepsilon}^k \rightarrow \chi^k$ weakly in H

where $\{\phi_{\varepsilon}^k\}_{k=1}^{\infty}$ and $\{\chi_{\varepsilon}^k\}_{k=1}^{\infty}$ satisfy

$$b_0(\phi^k, \chi) = \lambda^k(\phi^k, \chi), \quad \phi^k \in V_0, \quad \forall \chi \in V$$

$$b_{-1}(\chi^k, \chi) = \mu_{-1}^k(\phi^k, \chi), \quad \phi^k \in H_1, \quad \forall \chi \in V$$

Proof

Let $a_i(\phi, \chi) = \varepsilon b_{i-1}(\phi, \chi)$, $i=0,1$ and $\phi_{\varepsilon}^k = \varepsilon v_{\varepsilon}^k$ in Theorem 3.1 to get the desired results.

Remark 3.2:

The weak convergence in Theorem 3.1 cannot be improved in general. This will be illustrated by Example 3.2.

Remark 3.3:

A careful examination of the steps of the analysis undertaken in the present section yields the following observation: the weak limits $\{\phi^k\}_{k=1}^{\infty}$, $\{\psi^k\}_{k=1}^{\infty}$ form an orthonormal system in H . This remark is of paramount importance in approximating the solution of boundary value problems involving the operator A_{ε} .

Now some examples are given as concrete illustrations of the above abstract results. Only operators of order less than or equal to four are considered, due to their frequent usage in modeling of physical processes.

Let $\Omega = \Omega_0 \cup \Omega_1$ be a bounded set in \mathbb{R}^n with boundary $\Gamma = \Gamma_0 \cup \Gamma_1$. the manifold S denotes the interface between Ω_0 and Ω_1 , as indicated in Fig. 3-1:

Example 3.1: A second order operator

Let $H = L^2(\Omega)$, $V = H_0^1(\Omega)$

$$a_1(\phi, \psi) = \sum_{j=1}^n \int_{\Omega} \frac{\partial \phi}{\partial x_j} \frac{\partial \psi}{\partial x_j} dx, \quad i = 0, 1$$

then (2.4) becomes:

$$\left. \begin{aligned} -\Delta \chi_{\varepsilon 0}^k &= \gamma_{\varepsilon}^k \chi_{\varepsilon 0}^k \text{ on } \Omega_0 \\ -\varepsilon \Delta \chi_{\varepsilon 1}^k &= \gamma_{\varepsilon}^k \chi_{\varepsilon 1}^k \text{ on } \Omega_1 \\ \chi_{\varepsilon 0}^k|_{\Gamma_0} &= 0, \quad \chi_{\varepsilon 1}^k|_{\Gamma_1} = 0 \\ \chi_{\varepsilon 0}^k &= \chi_{\varepsilon 1}^k \\ \frac{\partial \chi_{\varepsilon 0}^k}{\partial \nu} &= \varepsilon \frac{\partial \chi_{\varepsilon 1}^k}{\partial \nu} \end{aligned} \right\} \text{ on } S \quad (3-24)$$

where: Δ stands for the Laplacian in \mathbb{R}^n .

ν is the unit normal on Γ or S , outward relative to Ω_0 .

In this example, (3-16) becomes

$$\left. \begin{aligned} \phi_0^k &= 0 \text{ on } \Omega_0 \\ -\Delta \phi_1^k &= \lambda_1^k \phi_1^k \text{ on } \Omega_1 \\ \phi_1^k|_{\Gamma_1} &= 0, \quad \phi_1^k|_S = 0 \end{aligned} \right\} \quad (3-25)$$

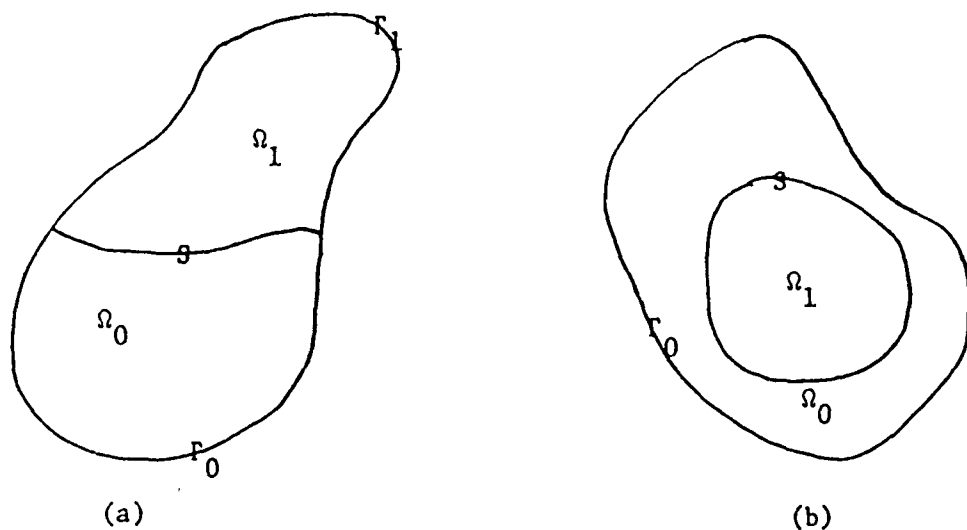


Figure 3-1. Examples of Interfaced Sets

which is a Dirichlet eigenvalue problem for the Laplacian operator in Ω_1 . The subspace V_0 of V is:

$$V_0 = \{ \chi \in V : \chi_0 = 0, \chi_1 \in H_0^1(\Omega_1) \}$$

The conclusions of Prop. 2.1 are applicable in this case. Hence $\{\phi^k\}_{k=1}^\infty$ is a complete orthonormal system in $L^2(\Omega_1)$.

Equation (3-17) becomes

$$\left. \begin{aligned} -\Delta \psi_1^k &= \mu_0^k \psi_0^k \text{ on } \Omega_0 \\ \psi_1^k &= 0 \text{ on } \Omega_1 \\ \psi_1^k|_{\Gamma_0} &= 0, \quad \frac{\partial \psi_0^k}{\partial \nu}|_S = 0 \end{aligned} \right\} \quad (3-26)$$

which is an eigenvalue problem with mixed boundary conditions for the Laplacian operator in Ω_0 . Again, the conclusions of Prop. 2.1 are applicable in this instance, provided the interface S is sufficiently smooth. Therefore, $\{\psi^k\}_{k=1}^\infty$ form an orthonormal system in $L^2(\Omega_0)$. It is noteworthy to observe that $\psi^k = 0$ because ψ^k must be orthogonal (in $L^2(\Omega)$) to ϕ^l , $l=1,2,\dots$.

The subspace H_1 of H is then

$$H_1 = \{ \chi \in H: \chi_0 \in H^1(\Omega_0; \Gamma_0), \frac{\partial \chi_0}{\partial \nu} = 0 \text{ on } S, \chi_1 = 0 \}.$$

Remark 3.4

In Example 3.1, one can consider

$$a_1(\phi, \psi) = \sum_{j=1}^n \sum_{k=1}^n \int_{\Omega_1} a_{jk}^1 \frac{\partial \phi}{\partial x_j} \frac{\partial \psi}{\partial x_k} dx, \quad i = 0, 1$$

which a_{jk}^1 satisfies

$$1) \quad a_{jk}^1 \in C^1(\overline{\Omega_1})$$

$$2) \quad a_{jk}^1 = a_{kj}^1$$

$$3) \quad \sum_{j=1}^n \sum_{k=1}^n a_{jk}^1 \zeta_j \zeta_k > \alpha_1 \sum_{k=1}^n \zeta_k^2, \quad \alpha_1 > 0, \quad \forall \zeta \in \mathbb{R}^n, \zeta \neq 0.$$

The discussion therein remains unchanged.

Example 3.2

Let $\Omega_0 = (-1, 0)$, $\Omega_1 = (0, 1)$, $S = \{0\}$, $\Gamma_0 = \{-1\}$, $\Gamma_1 = \{1\}$. Then the solutions of (3-25)-(3-26) become respectively

$$\left. \begin{aligned} \lambda_1^k &= (k\pi)^2 \\ \phi_0^k &= 0 \\ \phi_1^k &= \sqrt{2} \sin k\pi x \end{aligned} \right\}$$

$$\left. \begin{aligned} \mu_0^k &= ((2k-1) \pi/2)^2 \\ \phi_0^k &= \cos[(2k-1) \pi x/2] \\ \psi_1^k &= 0 \end{aligned} \right\}$$

The exact eigenvalues ϕ_2^k must satisfy the following transcendental equation:

$$\cos \sqrt{\gamma_\epsilon^k} \sin \sqrt{\frac{\gamma_\epsilon^k}{\epsilon}} + \sqrt{\epsilon} \sin \sqrt{\gamma_\epsilon^k} \cos \sqrt{\frac{\gamma_\epsilon^k}{\epsilon}} = 0. \quad (3-27)$$

It is not possible to solve for γ_ϵ^k as a function of ϵ . However, for some sequences of ϵ , e.g., $\epsilon = 1/(4l+1)^2$, l an integer, $\{\mu_{\epsilon l}^1, \psi_{\epsilon l}^1\}$ given below is an exact eigenvalue-eigenvector pair

$$\left. \begin{aligned} \mu_{\epsilon l}^1 &= \left(\frac{\pi}{2}\right)^2 \\ \psi_{\epsilon l}^1 &= \cos \frac{\pi}{2} x \\ \psi_{\epsilon l}^1 &= \cos \frac{\pi}{2\sqrt{\epsilon_l}} x \end{aligned} \right\} \quad (3-28)$$

Observe the oscillatory behavior of $\psi_{\epsilon l}^l$ as $l \rightarrow \infty$. This is the manifestation of its weak convergence in $(L^2(\Omega_1))$ to zero. Furthermore, this example shows that $\{\psi_{\epsilon k}^k\}_{k=1}^{\infty}$ are not analytic functions of ϵ . Consequently, the task of finding these eigenvectors (in order to solve boundary value problems) is impossible. The alternative is to use the weak limits of $\{\chi_{\epsilon k}^k\}_{k=1}^{\infty}$ and $\{\phi_{\epsilon k}^k\}_{k=1}^{\infty}$ to "approximate" the solutions of boundary value problems involving stiff operators. This will be the subject of a subsequent paper (see [9]).

Similarly, for $\epsilon_k = \frac{1}{k^2}$, $k=1,2,\dots$, $\{\lambda_{\epsilon_k}^k, \phi_{\epsilon_k}^k\}$ given below is an exact eigenvalue-eigenvector pair

$$\left. \begin{aligned} \lambda_{\epsilon_k}^k &= (\pi)^2 \\ \phi_{\epsilon_k 0}^k &= \sqrt{\epsilon_k} \sin \sqrt{\epsilon_k} k\pi x \\ \phi_{\epsilon_k 1}^k &= \sin k\pi x \end{aligned} \right\} \quad (3-29)$$

Note that in (3-29), ϵ_k depends on the index of the eigenvalue. Hence, one cannot let ϵ_k go to zero and observe what happens to this eigenvalue-eigenvector pair. However, the following conclusions can be drawn. First, the results of Theorem 2.1 show that $\phi_{\epsilon_0}^k \rightarrow 0$ in the present example. This is certainly reflected in (3-29) by the presence of the factor $\sqrt{\epsilon_k}$ multiplying $\phi_{\epsilon_k 0}^k$. Second, the presence of $\sqrt{\epsilon_k}$ in the argument of the sin function in (3-29) indicates that "flattening" occurs in ϕ_{ϵ}^k as $\epsilon \rightarrow 0$.

Example 3.3: A fourth order operator

Let $u = L^2(\Omega)$, $v = H_0^2(\Omega)$

$$a_1(\phi, \psi) = \int_{\Omega_1} \Delta \phi \Delta \psi \, dx, \quad i = 0, 1$$

then (2.4) becomes:

$$\left. \begin{aligned}
 \Delta^2 \chi_{\epsilon 0}^k &= \gamma^k \chi_{\epsilon 0}^k \text{ on } \Omega_0 \\
 \epsilon \Delta^2 \chi_{\epsilon 1}^k &= \gamma^k \chi_{\epsilon 1}^k \text{ on } \Omega_1 \\
 \chi_{\epsilon 0}^k &= \frac{\partial \chi_{\epsilon 0}^k}{\partial \nu} = 0 \text{ on } \Gamma_0 \\
 \chi_{\epsilon 1}^k &= \frac{\partial \chi_{\epsilon 1}^k}{\partial \nu} = 0 \text{ on } \Gamma_1 \\
 \chi_{\epsilon 0}^k &= \chi_{\epsilon 1}^k, \quad \frac{\partial \chi_{\epsilon 0}^k}{\partial \nu} = \frac{\partial \chi_{\epsilon 1}^k}{\partial \nu} \\
 \Delta \chi_{\epsilon 0}^k &= \epsilon \Delta \chi_{\epsilon 1}^k, \quad \frac{\partial \Delta \chi_{\epsilon 0}^k}{\partial \nu} = \epsilon \frac{\partial \Delta \chi_{\epsilon 1}^k}{\partial \nu}
 \end{aligned} \right\} \text{ on } S \quad (3-30)$$

Equation (3-16) becomes

$$\left. \begin{aligned}
 \phi_0^k &= 0 \text{ on } \Omega \\
 \Delta^2 \phi_1^k &= \lambda^k \phi_1^k \text{ on } \Omega_1 \\
 \phi_1^k &= \frac{\partial \phi_1^k}{\partial \nu} = 0 \text{ on } \Gamma_1 \\
 \phi_1^k &= \frac{\partial \phi_1^k}{\partial \nu} = 0 \text{ on } S
 \end{aligned} \right\}$$

This is a Dirichlet eigenvalue problem for the biharmonic operator in Ω_1 .

Equation (3-17) becomes

$$\left. \begin{aligned} \Delta^2 \psi_0^k &= \mu_{00}^k \psi_0^k \text{ on } \Omega_0 \\ \psi_1^k &= 0 \text{ on } \Omega_1 \\ \psi_0^k &= \frac{\partial \psi_0^k}{\partial \nu} = 0 \text{ on } \Gamma_0 \\ \Delta \psi_0^k &= \frac{\partial \Delta \psi_0^k}{\partial \nu} = 0 \text{ on } S \end{aligned} \right\} \quad (3-32)$$

Identical comments to those of Examples 3.1-3.2 can be made here, provided the function spaces are changed to reflect the increase in the operator order from two to four (as seen in (3-30)).

Remark 3.5:

Some of the properties discussed in this section are shared by many other stiff operators, which do not fit in the axiomatization of Section 2 (c.f. [9]).

SECTION 4

NUMERICAL RESULTS

In this section, Example 3.2 is analyzed numerically, using the Finite Element Method, to supplement the analysis undertaken in the preceding section. The set $\Omega = (-1,1)$ is divided into N equal intervals of length $h = \frac{2}{N}$. The roof functions $\{\phi_h^i\}_{i=1}^{N-1}$ [11], [13] are selected as a basis for the finite dimensional approximation of $H_0^1(\Omega)$. The finite dimensional approximation of the operator A_ϵ can be written in matrix form as

$$A_\epsilon^h = (M^h) - \frac{1}{\epsilon} K^h \quad (4-1)$$

where the entries of M^h are

$$(M^h)_{i,j} = \int_{\Omega} \phi_h^i \phi_h^j dx$$

$$i, j = 1, 2, \dots, N-1.$$

In the forthcoming example, the matrix M^h can be written explicitly, i.e.,

$$M^h = \frac{h}{6} \begin{bmatrix} 4 & 1 & & 0 \\ 1 & 4 & & \\ & & 1 & 4 & 1 \\ 0 & & & 1 & 4 \end{bmatrix}$$

For all computer runs, N is selected so that an accurate plot is obtained (N is indicated under each plot). The subroutine RSG from EISPACK with single precision is used to compute the eigenvalues and eigenvectors of A_{ϵ}^h .

Example 4.1: (Refer to Example 3.2)

In this example, the entries of K_{ϵ}^h are

$$(K_{\epsilon}^h)_{i,j} = \int_{\Omega} a(x) \frac{d\phi_i^h}{dx} \frac{d\phi_j^h}{dx} dx \quad (4-2)$$

$$i, j = 1, 2, \dots, N-1$$

where

$$a(x) = \begin{cases} 1 & \text{if } x \in (-1, 0) \\ \epsilon & \text{if } x \in (0, 1) \end{cases}$$

For N even, K_{ϵ}^h can be written as

$$K_{\epsilon}^h = \frac{1}{h} \begin{bmatrix} 2 & -1 & & & & & 0 \\ -1 & 2 & & & & & \\ & & -1 & 0 & & & \\ & -1 & 1+\epsilon & -\epsilon & & & \\ & 0 & -\epsilon & -2\epsilon & & & \\ & & & \ddots & \ddots & & \\ & & & & \ddots & \ddots & \\ & & & & & 2\epsilon & -\epsilon \\ 0 & & & & & -\epsilon & 2\epsilon \end{bmatrix} + \frac{N}{2} + 1 \quad (4-3)$$

The eigenvalues $\lambda_{\epsilon}^1, \lambda_{\epsilon}^2, \mu_{\epsilon}^1$ are tabulated in Table 4-1 for $\epsilon = 0.1, 0.04, 0.01, 0.001$. The corresponding eigenvectors are plotted in Figures (4-1a-4-1d), (4-2a-4-2d), (4-3a-4-3d).

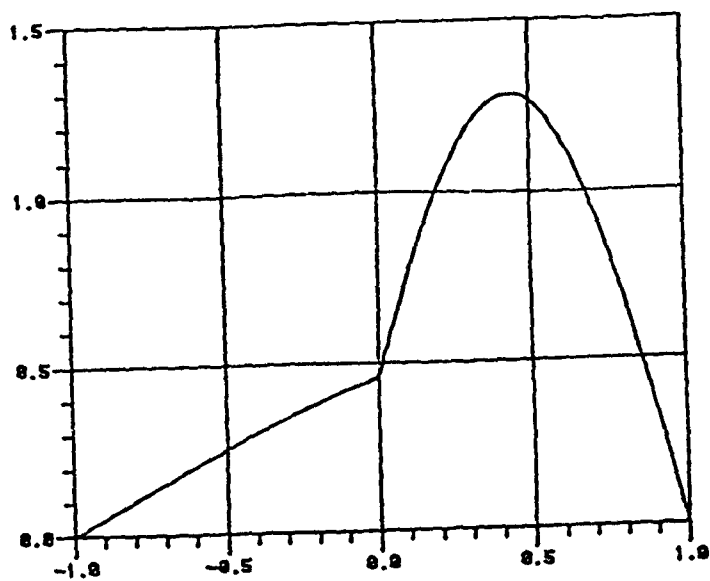


Figure 4-1a. ϕ_ϵ^l for $\epsilon = 0.04$, $N = 50$

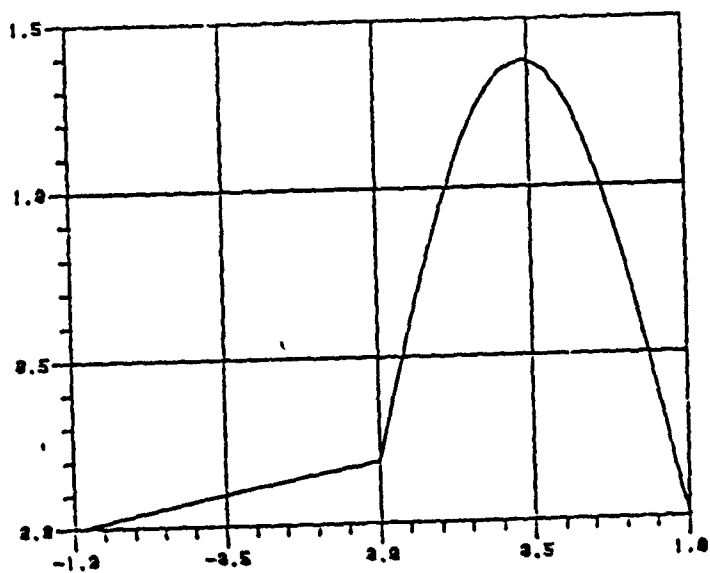


Figure 4-1b. ϕ_ϵ^l for $\epsilon = 0.04$, $N = 50$

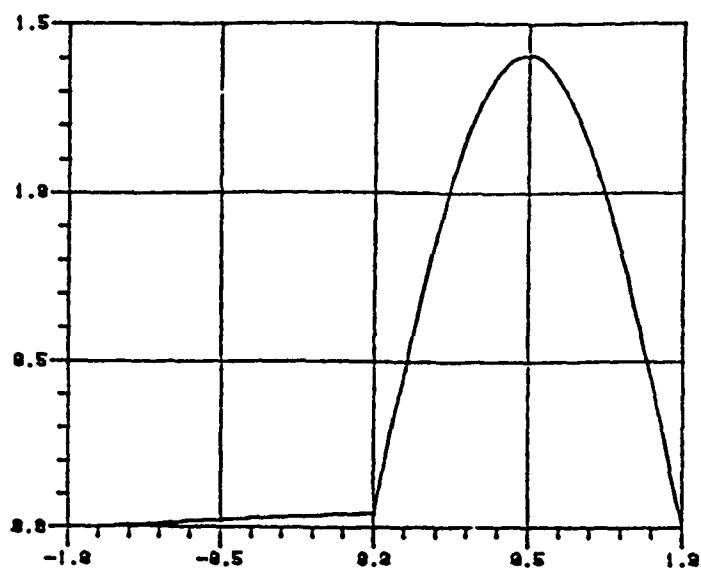


Figure 4-1c. ϕ_ϵ^1 for $\epsilon = 0.01$, $N = 100$

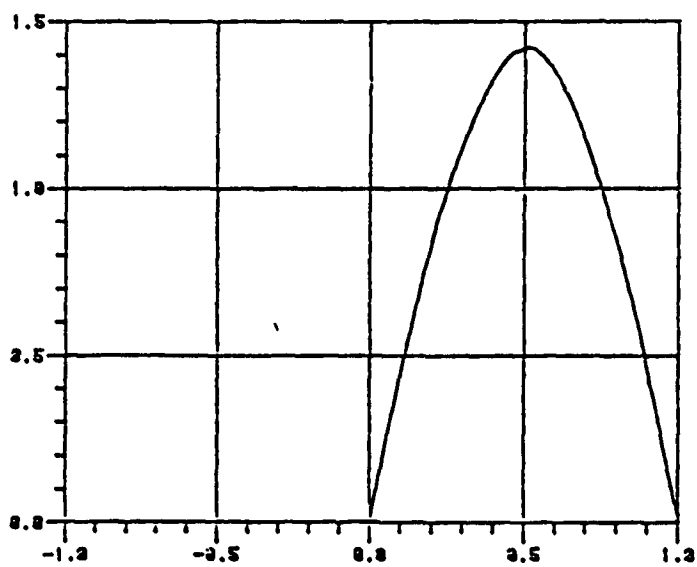


Figure 4-1d. ϕ_ϵ^1 for $\epsilon = 0.001$, $N = 150$

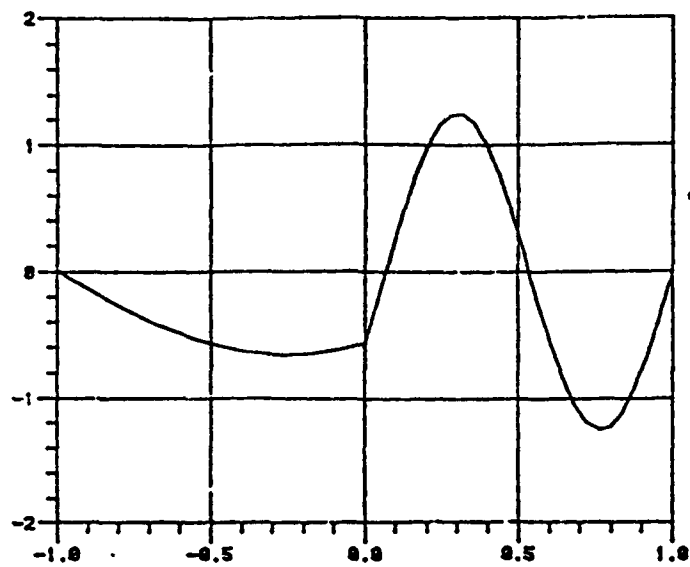


Figure 4-2a. ϕ_ϵ^2 for $\epsilon = 0.1$, $N = 50$

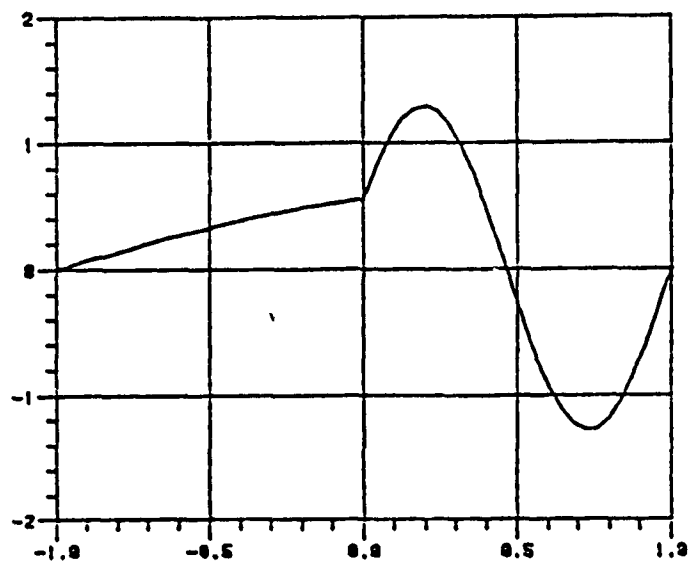


Figure 4-2b. ϕ_ϵ^2 for $\epsilon = 0.04$, $N = 50$

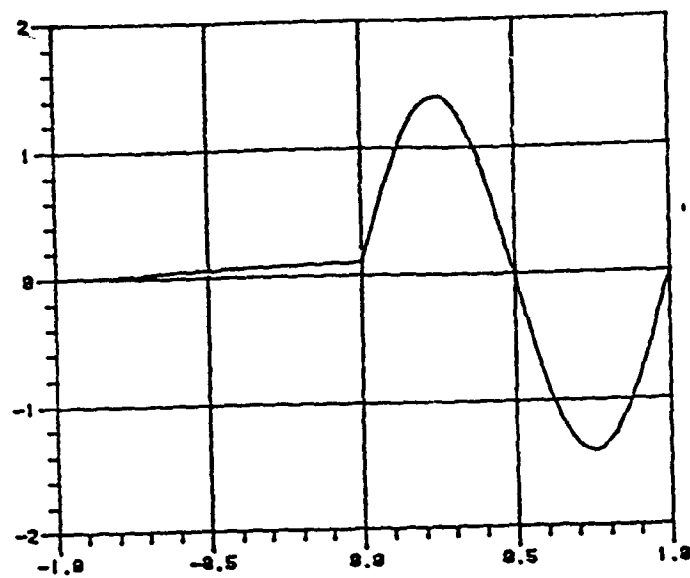


Figure 4-2c. ϕ_ϵ^2 for $\epsilon = 0.01$, $N = 100$

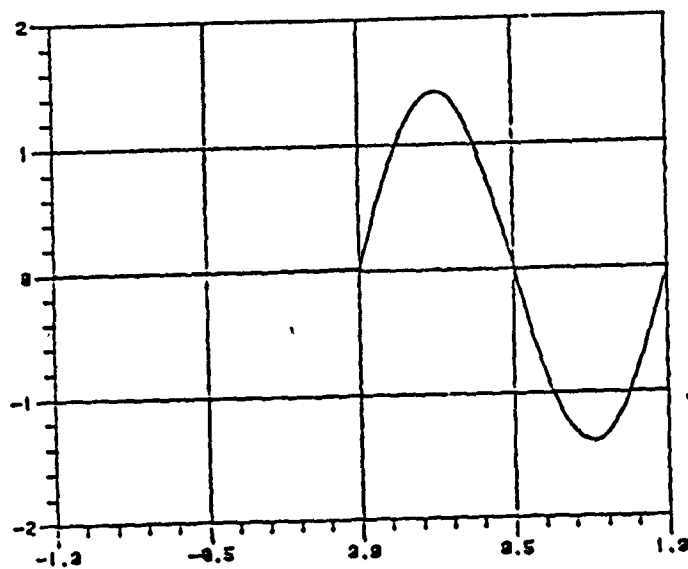


Figure 4-2d. ϕ_ϵ^2 for $\epsilon = 0.001$, $N = 150$

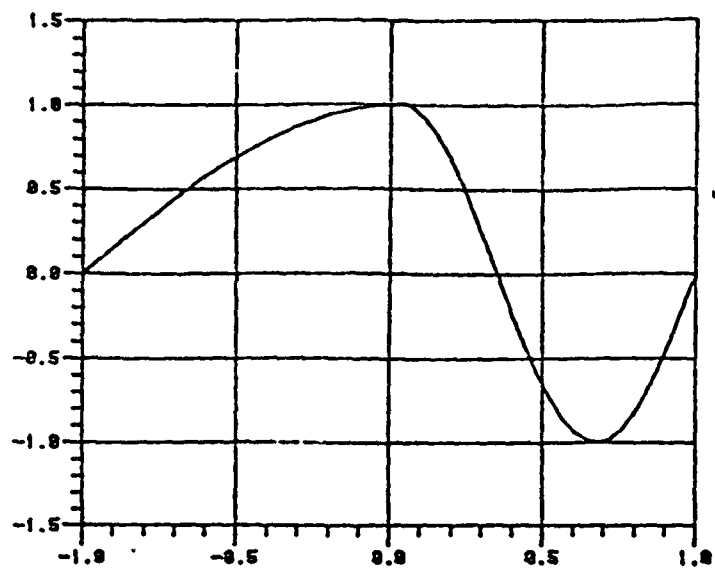


Figure 4-3a. ψ_ϵ^1 for $\epsilon = 0.1$, $N = 50$

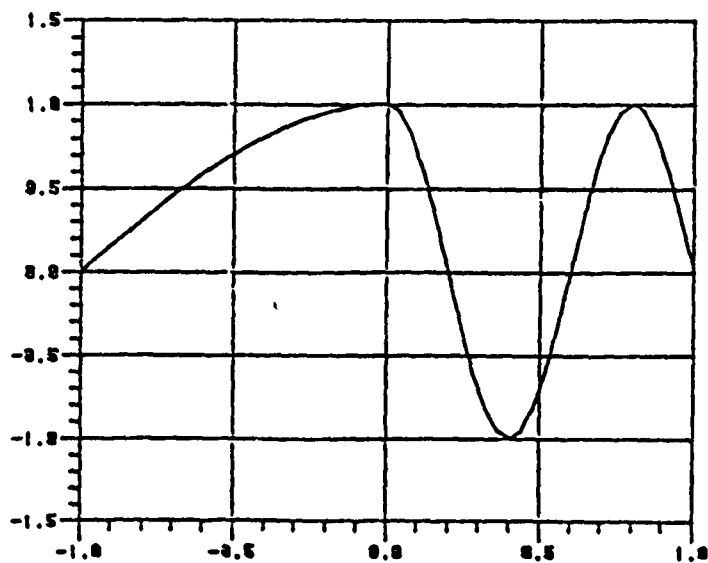


Figure 4-3b. ψ_ϵ^1 for $\epsilon = 0.04$, $N = 50$

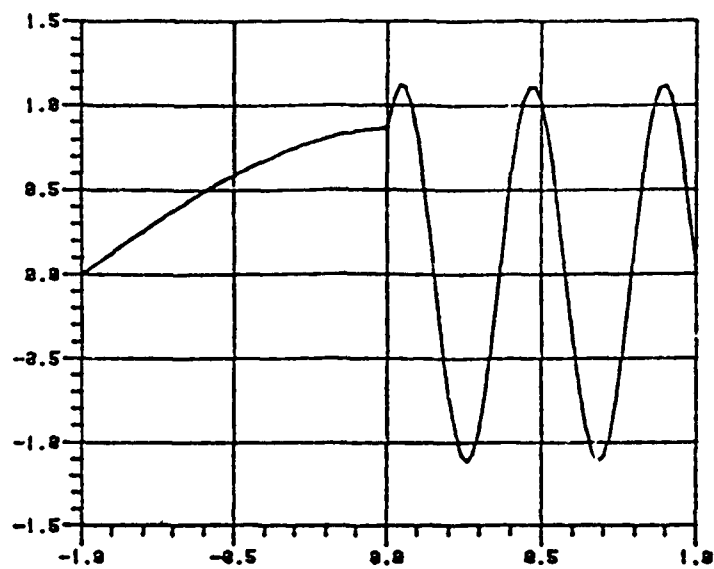


Figure 4-3c. ψ_ϵ^1 for $\epsilon = 0.01$, $N = 100$

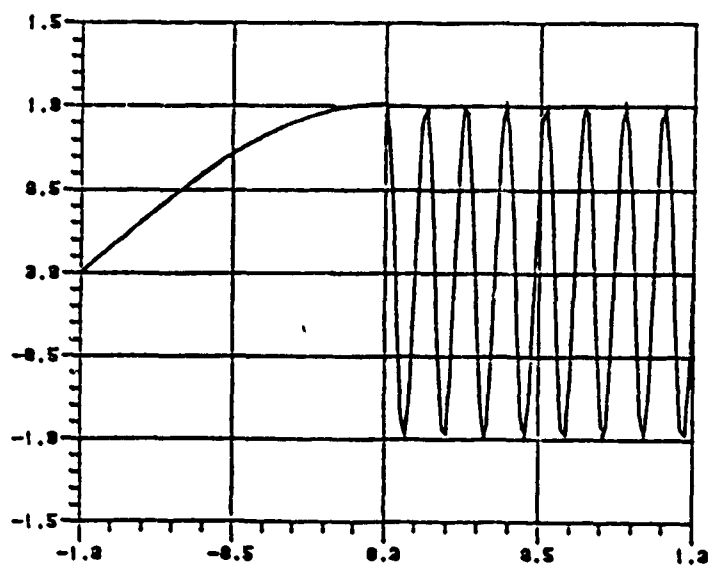


Figure 4-3d. ψ_ϵ^1 for $\epsilon = 0.001$, $N = 150$

TABLE 4-1. $\lambda_{\epsilon}^1, \lambda_{\epsilon}^2, \mu_{\epsilon}^1$ for $\epsilon = 0.1, 0.04, 0.01, 0.001$

ϵ	λ_{ϵ}^1	λ_{ϵ}^2	μ_{ϵ}^1
0.1	0.77230	4.5742	2.3462
0.04	0.36160	1.3715	2.4782
0.01	0.09650	0.38677	2.2153
0.001	0.01069	0.03997	2.2538

It is clear that most of the features described in Section 3 are exhibited in these plots. First, observe the attenuation of ϕ_{ϵ}^k , $k = 1, 2$ as $\epsilon \rightarrow 0$ on Ω_0 . Second, note the oscillatory behavior of ψ_{ϵ}^1 as $\epsilon \rightarrow 0$ on Ω_1 .

Furthermore, one may add that the first eigenvalue-eigenvector pairs are computed more accurately than their last counterparts [13]. Consequently, if the eigenvalues of A_{ϵ}^h are ordered ascendingly, $\{\mu_{\epsilon}^1, \psi_{\epsilon}^1\}$ is pushed higher and higher as $\epsilon \rightarrow 0$ and hence computed less and less accurately. Moreover, since h is fixed, the oscillatory behavior of ψ_{ϵ}^1 would not be captured by this approximation, unless h is made smaller and hence increasing the order of the matrix A_{ϵ}^h .

SECTION 5

CONCLUSION

The eigenvalue problem of a class of stiff operators has been analyzed in this paper, via a general formulation using bilinear forms, to avoid the complexity of explicitly keeping track of the various boundary and interface conditions. First, the intuitive idea that the eigenvalues of stiff operators are of different order of magnitude as functions of the parameter ϵ , is rigorously verified. Second, a terminology is introduced to describe the convergence of the eigenvector as $\epsilon \rightarrow 0$, i.e., flattening, alternation and oscillation. This analysis is of paramount importance, because it will yield insight into how to approximate boundary value problems involving stiff operators.

REFERENCES

1. J.P. Aubin, Applied Functional Analysis, John Wiley & Sons, New York, 1979.
2. A. Bensoussan, J.L. Lions, Applications des Inequations Variationnelles en Controle Stochastique, Dunod, Paris, 1978.
3. G. Duvant, J.L. Lions, Inequalities in Mechanics and Physics, Springer-Verlag, New York, 1976.
4. P.P.N. de Croen, "Singular Perturbations of Spectra," in Asymptotic Analysis, F. Verhulst, Lecture Notes in Mathematics, Springer-Verlag, New York, 1979.
5. T. Kato, Perturbation Theory for Linear Operators, Springer-Verlag, New York, 1980.
6. S. Kesavan, "Homegenization of Elliptic Eigenvalue Problems: Parts I & II", Appl. Math. Option., Vol. 5, 1979.
7. J.L. Lions, Perturbation Singulieres dans les Problemes aux Limites et in Controle Optimal, Lecture Notes in Mathematics, Springer-Verlag, New York, 1973.
8. J. Moser, "Singular Perturbation of Eigenvalue Problems for Linear Differential Equations of Even Order," Comm. Pure Appl. Math., Vol. 8, pp. 649-675, 1955.
9. H. Salhi, Ph.D. Thesis, University of Illinois, Urbana, Illinois, 1983.
10. B. Smith, et al., Matrix Eigensystem Routines Eispack Guide, Lecture Notes in Computer Sciene 6, Springer-Verlag, New York, 1974.
11. G. Strong, G.J. Fix, An Analysis of the Finite Element Method, Prentice-Hall, Englewood Cliffs, New Jersey, 1971.
12. J. Weidman, Linear Operators in Hilbert Spaces, Springer-Verlag, New York, 1980.
13. O.C. Zienkiewicz, The Finite Element Method, McGraw Hill, New York, 1977.

APPENDIX B

TP-221

APPROXIMATION OF A CLASS OF
OF STIFF SYSTEMS

By:

Hassan Salhi
Douglas P. Looze

May 1985

ALPHATECH, Inc.
2 Burlington Executive Center
111 Middlesex Turnpike
Burlington, MA 01803
617-273-3388

*This work was supported at the University of Illinois by the Joint Services Electronics Program under Contract N00014-79-C-0424, and at ALPHATECH by Contract No. F33615-84-C-3618.

ABSTRACT

In this paper, asymptotic approximations for a class of linear stiff systems are constructed, using the weak limits of the eigenvectors of the associated stiff operators.

SECTION 1

INTRODUCTION

A standard approach in solving many boundary value problems of mathematical physics is to employ eigenvector expansions. When such problems contain one (or several) small parameter ϵ , asymptotic expansions in (fractional) powers of ϵ can often be a powerful approximating process.

In a previous paper [5]*, the spectral decomposition of a class of stiff operators was investigated. The asymptotic properties of their eigenvalues and the corresponding eigenvectors were analyzed. More importantly, it was discovered that some of the aforementioned eigenvectors are not analytic functions of ϵ . This fact is intimately related to their convergence in a Hilbert space with a weaker topology. Despite this undesirable property, it is possible to derive asymptotic approximations of the solutions of boundary value problems involving stiff operators.

In the sequel, the results of [5] are employed to investigate the behavior of the solutions of the following three formal equations

$$A_{\epsilon} y_{\epsilon} = f \quad (1-1)$$

$$\frac{\partial y_{\epsilon}}{\partial t} + A_{\epsilon} y_{\epsilon} = f, \quad y_{\epsilon}(0) = h \quad (1-2)$$

*References are indicated by numbers in square brackets, the list appears at the end of this Appendix.

$$\frac{\partial^2 y_\epsilon}{\partial t^2} + A_\epsilon y_\epsilon = f, \quad y_\epsilon(0) = h, \quad \frac{\partial y_\epsilon}{\partial t}(0) = g \quad (1-3)$$

where A_ϵ is a stiff operator of the class studied in [5].

The occurrence of (1-1)-(1-3) is very frequent in mathematical models of distributed physical processes such as nuclear reactors, heat exchangers, chemical reactors, fluid systems, vibration systems, steel and glass processes, etc. Thus, it is important to focus on them. The major thrust of this paper is to derive asymptotic approximations of the solutions y_ϵ of (1-1)-(1-3). For elliptic problems (i.e., (1-1)), by appropriately modifying the weak limits of the eigenvectors, one may be able to compute an asymptotic expansion of any order for y_ϵ . In so doing, the formal results obtained in [3] are complemented. For revolution problems (i.e., (1-2)-(1-3)), the concept of weak solutions [2],[4] is used to define zeroth order approximations of the solutions of (1-2)-(1-3), which depend only upon the weak limits of the eigenvectors.

This paper is organized as follows. In Section 2, the main results of [5] are briefly reviewed. In Section 3, the solution of (1-1) is derived. In Section 4, the convergence of the solution of (1-2) is investigated and an asymptotic approximation is constructed for it. In Section 5, an analysis similar to that of Section 4 for a class of hyperbolic problems (i.e., (1-3)) is undertaken. In the last section, some concluding remarks are presented.

SECTION 2

REVIEW OF PREVIOUS RESULTS

Let V, H be two given real Hilbert spaces such that V is dense in H and

A1) the injection of V into H is compact.

Let V^* denote the dual space of V . After identification of H with H^* , one has

A2) $V \subset H \subset V^*$.

Let $a_i(\phi, \psi)$, $i = 0, 1$ be two forms on V such that the following assumptions hold:

A3) $a_1(\phi, \psi)$ is bilinear, symmetric on V

A4) $a_1(\phi, \psi)$ is continuous on V , i.e., there exists β_1 such that

$$a_1(\phi, \psi) \leq \beta_1 \|\phi\|_V \|\psi\|_V, \quad \forall \phi \in V, \quad \forall \psi \in V$$

A5) $a_1(\phi, \phi) \geq \alpha_1 p_1(\phi)^2$, where $\alpha_1 > 0$ and $p_1(\cdot)$ is continuous semi-norm on V .

A6) $p_0(\phi) + p_1(\phi)$ is a norm equivalent to $\|\phi\|_V$

A7) $a_1(\phi, \phi) = 0$ on $V_i \subset V$, where V_i is an infinite-dimensional subspace of V , $i=0, 1$.

A8) If $\psi \mapsto L_0(\psi)$ is a continuous linear form on V , null on V_0 , there exists $\phi \in V$ (module V_0) such that

$$a_0(\phi, \psi) = L_0(\psi), \quad \forall \psi \in V$$

Let $a_\epsilon(\phi, \psi)$ be defined as

$$a_\epsilon(\phi, \psi) = a_0(\phi, \psi) + \epsilon a_1(\phi, \psi) \tag{2-1}$$

Remark 2.1:

Clearly, the form $a_\epsilon(\phi, \psi)$ is bilinear, symmetric, coercive and bounded on V . Hence, it defines uniquely a selfadjoint operator A_ϵ

$$A_\epsilon \in L(V; V^*) ,$$

i.e.,

$$a_\epsilon(\phi, \psi) = \langle A_\epsilon \phi, \psi \rangle , \text{ for all } \phi, \psi \in V$$

where $\langle \cdot, \cdot \rangle$ denotes the duality pairing between V and its dual V^* .

From the above remark, one concludes that the spectrum of A_ϵ is a subset of \mathbb{R}^+ , consisting only of the point spectrum [1].

The eigenvalue problem for A_ϵ is, then, to seek $\{\gamma_\epsilon^k, \chi_\epsilon^k\}_{k=1}^\infty \in \mathbb{R}^+ \times V$ such that

$$A_\epsilon \chi_\epsilon^k = \gamma_\epsilon^k \chi_\epsilon^k \quad (2-2)$$

or equivalently

$$a(\chi_\epsilon^k, \phi) = \gamma_\epsilon^k (\chi_\epsilon^k, \psi) , \text{ for all } y \in V \quad (2-3)$$

Now the properties of $\{\gamma_\epsilon^k, \chi_\epsilon^k\}_{k=1}^\infty$ are summarized in:

Theorem 2.1:

Let $\{\gamma_\epsilon^k\}_{k=1}^\infty$ be the eigenvalues of A_ϵ and $\{\chi_\epsilon^k\}_{k=1}^\infty$ the corresponding normalized system of eigenvectors. Then, given a sequence of ϵ converging to zero, $\{\gamma_\epsilon^k, \chi_\epsilon^k\}_{k=1}^\infty$ can be decomposed into $\{\lambda_\epsilon^k, \phi_\epsilon^k\}_{k=1}^\infty$ and $\{\mu_\epsilon^k, \psi_\epsilon^k\}_{k=1}^\infty$ such that, for each k ,

1) $\lambda_{\epsilon}^k \rightarrow 0$ linearly in ϵ , $\phi_{\epsilon}^k \rightarrow \psi^k$ weakly in V

2) $\mu_0^k \rightarrow \mu_0^k > 0$, $\psi_{\epsilon}^k \rightarrow \psi^k$ weakly in H

where $\{\phi^k\}_{k=1}^{\infty}$ and $\{\psi^k\}_{k=1}^{\infty}$ satisfy

$$a_1(\phi^k, \chi) = \lambda_1^k(\phi^k, \chi), \quad \phi^k \in V_0 \subset V, \text{ for all } \chi \in V_0 \quad (2-4)$$

$$a_0(\psi^k, \chi) = \mu_0^k(\psi^k, \chi), \quad \psi^k \in H_1 \subset H, \text{ for all } \chi \in V_1 \quad (2-5)$$

Moreover, the following estimates hold for $\epsilon > 0$:

$$3) \quad \|\phi_{\epsilon}^k\|_{V_1} \leq C_1 \quad (2-6)$$

$$4) \quad \sqrt{\epsilon} \|\psi_{\epsilon}^k\|_{V_2} \leq C_2 \quad (2-7)$$

where C_1, C_2 are two positive constants, independent of ϵ .

Proof: See [5].

Remark 2.2:

The subspace H_1 of H in (2-5) is uniquely determined as the span of $\{\psi^k\}_{k=1}^{\infty}$.

Remark 2.3:

The weak limits $\{\phi^k\}_{k=1}^{\infty}$ and $\{\psi^k\}_{k=1}^{\infty}$ form an orthonormal system in H .

SECTION 3

ELLIPTIC BOUNDARY VALUE PROBLEMS

In this section, an asymptotic expansion of the solution y_ϵ of

$$A_\epsilon y_\epsilon = f, \quad f \in H \quad (3-1)$$

or equivalently

$$a_0(y_\epsilon, \phi) + \epsilon a_1(y_\epsilon, \phi) = (f, \phi), \quad \epsilon \in V, \quad \text{for all } \phi \in V \quad (3-2)$$

is desired. This problem is studied in a more general context (namely without assumption A1) in [3].

The modifications of the weak limits of the eigenvectors are now considered. Since $\psi_\epsilon^k \in H_1$, one may add to it a function

$$\xi_\epsilon^k = \xi_0^k + \epsilon \xi_1^k + \epsilon^2 \xi_2^k + \dots \quad (3-3)$$

where

$$\xi_0^k \in H \text{ such that } \psi^k + \xi_0^k \in V \quad (3-4)$$

$$\xi_l^k \in V, \quad l = 1, 2, \dots \quad (3-5)$$

This amounts to solving the following boundary value problem, using the iterative process of [3]:

$$a_0(\psi^k + \xi_\epsilon^k, \chi) + \epsilon a_1(\psi^k + \xi_\epsilon^k, \chi) = \mu_0^k(\psi^k, \chi), \quad \text{for all } \chi \in V \quad (3-6)$$

Consequently, $\{\xi_l^k\}_{l=0}^{\infty}$ satisfy

$$a_1(\xi_0^k, \chi) = 0, \quad \psi^k + \xi_0^k \in V, \quad \text{for all } \chi \in V_0 \quad (3-7)$$

...

$$\left. \begin{aligned} a_0(\xi_l^k, \chi) &= -a_1(\xi_{l-1}^k, \chi), \quad \text{for all } \chi \in V \\ a_1(\xi_l^k, \chi) &= 0, \quad \text{for all } \chi \in V_0 \\ l &= 1, 2, \dots \\ k &= 1, 2, \dots \end{aligned} \right\} \quad (3-8)$$

Remark 3.1:

It is worthy of mention that the iterative process described by (3-7)-(3-8) appears to average the oscillatory behavior of ψ_ϵ^k [5].

Similarly, one adds to ϕ^k

$$\theta_\epsilon^k = \epsilon \theta_1^k + \epsilon^2 \theta_2^k + \dots \quad (3-9)$$

where

$$\theta_l^k \in V, \quad l = 1, 2, \dots$$

The function θ_ϵ^k is chosen such that

$$a_0(\phi^k + \theta_\epsilon^k, \chi) + \epsilon a_1(\phi^k, \chi) = \epsilon a_1(\phi^k, \chi), \quad \text{for all } \chi \in V$$

from which one concludes (using the fact that $\phi^k \in V_0$) that $\{\theta_l^k\}_{l=1, k=1}^{\infty}$ satisfy

$$\left. \begin{aligned}
 a_{01}(\theta^k, \chi) &= a_1(\phi^k, \chi) \quad , \quad \text{for all } \chi \in V \\
 a_{11}(\theta^k, \chi) &= 0 \quad , \quad \text{for all } \chi \in V_0 \\
 &\dots \\
 a_{0\ell}(\theta^k, \chi) &= -a_{1\ell-1}(\theta^k, \chi) \quad , \quad \text{for all } \chi \in V \\
 a_{1\ell}(\theta^k, \chi) &= 0 \quad , \quad \text{for all } \chi \in V_0
 \end{aligned} \right\} \quad (3-10)$$

$$\ell = 2, 3, \dots$$

$$k = 1, 2, \dots$$

Remark 3.2:

The zeroth term in (3-9) is zero because $\phi^k \in V$.

Remark 3.3:

The iterative process presented above appears to average the flattening (and attenuation) of $\{\phi^k\}_{k=1}^{\infty}$ [5].

Before proceeding further, consider the following example to examine what (3-7)-(3-8), and (3-10) yield:

Example 3.1:

Let $H = L^2(\Omega)$, $V = H_0^1(\Omega)$ where $\Omega = \Omega_0 \cup \Omega_1 \cup S$, $\Gamma = \Gamma_0 \cup \Gamma_1$ as indicated in Fig. 3-1. Let

$$a_1(\phi, \psi) = \sum_{j=1}^n \int_{\Omega_1} \frac{\partial \phi}{\partial x_j} \frac{\partial \psi}{\partial x_j} dx$$

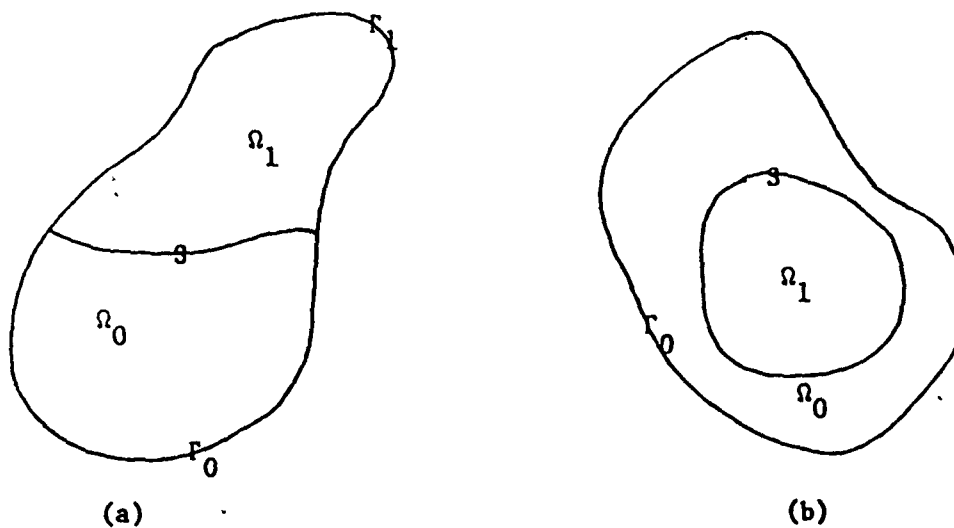


Figure 3-1. Examples of Interfaced Sets

then (3-7)-(3-8), and (3-10) become

$$\left. \begin{aligned}
 &\xi_{00}^k = 0 \text{ on } \Omega_0 \\
 &-\Delta \xi_{01}^k = 0 \text{ on } \Omega_1 \\
 &\xi_{01}^k \Big|_{\Gamma_1} = 0, \quad \xi_{01}^k \Big|_S = \psi_{01}^k \Big|_S
 \end{aligned} \right\}$$

...

$$-\Delta \xi_{l0}^k = 0 \text{ on } \Omega_0$$

$$\xi_{l0}^k \Big|_{\Gamma_0} = 0, \quad \frac{\partial \xi_{l0}^k}{\partial \nu} \Big|_S = \frac{\partial \xi_{l-1,1}^k}{\partial \nu} \Big|_S$$

$$-\Delta \xi_{l1}^k = 0 \text{ on } \Omega_1$$

$$\xi_{l1}^k \Big|_{\Gamma_1} = 0, \quad \xi_{l1}^k \Big|_S = \xi_{l0}^k \Big|_S$$

$$l = 1, 2, \dots$$

$$k = 1, 2, \dots$$

...

$$-\Delta \theta_{l0}^k = 0 \text{ on } \Omega_0$$

$$\theta_{l0}^k \Big|_{\Gamma_1} = 0, \quad \frac{\partial \theta_{l0}^k}{\partial \nu} \Big|_S = \frac{\partial \phi_1^k}{\partial \nu} \Big|_S$$

$$-\Delta \theta_{l1}^k = 0 \text{ on } \Omega_1$$

$$\theta_{l1}^k \Big|_{\Gamma_1} = 0, \quad \theta_{l1}^k \Big|_S = \theta_{l0}^k \Big|_S$$

...

$$\left. \begin{aligned}
 -\Delta \theta_{\ell 0}^k &= 0 \text{ on } \Omega_0 \\
 \xi_{\ell 0}^k \Big|_{\Gamma_0} &= 0, \quad \frac{\partial \theta_{\ell 0}^k}{\partial \nu} \Big|_S = \frac{\partial \theta_{\ell-1,1}^k}{\partial \nu} \Big|_S \\
 -\Delta \theta_{\ell 1}^k &= 0 \text{ on } \Omega_1 \\
 \theta_{\ell 1}^k \Big|_{\Gamma_1} &= 0, \quad \theta_{\ell 1}^k \Big|_S = \theta_{\ell 0}^k \Big|_S
 \end{aligned} \right\}$$

$$\ell = 2, 3, \dots$$

$$k = 1, 2, \dots$$

Remark 3.4:

The computation of these modifications is greatly simplified since the dependence on the parameter ε is eliminated.

Now attention is focused into obtaining an asymptotic expansion of the solution of the boundary value problem (3-1) using the modified weak limits of the eigenvectors of A_ε .

Theorem 3.1:

For sufficiently small ε , the solution of (3-1) is given by

$$y_\varepsilon = \sum_{k=1}^{\infty} \frac{c^k}{\mu_0^k} (\psi_{\varepsilon}^{k+\xi^k}) + \sum_{k=1}^{\infty} \frac{d^k}{\varepsilon \lambda_1^k} (\phi_{\varepsilon}^{k+\theta^k}) \quad (3-11)$$

where

$$\{\mu_0^k, \psi^k\}_{k=1}^{\infty} \text{ and } \{\lambda_1^k, \phi^k\}_{k=1}^{\infty} \text{ satisfy (2-4)-(2-5)}$$

$$\{\xi_{\epsilon}^k\}_{k=1}^{\infty} \text{ and } \{\theta_{\epsilon}^k\}_{k=1}^{\infty} \text{ are given by (3-3) and (3-9)}$$

$\{c^k\}_{k=1}^{\infty}$ and $\{d^k\}_{k=1}^{\infty}$ are the Fourier coefficients of f , i.e.,

$$c^k = (f, \psi^k)_H \quad (3-12)$$

$$d^k = (f, \phi^k)_H \quad (3-13)$$

Proof:

The eigenvectors $\{\phi^k\}_{k=1}^{\infty}$ and $\{\psi^k\}_{k=1}^{\infty}$ form a complete orthonormal¹ basis of H and $\phi^k + \theta_{\epsilon}^k \in V$, $\psi^k + \xi_{\epsilon}^k \in V$ by construction. Now it is straightforward to verify that (3-11) is the unique asymptotic expansion of y_{ϵ} .

Remark 3.5:

Truncate ξ_{ϵ}^k and θ_{ϵ}^k to the p th term and denote these truncated series, respectively, by $\xi_{\epsilon}^{k,p}$ and $\theta_{\epsilon}^{k,p}$. Define e_{ϵ}^p by

$$e_{\epsilon}^p = y_{\epsilon} - y_{\epsilon}^p$$

where

$$y_{\epsilon}^p = \sum_{k=1}^{\infty} \frac{c^k}{\mu_0^k} (\psi^k + \xi_{\epsilon}^{k,p}) + \sum_{k=1}^{\infty} \frac{d^k}{\epsilon \lambda_1^k} (\phi^k + \theta_{\epsilon}^{k,p})$$

¹Note that $\{\psi^k\}_{k=1}^{\infty}$ must be renormalized in H .

Then it can be shown ([3], p. 13) that

$$\|eP\|_{\epsilon} < C \epsilon^P$$

where C is a constant independent of ϵ .

Example 3.2 (Example 3.1 Cont.)

In this case, (3-11)-(3-13) become

$$\left. \begin{aligned} y_{\epsilon 0} &= \sum_{k=1}^{\infty} \frac{c^k}{\mu_0^k} (\psi_0^{k+\xi^k}) + \sum_{k=1}^{\infty} \frac{d^k}{\epsilon \lambda_1^k} \theta_0^k \\ y_{\epsilon 1} &= \sum_{k=1}^{\infty} \frac{c^k}{\mu_0^k} \xi_1^k + \sum_{k=1}^{\infty} \frac{d^k}{\epsilon \lambda_1^k} (\phi_1^{k+\theta^k}) \end{aligned} \right\}$$

where

$$c^k = (f, \psi^k)_{L^2(\Omega)} = (f_0, \psi_0^k)_{L^2(\Omega_0)}$$

$$d^k = (f, \psi^k)_{L^2(\Omega)} = (f_1, \psi_1^k)_{L^2(\Omega_1)}$$

$\xi_{\epsilon}^k, \theta_{\epsilon}^k$ are computed in Example 3.1.

SECTION 4

PARABOLIC BOUNDARY VALUE PROBLEMS

In this section, an evolution problem of parabolic type is considered. Hence, let the variable t denote time. It is assumed that $t \in (0, T)$, $T < \infty$, and that all the assumptions made in Section 2 hold. Let $L^2(0, T; V)$, $L^2(0, T; H)$, $L^2(0, T; V^*)$ denote the Hilbert spaces of Lebesgue square integrable functions with values in V , H , V^* , respectively. Let prime denote the distributional derivative with respect to time [4]. In the sequel, the following parabolic boundary value problem is analyzed

$$(y'_\epsilon, \phi) + a_0(y_\epsilon, \phi) + \epsilon a_1(y_\epsilon, \phi) = (f, \phi) \quad , \quad \text{for all } \phi \in V \quad (4-1)$$

$$y_\epsilon(0) = h \quad , \quad h \text{ given in } H \quad (4-2)$$

$$y_\epsilon \in L^2(0, T; V) \quad , \quad f \in L^2(0, T; H) \quad . \quad (4-3)$$

Under the assumptions made, problem (4-1)-(4-3) admits a unique solution $y_\epsilon \in L^2(0, T; V)$ [4]. Using the results derived in Section 2, the convergence of y_ϵ as $\epsilon \rightarrow 0$ is studied. Then an asymptotic approximation of y_ϵ is constructed and an asymptotic error estimate is derived.

4.1 CONVERGENCE OF y_ϵ as $\epsilon \rightarrow 0$

As in Section 2, let $\{\lambda^k, \phi^k\}_{\epsilon, k=1}^{\infty}$ and $\{\mu^k, \psi^k\}_{\epsilon, k=1}^{\infty}$ be the exact eigenvalue-eigenvector pairs of A_ϵ with the eigenvectors normalized to one in H .

Let

$$y_\epsilon = \sum_{k=1}^{\infty} c_\epsilon^k(t) \psi_\epsilon^k + \sum_{k=1}^{\infty} d_\epsilon^k(t) \phi_\epsilon^k \quad (4-4)$$

$$f = \sum_{k=1}^{\infty} (f, \psi_\epsilon^k) \psi_\epsilon^k + (f, \phi_\epsilon^k) \phi_\epsilon^k \quad (4-5)$$

$$h = \sum_{k=1}^{\infty} (h, \psi_\epsilon^k) \psi_\epsilon^k + \sum_{k=1}^{\infty} (h, \phi_\epsilon^k) \phi_\epsilon^k \quad (4-6)$$

Substitute (4-4)-(4-6) into (4-1)-(4-3) to find that $\{c_\epsilon^k\}_{k=1}^{\infty}$, $\{d_\epsilon^k\}_{k=1}^{\infty}$ satisfy the following ordinary differential equations:

$$\frac{dc_\epsilon^k}{dt} + \mu_\epsilon^k c_\epsilon^k = (f, \psi_\epsilon^k), \quad c_\epsilon^k(0) = (h, \psi_\epsilon^k)$$

$$\frac{dd_\epsilon^k}{dt} + \lambda_\epsilon^k d_\epsilon^k = (f, \phi_\epsilon^k), \quad d_\epsilon^k(0) = (h, \phi_\epsilon^k)$$

$$k = 1, 2, \dots$$

whose solutions are

$$c_\epsilon^k(t) = e^{-\mu_\epsilon^k t} (h, \psi_\epsilon^k) + \int_0^t e^{-\mu_\epsilon^k(t-\tau)} (f, \psi_\epsilon^k) d\tau$$

$$d_\epsilon^k(t) = e^{-\lambda_\epsilon^k t} (h, \phi_\epsilon^k) + \int_0^t e^{-\lambda_\epsilon^k(t-\tau)} (f, \phi_\epsilon^k) d\tau.$$

Using Theorem 2.1, one concludes with no difficulty that

$$y_\epsilon \rightarrow y \text{ weakly in } L^2(0, T; H)$$

where

$$y = \sum_{k=1}^{\infty} c^k \psi^k + \sum_{k=1}^{\infty} d^k \phi^k$$

$\{\phi^k\}_{k=1}^{\infty}$, $\{\psi^k\}_{k=1}^{\infty}$ are the weak limits of $\{\phi^k\}_{\varepsilon k=1}^{\infty}$ (respectively, $\{\psi^k\}_{\varepsilon k=1}^{\infty}$)

in V , (respectively, in H) given by (2-4) (respectively, 2-5)

$$c^k(t) = e^{-\mu^k t} (h, \psi^k) + \int_0^t e^{-\mu^k(t-\tau)} (f, \psi^k) d\tau$$

$$d^k(t) = (h, \phi^k) + \int_0^t (f, \phi^k) d\tau.$$

The preceding discussion is summarized in:

Theorem 4.1:

Let y_{ε} denote the solution of (4-1)-(4-3). Given a sequence of ε converging to zero,

$$y_{\varepsilon} \rightarrow y \text{ weakly in } L^2(0, T; H) \quad (4-8)$$

where y is given by (4-7). Moreover,

$$\sqrt{\varepsilon} \|y\|_{L^2(0, T; V)} < C \quad (4-9)$$

Where C is a constant independent of ε .

Proof:

Use the eigenvalue-eigenvector pairs of the operator A_{ε} and their properties, as described by theorem 2.1, to obtain (4-8). The estimate (4-9) is then readily derived by employing (2-6)-(2-7).

4.2 ASYMPTOTIC APPROXIMATION OF y

It should be noted that the method by which stiff elliptic boundary value problems were solved in Section 3 does not yield an iterative process for evolution problems in general. Therefore, one would be content to obtain a "weak" approximation of the solution of (4-1)-(4-3) using only the weak limits of the eigenvectors of A_ϵ .

In the sequel, an approximation of the solution of the following boundary value problem is derived:

$$\left. \begin{aligned} \frac{\partial y_{\epsilon 0}}{\partial t} + A_0 y_{\epsilon 0} &= f_0 \text{ on } Q_0 \\ \frac{\partial y_{\epsilon 1}}{\partial t} + \epsilon A_1 y_{\epsilon 1} &= f_1 \text{ on } Q_1 \end{aligned} \right\} \quad (4-10)$$

$$y_{\epsilon 0} = 0 \text{ on } \Sigma_0, \quad y_{\epsilon 1} = 0 \text{ on } \Sigma_1 \quad (4-11)$$

$$\left. \begin{aligned} y_{\epsilon 0} &= y_{\epsilon 1} \\ \frac{\partial y_{\epsilon 0}}{\partial \nu_{A_0}} &= \epsilon \frac{\partial y_{\epsilon 1}}{\partial \nu_{A_1}} \end{aligned} \right\} \text{ on } R \quad (4-12)$$

$$y_\epsilon(0) = h \text{ on } \Omega \quad (4-13)$$

where

$$Q_i = \Omega_i \times (0, T), \quad i = 0, 1$$

$$\Sigma_i = \Gamma_i \times (0, T), \quad i = 0, 1$$

$$R = S \times (0, T) .$$

$$A_k = \sum_{i=1}^n \sum_{j=1}^n \frac{\partial}{\partial x_i} a_{ij}^k(x) \frac{\partial}{\partial x_j}, \quad k = 0, 1$$

a_{ij}^k satisfy

$$1) \quad a_{ij}^k \in C^1(\Omega_k)$$

$$2) \quad a_{ij}^k = a_{ji}^k$$

$$3) \quad \sum_{i=1}^n \sum_{j=1}^n a_{ij}^k \xi_i \xi_j > \alpha_k \sum_{i=1}^n \xi_i^2, \quad \alpha_k > 0,$$

for all $\xi \in \mathbb{R}^n$, $\xi \neq 0$.

The chief reason for this digression is that one can explicitly specify the regularity conditions of the functions involved in the construction of the approximation of y_ϵ . However, the concepts involve herein are equally applicable to the general case.

Now, let the zeroth order approximation be denoted by $y_\epsilon^0 = (y_0^0, y_{\epsilon 1}^0)$ and defined as follows:

$$\left. \begin{aligned} \frac{\partial y_0^0}{\partial t} + A_0 y_0^0 &= f_0 \text{ on } Q_0 \\ y_0^0 &= 0 \text{ on } \Sigma_0 \\ \frac{\partial y_0^0}{\partial \nu_{A_0}} &= 0 \text{ on } R \\ y_0^0(0) &= h_0 \text{ on } \Omega_0 \end{aligned} \right\} \quad (4-14)$$

$$\left. \begin{aligned}
 \frac{\partial y_{\epsilon 1}^0}{\partial t} + \epsilon A_1 y_{\epsilon 1}^0 &= f_1 \text{ on } Q_1 \\
 y_{\epsilon 1}^0 &= 0 \text{ on } \Sigma_1 \\
 y_{\epsilon 1}^0 &= y_0^0 \text{ on } R \\
 y_{\epsilon 1}^0(0) &= h_1 \text{ on } \Omega_0
 \end{aligned} \right\} \quad (4-15)$$

Remark 4.1:

The solution of y_0^0 of (4-14) is regular. Actually, $y_0^0 \in L^2(0, T; H^1(\Omega_0; \Gamma_0)) \subset L^2(Q_0)$. Hence $y_0^0|_R \in L^2(0, T; H^{1/2}(S)) \subset L^2(R)$. Problem (4-15) is a nonhomogeneous boundary value problem. Consequently, $y_{\epsilon 1}^0$ has meaning in a weak sense using transposition [4].

Since the zeroth order approximation y_{ϵ}^0 is weak, one rewrites (4-14)-(4-15) in the proper form, using transposition as follows. Let

$$\begin{aligned}
 \phi_0 &= \left\{ x_0 : x_0 \in H^{2,1}(Q_0) , \quad x_0 \Big|_{\Sigma_0} = 0 , \quad \frac{\partial x_0}{\partial \nu_{A_0}} \Big|_R = 0 , \quad x_0(T) = 0 \right\} \\
 \phi_1 &= \left\{ x_1 : x_1 \in H^{2,1}(Q_1) , \quad x_1 \Big|_{\Sigma_1} = 0 , \quad x_1 \Big|_R = 0 , \quad x_1(T) = 0 \right\} .
 \end{aligned}$$

Now consider the following isomorphisms

$$x_0 \mapsto -\frac{\partial x_0}{\partial t} + A_0 x_0 \text{ from } \phi_0 \text{ to } L^2(Q_0)$$

$$x_1 \mapsto -\frac{\partial x_1}{\partial t} + \varepsilon A_1 x_1 \text{ from } \phi_1 \text{ to } L^2(Q_1) \quad .$$

By transposition, one concludes that $x_0 \mapsto M^0(x_0)$, being a continuous linear form on ϕ_0 (endowed with the topology induced by $H^{2,1}(Q_0)$), there exists a unique $y_0^0 \in L^2(Q_0)$ such that

$$\int_{Q_0} y_0^0 \left(-\frac{\partial x_0}{\partial t} + A_0 x_0 \right) dQ_0 = M^0(x_0) \quad , \quad \text{for all } x_0 \in \phi_0 \quad (4-16)$$

and

$M^0 \mapsto y_0^0$ is a continuous linear mapping of

$\phi_0^* \mapsto L^2(Q_0)$ (cf. Remark 4.2).

Similarly, $x_1 \mapsto M_\varepsilon^1(x_1)$ being a continuous linear form on ϕ_1 (endowed with the topology of $H^{2,1}(Q_1)$), there exists a unique $y_{\varepsilon 1}^0 \in L^2(Q_1)$ such that

$$\int_{Q_1} y_{\varepsilon 1}^0 \left(-\frac{\partial x_1}{\partial t} + \varepsilon A_1 x_1 \right) dQ_1 = M_\varepsilon^1(x_1) \quad , \quad \text{for all } x_1 \in \phi_1 \quad (4-17)$$

and

$M_\varepsilon^1 \mapsto y_{\varepsilon 1}^0$ is a continuous linear mapping of $\phi_1^* \mapsto L^2(Q_1)$.

Select $M^0(\chi_0)$ and $M^1_\epsilon(\chi_1)$ as

$$M^0(\chi_0) = \int_{Q_0} f_0 \chi_0 dQ_0 + \int_{\Omega_0} h_0 \chi_0(x,0) d\Omega_0$$

$$M^1_\epsilon(\chi_1) = \int_{Q_1} f_1 \chi_1 dQ_1 + \int_{\Omega_1} h_1 \chi_1(x,0) d\Omega_1 - \epsilon \int_R y^0_0 \frac{\partial \chi_1}{\partial \nu_{A_1}} dR$$

Remark 4.2:

Since $C^\infty_0(Q_0) \not\subset \Phi_0$, the dual of Φ_0 is not a space of distributions. Therefore, the introduction of Θ_{Γ_0} is required to interpret duality [4].

It can be easily verified that the solutions of (4-14)-(4-15) and (4-16)-(4-17) are identical [2].

Now an error estimate between the exact solution y_ϵ and its approximation y^0_ϵ is derived.

Theorem 4.2:

Let y_ϵ be the solution of (4-15)-(4-16) and y^0_ϵ the solution of (4-16)-(4-17). Then, for sufficiently small ϵ , one has

$$\|y_\epsilon - y^0_\epsilon\|_{\epsilon L^2(Q)} \leq C \epsilon^{1/2} \quad (4-18)$$

where

$$Q = Q_0 \times Q_1$$

and C is a positive constant, independent of ϵ .

Proof:

First, rewrite (4-10)-(4-13) in the weak form, i.e.,

$$\int_{Q_0} y_{\epsilon 0} \left(-\frac{\partial \chi_0}{\partial t} + A_0 \chi_0 \right) dQ_0 = \int_{Q_0} f_0 \chi_0 dQ_0 + \int_{\Omega_0} h_0 \chi_0(x,0) d\Omega_0$$

$$- \int_R \frac{\partial y_{\epsilon 0}}{\partial v_{A_0}} \chi_0 dR, \text{ for all } \chi_0 \in \Phi_0 \quad (4-19)$$

$$\int_{Q_1} y_{\epsilon 1} \left(-\frac{\partial \chi_1}{\partial t} + \epsilon A_1 \chi_1 \right) dQ_1 = \int_{Q_1} f_1 \chi_1 dQ_1 + \int_{\Omega_1} h_1 \chi_1(x,0) d\Omega_1$$

$$- \epsilon \int_R y_{\epsilon 1} \frac{\partial \chi_1}{\partial v_{A_1}} dR, \text{ for all } \chi_1 \in \Phi_1 \quad (4-20)$$

Subtract (4-16) from (4-19) and (4-17) from (4-20) to obtain

$$\int_{Q_0} \left(y_{\epsilon 0} - y_0^0 \right) \left(-\frac{\partial \chi_0}{\partial t} + A_0 \chi_0 \right) dQ_0 = \epsilon \int_R \frac{\partial y_{\epsilon 1}}{\partial v_{A_1}} \chi_0 dR, \text{ for all } \chi_0 \in \Phi_0$$

$$(4-21)$$

$$\int_{Q_1} \left(y_{\epsilon 1} - y_{\epsilon 1}^0 \right) \left(-\frac{\partial \chi_1}{\partial t} + \epsilon A_1 \chi_1 \right) dQ_1 = \epsilon \int_R \left(y_{\epsilon 0} - y_0^0 \right) \frac{\partial \chi_1}{\partial v_{A_1}} dR, \text{ for all } \chi_1 \in \Phi_1$$

$$(4-22)$$

where the interface condition (4-12) is used.

Now consider the following equations:

$$\left. \begin{aligned} -\frac{\partial \chi_{\epsilon 0}}{\partial t} + A_0 \chi_{\epsilon 0} &= y_{\epsilon 0} - y_0^0 \text{ on } Q_0 \\ \chi_{\epsilon 0} &= 0 \text{ on } \Sigma_0 \\ \frac{\partial \chi_{\epsilon 0}}{\partial v_{A_0}} &= 0 \text{ on } R \\ \chi_{\epsilon 0}(x, T) &= 0 \end{aligned} \right\} \quad (4-23)$$

$$\left. \begin{aligned} -\frac{\partial \chi_{\varepsilon 1}}{\partial t} + \varepsilon A_0 \chi_{\varepsilon 1} &= y_{\varepsilon 1} - y_{\varepsilon 1}^0 \text{ on } Q_1 \\ \chi_{\varepsilon 1} &= 0 \text{ on } \Sigma_1 \\ \chi_{\varepsilon 1} &= 0 \text{ on } R \\ \chi_{\varepsilon 1}(x, T) &= 0 \end{aligned} \right\} \quad (4-24)$$

Since the coefficients of A_i , $i = 0, 1$ are assumed to be sufficiently regular and $y_{\varepsilon 0} - y_0^0 \in L^2(0, T; L^2(\Omega_0))$, $y_{\varepsilon 1} - y_{\varepsilon 1}^0 \in L^2(0, T; L^2(\Omega_1))$, one concludes that

$$\chi_{\varepsilon i} \in \Phi_i, \quad i = 0, 1.$$

Let $\chi_0 = \chi_{\varepsilon 0}$ in (4-21) and $\chi_1 = \chi_{\varepsilon 1}$ in (4-22), and use (4-23)-(4-24) to obtain

$$\|y_{\varepsilon 0} - y_0^0\|_{L^2(Q_0)} < C_1 \varepsilon^{1/2}$$

$$\|y_{\varepsilon 1} - y_{\varepsilon 1}^0\|_{L^2(Q_1)} < C_2 \varepsilon^{1/2}$$

where C_1, C_2 are some positive constants, independent of ε . Hence,

$$\|y_{\varepsilon} - y_{\varepsilon}^0\|_{L^2(Q)} = \|y_{\varepsilon 0} - y_0^0\|_{L^2(Q_0)} + \|y_{\varepsilon 1}\|_{L^2(Q_1)} < C \varepsilon^{1/2}.$$

Remark 4.3:

It should be noted that (4-18) holds for ε small, but strictly positive, because of the heavy reliance upon the fact that the solution of (4-24)

belongs to Φ_1 . It is easy to see that if one formally sets $\epsilon = 0$ in the first equation of (4-24), its right-hand side would be in $L^2(0, T; L^2(\Omega_1))$ but $\chi_{\epsilon 1}$ for $\epsilon = 0$ would not be in Φ_1 .

Recall that it was shown in Section 2 that the eigenvalue-eigenvector pairs of A_ϵ , i.e., $\{\gamma_\epsilon^k, \chi_\epsilon^k\}_{k=1}^\infty$ are decomposable into two groups $\{\lambda_\epsilon^k, \phi_\epsilon^k\}_{k=1}^\infty$ and $\{\mu_\epsilon^k, \psi_\epsilon^k\}_{k=1}^\infty$.

The normalized weak limits (in $H_0^1(\Omega)$) of $\{\phi_\epsilon^k\}_{k=1}^\infty$ satisfy

$$\left. \begin{aligned} \phi_0^k &= 0 \text{ on } \Omega_0 \\ A_1 \phi_1^k &= \lambda_1^k \phi_1^k \text{ on } \Omega_1 \\ \phi_1^k \Big|_{\Gamma_1} &= 0, \quad \phi_1^k \Big|_S = 0 \end{aligned} \right\} \quad k = 1, 2, \dots \quad (4-25)$$

The normalized weak limits (in $L^2(\Omega)$) of $\{\psi_\epsilon^k\}_{k=1}^\infty$ obey

$$\left. \begin{aligned} A_0 \psi_0^k &= \mu_0^k \psi_0^k \text{ on } \Omega_0 \\ \psi_0^k &= 0 \text{ on } \Omega_1 \\ \psi_0^k \Big|_{\Gamma_0} &= 0, \quad \frac{\partial \psi_0^k}{\partial \nu_{A_0}} \Big|_S = 0 \end{aligned} \right\} \quad k = 1, 2, \dots \quad (4-26)$$

Then the solution of (4-14)-(4-15) may be represented by

$$\left. \begin{aligned} y_0^0 &= \sum_{k=1}^{\infty} c^k(t) \psi_0^k \\ c^k &\in L^2(0, T), \quad \sum_{k=1}^{\infty} \int_0^T |c^k(t)|^2 dt < \infty \end{aligned} \right\}$$

$$\left. \begin{aligned} y_{\epsilon}^0 &= \sum_{k=1}^{\infty} \frac{d^k(t)}{\epsilon} \phi_1^k \\ d_{\epsilon}^k &\in L^2(0, T), \quad \sum_{k=1}^{\infty} \int_0^T \left| \frac{d^k(t)}{\epsilon} \right|^2 dt < \infty \end{aligned} \right\}$$

In order to determine $c^k(t)$, $\frac{d^k(t)}{\epsilon}$, let

$$\chi_0(x, t) = \theta(t) \psi_0^k(x), \quad \theta \in C^1([0, T]), \quad \theta(T) = 0 \quad (\text{so that } \chi_0 \in \Phi_0)$$

$$\chi_1(x, t) = v(t) \phi_1^k(x), \quad v \in C^1([0, T]), \quad v(T) = 0 \quad (\text{so that } \chi_1 \in \Phi_1)$$

in (4-16)-(4-17) to get

$$\int_0^T c^k \left(-\frac{d\theta}{dt} + \mu_0^k \theta \right) dt = \int_0^T (f_0, \psi_0^k) \theta dt - (h_0, \psi_0^k) \theta(0)$$

$$\int_0^T \frac{d^k}{\epsilon} \left(-\frac{dv}{dt} + \lambda_1^k v \right) dt = \int_0^T (f_1, \phi_1^k) v dt - (h_1, \phi_1^k) v(0)$$

$$- \epsilon \int_0^T \left(\sum_{\ell=1}^{\infty} c^{\ell} \int_S \psi^{\ell} \frac{\partial \phi_1^k}{\partial \nu_{A_1}} dS \right) v dt,$$

which are equivalent to

$$\left. \begin{aligned} \frac{dc^k}{dt} + \mu_0^k c^k &= (f_0, \phi_1^k) \\ c^k(0) &= (h_0, \psi_0^k) \end{aligned} \right\}$$

$$\left. \begin{aligned} \frac{d}{dt} \frac{d^k}{\epsilon} + \lambda_1^k \epsilon \frac{d^k}{\epsilon} &= (f_1, \phi_1^k) - \epsilon \sum_{\ell=1}^{\infty} c^\ell \int_S \psi_0^\ell \frac{\partial \phi_1^k}{\partial \nu_{A_1}} dS \\ \frac{d^k}{\epsilon}(0) &= (h_1, \phi_1^k) \end{aligned} \right\}$$

Remark 4.4:

Using the terminology of singular perturbation, a two time-scale decomposition is achieved. Namely, y_0^0 is "fast" and $y_{\epsilon 1}^0$ is predominantly "slow".

SECTION 5

HYPERBOLIC BOUNDARY VALUE PROBLEMS

In this section, an evolution of hyperbolic type is investigated, namely, the following boundary value problem:

$$(y''_{\epsilon}, \chi) + a_0(y_{\epsilon}, \chi) + \epsilon a_1(y_{\epsilon}, \chi) = (f, \chi), \text{ for all } \chi \in V \quad (5-1)$$

$$y_{\epsilon}(0) = h, \text{ } h \text{ given in } V \quad (5-2)$$

$$y'_{\epsilon}(0) = g, \text{ } g \text{ given in } H \quad (5-3)$$

$$y_{\epsilon} \in L^2(0, T; V), \text{ } y'_{\epsilon} \in L^2(0, T; H), \text{ } f \in L^2(0, T; H) \quad (5-4)$$

The present analysis will be parallel to that of Section 4. Hence, the convergence of y_{ϵ} as $\epsilon \rightarrow 0$ is studied. Then a zeroth order approximation of y_{ϵ} is constructed, using the weak limits of the eigenvectors of A_{ϵ} (i.e., the operator associated with the bilinear form $a_{\epsilon}(\phi, \psi) = a_0(\phi, \psi) + \epsilon a_1(\phi, \psi)$ (cf. Section 2). As previously indicated, (5-1)-(5-4) have to be specialized to second order operators A_{ϵ} , so that one can specify precisely what is required for the present analysis to hold. Therefore, the following problem is considered in the sequel:

$$\left. \begin{aligned} \frac{\partial^2 y_{\epsilon 0}}{\partial t^2} + A_0 y_{\epsilon 0} &= f_0 \text{ on } Q_0 \\ \frac{\partial^2 y_{\epsilon 1}}{\partial t^2} + \epsilon A_1 y_{\epsilon 1} &= f_1 \text{ on } Q_1 \end{aligned} \right\} \quad (5-5)$$

$$y_{\epsilon 0} = 0 \text{ on } \Sigma_0, y_{\epsilon 1} = 0 \text{ on } \Sigma_1 \quad (5-6)$$

$$\left. \begin{aligned} y_{\epsilon 0} &= y_{\epsilon 1} \\ \frac{\partial y_{\epsilon 0}}{\partial \nu_{A_0}} &= \epsilon \frac{\partial y_{\epsilon 1}}{\partial \nu_{A_1}} \end{aligned} \right\} \text{ on } R \quad (5-7)$$

$$y_{\epsilon}(0) = h, \quad h = (h_0, h_1), \quad h_i \in H_0^1(\Omega_i), \quad i = 0, 1 \quad (5-8)$$

$$\frac{\partial y_{\epsilon}}{\partial t}(0) = g, \quad g \in L^2(\Omega) \quad (5-9)$$

$$y_{\epsilon} \in L^2(0, T; H_0^1(\Omega)), \quad \frac{\partial y_{\epsilon}}{\partial t} \in L^2(0, T; L^2(\Omega)) \quad (5-10)$$

$$f \in L^2(0, T; L^2(\Omega)) \quad (5-11)$$

where $A_i, i = 0, 1$ satisfy the conditions of subsection 4.2

5.1 CONVERGENCE OF y_{ϵ} AS $\epsilon \rightarrow 0$

Theorem 5.1:

Let y_{ϵ} be the solution of (5-5)-(5-11). Then, given a sequence of ϵ converging to zero,

$$y_{\epsilon} \rightharpoonup \text{weakly in } L^2(0, T; L^2(\Omega)) \quad (5-12)$$

$$\frac{\partial y_{\epsilon}}{\partial t} \rightharpoonup \frac{\partial y}{\partial t} \text{ weakly in } L^2(0, T; L^2(\Omega)) \quad (5-13)$$

Moreover,

$$\sqrt{\epsilon} \|y\|_{\epsilon L^2(0,T; H_0^1(\Omega))} \leq C \quad (5-14)$$

C is a constant independent of ϵ .

Proof:

Let $\{\lambda_k^{\epsilon}, \phi_k^{\epsilon}\}_{k=1}^{\infty}$ and $\{\mu_k^{\epsilon}, \psi_k^{\epsilon}\}_{k=1}^{\infty}$ be the exact eigenvalue-eigenvector pairs

of A_{ϵ} , with the eigenvectors normalized (in $L_2(\Omega)$) for fixed ϵ . Using a finite dimensional approximation of y_{ϵ} such as

$$y_{\epsilon}^m = \sum_{k=1}^m c_k^{\epsilon} \psi_k^{\epsilon} + \sum_{k=1}^m d_k^{\epsilon} \phi_k^{\epsilon}$$

is is shown in [2] that

$$y_{\epsilon}^m \rightarrow y_{\epsilon} \text{ strongly in } L^2(0,T; H_0^1(\Omega)) \text{ as } m \rightarrow +\infty$$

$$\frac{\partial y_{\epsilon}^m}{\partial t} \rightarrow \frac{\partial y_{\epsilon}}{\partial t} \text{ strongly in } L^2(0,T; L_2(\Omega)) \text{ as } m \rightarrow +\infty$$

where

$$y_{\epsilon} = \sum_{k=1}^{\infty} c_k^{\epsilon} \psi_k^{\epsilon} + \sum_{k=1}^{\infty} d_k^{\epsilon} \phi_k^{\epsilon} \quad (5-15)$$

$\{c_k^{\epsilon}\}_{k=1}^{\infty}$, $\{d_k^{\epsilon}\}_{k=1}^{\infty}$ satisfy the following set of ordinary differential equations

$$\left. \begin{aligned} \frac{d^2 c_{\epsilon}^k}{dt^2} + \mu_{\epsilon}^k c_{\epsilon}^k &= (f, \psi_{\epsilon}^k) \\ c_{\epsilon}^k(0) &= (h, \psi_{\epsilon}^k) \\ \frac{dc_{\epsilon}^k}{dt}(0) &= (g, \psi_{\epsilon}^k) \end{aligned} \right\}$$

$$\left. \begin{aligned} \frac{d^2 d_{\epsilon}^k}{dt^2} + \lambda_{\epsilon}^k d_{\epsilon}^k &= (f, \phi_{\epsilon}^k) \\ d_{\epsilon}^k(0) &= (h, \phi_{\epsilon}^k) \\ \frac{dd_{\epsilon}^k}{dt}(0) &= (g, \phi_{\epsilon}^k) \end{aligned} \right\}$$

whose solutions are given respectively by

$$c_{\epsilon}^k(t) = (h, \psi_{\epsilon}^k) \cos \sqrt{\mu_{\epsilon}^k} t + \frac{(g, \psi_{\epsilon}^k)}{\sqrt{\mu_{\epsilon}^k}} \sin \sqrt{\mu_{\epsilon}^k} t + \int_0^t \frac{\sin \sqrt{\mu_{\epsilon}^k} (t-\tau)}{\sqrt{\mu_{\epsilon}^k}} (f, \psi_{\epsilon}^k) d\tau \quad (5-16)$$

$$d_{\epsilon}^k(t) = (h, \phi_{\epsilon}^k) \cos \sqrt{\lambda_{\epsilon}^k} t + \frac{(g, \phi_{\epsilon}^k)}{\sqrt{\lambda_{\epsilon}^k}} \sin \sqrt{\lambda_{\epsilon}^k} t + \int_0^t \frac{\sin \sqrt{\lambda_{\epsilon}^k} (t-\tau)}{\sqrt{\lambda_{\epsilon}^k}} (f, \phi_{\epsilon}^k) d\tau \quad (5-17)$$

Now, let ϵ be a sequence converging to zero. The convergence property (5-12) and the estimate (5-14) are easily deduced from the results of Theorem 2.1, where y is written as

$$y = \sum_{k=1}^{\infty} c^k \psi^k + \sum_{k=1}^{\infty} d^k \phi^k \quad (5-18)$$

where $\{c^k\}_{k=1}^{\infty}$, $\{d^k\}_{k=1}^{\infty}$ satisfy (5-16)-(5-17) after letting $\epsilon \rightarrow 0$, i.e.,

$$c^k(t) = (h, \psi^k) \cos \sqrt{\mu_0^k} t + \frac{(g, \psi^k)}{\sqrt{\mu_0^k}} \sin \sqrt{\mu_0^k} t + \int_0^t \frac{\sin \sqrt{\mu_0^k}(t-\tau)}{\sqrt{\mu_0^k}} (f, \psi^k) d\tau$$

$$d^k(t) = (h, \phi^k) + (g, \phi^k)t + \int_0^T (t-\tau)(f, \phi^k) d\tau.$$

Differentiate (5-15) with respect to time and take limit as $\epsilon \rightarrow 0$ using the results of Theorem 2.1 to get (5-13).

5.2 ASYMPTOTIC APPROXIMATION OF y_{ϵ}

In the sequel, the zeroth order approximation y_{ϵ}^0 of y_{ϵ} is constructed using the same approach as in subsection 4.2. An error estimate is then derived. An outline on how to solve for y_{ϵ}^0 using the weak limits of the eigenvectors of A_{ϵ} is also given. Let $y_{\epsilon}^0 = (y_{0\epsilon}^0, y_{\epsilon 1}^0)$ be defined by

$$\left. \begin{aligned}
 \frac{\partial^2 y_0^0}{\partial t^2} + A_0 y_0^0 &= f_0 \text{ on } Q_0 \\
 y_0^0 &= 0 \text{ on } \Sigma_0 \\
 \frac{\partial y_0^0}{\partial \nu_{A_0}} &= 0 \text{ on } R \\
 y_0^0(0) &= h_0 \text{ on } \Omega_0 \\
 \frac{\partial y_0^0}{\partial t}(0) &= g_0 \text{ on } \Omega_0
 \end{aligned} \right\} \quad (5-19)$$

$$\left. \begin{aligned}
 \frac{\partial^2 y_{\epsilon 1}^0}{\partial t^2} + \epsilon A_1 y_{\epsilon 1}^0 &= f_1 \text{ on } Q_1 \\
 y_{\epsilon 1}^0 &= 0 \text{ on } \Sigma_1 \\
 y_{\epsilon 1}^0 &= y_0^0 \text{ on } R \\
 \frac{\partial y_{\epsilon 1}^0}{\partial t}(0) &= g_1 \text{ in } \Omega_1
 \end{aligned} \right\} \quad (5-20)$$

Problem (5-20) is a nonhomogeneous boundary value problem. Using transposition, $y_{\epsilon 1}^0$ is defined in a weak sense as in subsection 4.2.

In order to derive an asymptotic error estimate between y_{ϵ} and y_{ϵ}^0 , they must be redefined using transposition. For this purpose, let

$$\phi_0 = \left\{ \begin{aligned} & \chi_0: \chi_0 \in L^2(0,T; H^1(\Omega)), \frac{\partial \chi_0}{\partial t} \in L^2(Q_0), \frac{\partial^2 \chi_0}{\partial t^2} + A_0 \chi_0 \in L^2(Q_0), \chi_0 = 0 \text{ on } \Sigma_0, \\ & \frac{\partial \chi_0}{\partial \nu_{A_0}} = 0 \text{ on } R, \chi_0(x,T) = 0, \frac{\partial \chi_0}{\partial t}(x,T) = 0 \end{aligned} \right\}^1$$

$$\phi_1 = \left\{ \begin{aligned} & \chi_1: \chi_1 \in L^2(0,T; H^1(\Omega_1)), \frac{\partial \chi_1}{\partial t} \in L^2(Q_1), \frac{\partial^2 \chi_1}{\partial t^2} + \epsilon A_1 \chi_1 \in L^2(Q_1), \chi_1 = 0 \\ & \text{on } \Sigma_1 \cup R, \chi_1(x,T) = 0, \frac{\partial \chi_1}{\partial t}(x,T) = 0 \end{aligned} \right\}^1$$

It can be easily verified that y_ϵ, y_ϵ^0 satisfy

$$\int_{Q_0} y_\epsilon \left(\frac{\partial^2 \chi_0}{\partial t^2} + A_0 \chi_0 \right) dQ_0 = \int_{Q_0} f_0 \chi_0 dQ_0 - \int_{\Omega_0} h_0 \frac{\partial \chi_0}{\partial t}(x,0) d\Omega_0 \quad (5-21)$$

$$+ \int_{\Omega_0} g_0 \chi_0(x,0) d\Omega_0 + \epsilon \int_R \frac{\partial y_{\epsilon 1}}{\partial \nu_{A_1}} \chi_0 dR, \text{ for all } \chi_0 \in \phi_0$$

$$\int_{Q_1} y_{\epsilon 1} \left(\frac{\partial^2 \chi_1}{\partial t^2} + \epsilon A_1 \chi_1 \right) dQ_1 = \int_{Q_1} f_1 \chi_1 dQ_1 - \int_{\Omega_1} h_1 \frac{\partial \chi_1}{\partial t}(x,0) d\Omega_1 \quad (5-22)$$

$$+ \int_{\Omega_1} g_1 \chi_1(x,0) d\Omega_1 - \epsilon \int_R y_{\epsilon 0} \frac{\partial \chi_1}{\partial \nu_{A_1}} dR, \text{ for all } \chi_1 \in \phi_1$$

ϕ_1 is endowed with the topology carried over by the mapping

$$\phi_1 \in L^2(0,T; L^2(\Omega_1)) \mapsto \chi_1, \quad i = 0, 1.$$

$$\int_{Q_0} y_0^0 \left(\frac{\partial^2 x_0}{\partial t^2} + A_0 x_0 \right) dQ_0 = \int_{Q_0} f_0 x_0 dQ_0 - \int_{\Omega_0} h_0 \frac{\partial x_0}{\partial t} (x, 0) d\Omega_0 \quad (5-23)$$

$$+ \int_{\Omega_0} g_0 x_0 (x, 0) d\Omega_0, \text{ for all } x_0 \in \Phi_0$$

$$\int_{Q_1} y_{\epsilon 1}^0 \left(\frac{\partial^2 x_1}{\partial t^2} + \epsilon A_1 x_1 \right) dQ_1 = \int_{Q_1} f_1 x_1 dQ_1 - \int_{\Omega_1} h_1 \frac{\partial x_1}{\partial t} (x, 0) d\Omega_1 \quad (5-24)$$

$$+ \int_{\Omega_1} g_1 x_1 (x, 0) d\Omega_1 - \epsilon \int_R y_0 \frac{\partial x}{\partial v_{A1}} dR, \text{ for all } x_1 \in \Phi_1.$$

Theorem 5.2:

Let $y_{\epsilon}^0, y_{\epsilon}^1$ be the solutions of (5-21)-(5-24). Then for sufficiently small ϵ , the following estimate holds

$$\|y_{\epsilon}^0 - y_0^0\|_{L^2(Q)} \leq C \epsilon^{1/4} \quad (5-25)$$

Proof:

Subtract (5-22) from (5-21) and (5-24) from (5-23) to get:

$$\int_{Q_0} (y_{\epsilon 0}^0 - y_0^0) \left(\frac{\partial^2 x_0}{\partial t^2} + A_0 x_0 \right) dQ_0 = - \epsilon \int_R \frac{\partial y_{\epsilon 1}^0}{\partial v_{A1}} x_0 dR \quad (5-26)$$

$$\int_{Q_1} (y_{\epsilon 1}^0 - y_0^1) \left(\frac{\partial^2 x_1}{\partial t^2} + \epsilon A_1 x_1 \right) dQ_1 = - \epsilon \int_R (y_{\epsilon 0}^0 - y_0^0) \frac{\partial x_1}{\partial v_{A1}} dR. \quad (5-27)$$

Now consider the following equations

$$\left. \begin{aligned}
 \frac{\partial^2 \chi_{\varepsilon 0}}{\partial t^2} + A_0 \chi_{\varepsilon 0} &= y_{\varepsilon 0} - y_0^0 \text{ on } Q_0 \\
 \chi_{\varepsilon 0} &= 0 \text{ on } \Sigma_0 \\
 \frac{\partial \chi_{\varepsilon 0}}{\partial \nu_{A_0}} &= 0 \text{ on } R \\
 \chi_{\varepsilon 0}(x, T) &= 0 \text{ on } \Omega_0 \\
 \frac{\partial \chi_{\varepsilon 0}}{\partial t}(x, T) &= 0 \text{ on } \Omega_0
 \end{aligned} \right\} \quad (5-28)$$

$$\left. \begin{aligned}
 \frac{\partial^2 \chi_{\varepsilon 1}}{\partial t^2} + \varepsilon A_1 \chi_{\varepsilon 1} &= y_{\varepsilon 1} - y_{\varepsilon 1}^0 \text{ on } Q_1 \\
 \chi_{\varepsilon 1} &= 0 \text{ on } \Sigma_1 \\
 \chi_{\varepsilon 1} &= 0 \text{ on } R \\
 \chi_{\varepsilon 1}(x, T) &= 0 \text{ on } \Omega_1 \\
 \frac{\partial \chi_{\varepsilon 1}}{\partial t}(x, T) &= 0 \text{ on } \Omega_1
 \end{aligned} \right\} \quad (5-29)$$

It can be shown [4] that

$$\chi_{\epsilon i} \in \phi_i, \quad i = 0, 1.$$

Consequently

$$\begin{aligned} \chi_{\epsilon 0} \Big|_R &\in L^2(0, T; H^{1/2}(S)) \\ \frac{\partial \chi_{\epsilon 1}}{\partial \nu_{A_1}} \Big|_R &\in L^2(0, T; H^{-1/2}(S)). \end{aligned}$$

From (5-13), one concludes that

$$\sqrt{\epsilon} \left\| y_{\epsilon 0} \right\|_{L^2(0, T; H^{1/2}(S))} \leq C_1 \quad (5-30)$$

$$\sqrt{\epsilon} \left\| \frac{\partial y_{\epsilon 1}}{\partial \nu_{A_1}} \right\|_{L^2(0, T; H^{-1/2}(S))} \leq C_2. \quad (5-31)$$

Let $\chi_0 = \chi_{\epsilon 0}$ in (5-26) and $\chi_1 = \chi_{\epsilon 1}$ in (5-27) and use (5-28)-(5-29), (5-30)-(5-31), to get

$$\left\| y_{\epsilon 0} - y_0^0 \right\|_{L^2(Q_0)} \leq C_3 \epsilon^{1/4}$$

$$\left\| y_{\epsilon 1} - y_{\epsilon 1}^0 \right\|_{L^2(Q_1)} \leq C_4 \epsilon^{1/4}$$

from which one obtains (5-25).

Now the weak limits of the eigenvectors of A_ϵ , i.e., (4-25)-(4-26) are employed to solve (5-13)-(5-20). First, renormalize $\{\psi^k\}_{k=1}^\infty$. Then, the solution of (5-19)-(5-20) may be represented by:

$$\left. \begin{aligned} y_0^0 &= \sum_{k=1}^{\infty} c^k \psi_0^k \\ c^k &\in L^2(0, T), \quad \sum_{k=1}^{\infty} \int_0^T |c^k(t)|^2 dt < \infty \end{aligned} \right\}$$

$$\left. \begin{aligned} y_{\varepsilon 1}^0 &= \sum_{k=1}^{\infty} \frac{d^k}{\varepsilon} \phi_1^k \\ \frac{d^k}{\varepsilon} &\in L^2(0, T), \quad \sum_{k=1}^{\infty} \int_0^T \left| \frac{d^k(t)}{\varepsilon} \right|^2 dt < \infty \end{aligned} \right\}$$

In order to obtain $c^k(t)$, $d^k(t)$, let

$$\chi_0(x, t) = \theta(t) \phi_0^k(x), \quad \theta \in C^2([0, T]), \quad \theta(T) = \frac{d\theta}{dt}(T) = 0$$

$$\chi_1(x, t) = v(t) \phi_1^k(x), \quad v \in C^2([0, T]), \quad v(T) = \frac{dv}{dt}(T) = 0$$

in (5-23)-(5-29) to get

$$\int_0^T c^k \left(\frac{d^2 \theta}{dt^2} + \mu_0^k \theta \right) dt = \int_0^T (f_0, \psi_0^k) \theta dt - (h_0, \psi_0^k) \frac{d\theta}{dt}(0) + (g_0, \psi_0^k) \theta(0)$$

$$\int_0^T \frac{d^k}{\varepsilon} \left(\frac{d^2 v}{dt^2} + \lambda_1^k \varepsilon v \right) dt = \int_0^T (f_1, \phi_1^k) v dt - (h_1, \phi_1^k) \frac{dv}{dt}(0)$$

$$+ (g_1, \phi_1^k) v(0) - \varepsilon \int_0^T \left(\sum_{\ell=1}^{\infty} c^{\ell} \int_S \psi_0^{\ell} \frac{\partial \phi_1}{\partial \nu_{A_1}} d\Omega \right) v dt$$

which are equivalent to

$$\left. \begin{aligned} \frac{d^2 c^k}{dt^2} + \mu_0^k c^k &= (f_0, \psi_0^k) \\ c^k(0) &= (h_0, \psi_0^k) \\ \frac{dc^k}{dt}(0) &= (g_0, \psi_0^k) \end{aligned} \right\}$$

$$\left. \begin{aligned} \frac{d^2 d_\epsilon^k}{dt^2} + \lambda_1^k \epsilon \frac{d^k}{dt} &= (f_1, \phi_1^k) - \epsilon \sum_{\ell=1}^{\infty} c^\ell \int_S \psi_0^\ell \frac{\partial \phi_1^k}{\partial \nu_{A_1}} dS \\ d_\epsilon^k(0) &= (h_1, \phi_1^k) \\ \frac{d d_\epsilon^k}{dt}(0) &= (g_1, \phi_1^k) \end{aligned} \right\}$$

Remark 5.1:

It should be stressed once more that the concepts used in approximating (5-5)-(5-11) can be employed to approximate any boundary value problem that fits into (5-1)-(5-5).

SECTION 6

CONCLUSIONS

In this paper, three stiff classical boundary value problems (namely elliptic, parabolic and hyperbolic) have been analyzed, using the spectral analysis of stiff operators [5].

For elliptic problems, it has been shown, that by appropriately modifying the weak limits of the eigenvectors of A_ϵ , a Laurent series expansion of any order can be derived. For evolution problems, zeroth order approximations in $L^2(0,T; L^2(\Omega))$ were easily constructed, using only the weak limits of the eigenvectors of A_ϵ .

Many other similar problems (including control problems) can be analyzed using the concepts used in the present paper.

Nice physical interpretations can be associated with the behavior of the solutions of (1-1)-(1-3) as $\epsilon \rightarrow 0$ in the fields of heat transfer and electromagnetic wave propagation. In a future publication [6], these interpretations are discussed using several examples of stiff boundary value problems.

The approximations obtained in this paper are also compared with finite dimensional approximations.

REFERENCES

1. Aubin, J.P., Applied Functional Analysis, John Wiley and Sons, New York, 1979.
2. Lions, J.L., Optimal Control of Systems Governed by Partial Differential Equations, Springer-Verlag, New York, 1971.
3. Lions, J.L., Perturbations Singulieres dans les Problems aux Limites et en Controle Optimal, Springer-Verlag, New York, 1973.
4. Lions, J.L. and E. Magenes, Nonhomogeneous Boundary Value Problems and Their Applications, Volumes I and II, Springer-Verlag, New York, 1972.
5. Salhi, H. and D.P. Looze, "Spectral Analysis of Stiff Operators," Technical Paper, TP-220, ALPHATECH, Inc., Burlington, MA, 1985.
6. Salhi, H. and D.P. Looze, "Analysis and Approximation of a Class of Stiff Boundary Value Problems with Applications to Heat Transfer and Electromagnetics," in preparation.

APPENDIX C

C.1 INTRODUCTION

four different models have been used during the design and analysis of the report. The models are the subsystem design model, the subsystem truth model, the coupled system analysis model, and the coupled system truth model. Each model is a low-order finite element approximation of a set of masses corrected by flexible beams. The models take the form:

$$M\ddot{p} + D\dot{p} + Kp = Bf \quad (C-1)$$

$$y = Cp \quad (C-2)$$

where

- N = number of elements
- m = number of forces
- p = N vector of positions of the elements
- f = N vector of forces on the elements
- y = r vector of measurements
- M = NxN mass matrix
- K = NxN spring constant matrix
- K = NxN damping matrix
- B = Nxm force coefficient matrix
- C = rxN output matrix

The remaining sections present the data for each of the finite element models that has been used.

C.2 SUBSYSTEM DESIGN MODEL

Number of masses = 3

N = 5

M =	5.5000	0.3536	0.0000
	0.3536	5.5000	0.3536
	0.0000	0.3536	5.5000

K =	5.3924	-3.8130	0.0000
	-3.8130	5.3924	-3.8130
	0.0000	-3.8130	5.3924

D =	0.3300	0.0212	0.0000
	0.0212	0.3300	0.0212
	0.0000	0.0212	0.3300

B =	2.1213	0.0000	0.0000
	0.0000	2.1213	0.0000
	0.0000	0.0000	2.1213

C =	1.0000	-0.7071	0.0000
	0.0000	0.7071	-1.0000

Note: The inputs for subsystems 1 and 2 are defined in Fig. 2-1.

C.3 SUBSYSTEM TRUTH MODEL

Number of masses = 3

N = 5

M =	B.5000	0.3536	0.0000	0.0000	0.0000
	0.3536	1.0000	0.2500	0.0000	0.0000
	0.0000	0.2500	B.5000	0.2500	0.0000
	0.0000	0.0000	0.2500	1.0000	0.3536
	0.0000	0.0000	0.0000	0.3536	B.5000

K =	18.7500	-13.2583	0.0000	0.0000	0.0000
	-13.2583	18.7500	-9.3750	0.0000	0.0000
	0.0000	-9.3750	18.7500	-9.3750	0.0000
	0.0000	0.0000	-9.3750	18.7500	-13.2583
	0.0600	0.0000	0.0000	-13.2583	18.7500

D =	0.5100	0.0212	0.0000	0.0000	0.0000
	0.0212	0.0600	0.0150	0.0000	0.0000
	0.0000	0.0150	0.5100	0.0150	0.0000
	0.0000	0.0000	0.0150	0.0600	0.0212
	0.0000	0.0000	0.0000	0.0212	0.5100

B =	2.7386	0.0000	0.0000
	0.0000	0.0000	0.0000
	0.0000	2.7386	0.0000
	0.0000	0.0000	0.0000
	0.0000	0.0000	2.7386

C =	1.0000	0.0000	-0.7071	0.0000	0.0000
	0.0000	0.0000	0.7071	0.0000	-1.0000

C.4 COUPLED ANALYSIS MODEL

Number of masses = 6

N = 6

M =	5.5000	0.3536	0.0000	0.0000	0.0000	0.0000
	0.3536	5.5000	0.3518	0.0000	0.0000	0.0000
	0.0000	0.3518	5.5000	0.0025	0.0000	0.0000
	0.0000	0.0000	0.0025	5.5000	0.3518	0.0000
	0.0000	0.0000	0.0000	0.3518	5.5000	0.3536
	0.0000	0.0000	0.0000	0.0000	0.3536	5.5000

K =	5.3924	-3.8130	0.0000	0.0000	0.0000	0.0000
	-3.8130	5.3924	-3.7941	0.0000	0.0000	0.0000
	0.0000	-3.7941	5.3924	-0.0270	0.0000	0.0000
	0.0000	0.0000	-0.0270	5.3924	-3.7941	0.0000
	0.0000	0.0000	0.0000	-3.7941	5.3924	-3.8130
	0.0000	0.0000	0.0000	0.0000	-3.8130	5.3924

D =	0.3300	0.0212	0.0000	0.0000	0.0000	0.0000
	0.0212	0.3300	0.0211	0.0000	0.0000	0.0000
	0.0000	0.0211	0.3300	0.0002	0.0000	0.0000
	0.0000	0.0000	0.0002	0.3300	0.0211	0.0000
	0.0000	0.0000	0.0000	0.0211	0.3300	0.0212
	0.0000	0.0000	0.0000	0.0000	0.0212	0.3300

B =	2.1213	0.0000	0.0000	0.0000	0.0000	0.0000
	0.0000	2.1213	0.0000	0.0000	0.0000	0.0000
	0.0000	0.0000	2.1213	0.0000	0.0000	0.0000
	0.0000	0.0000	0.0000	2.1213	0.0000	0.0000
	0.0000	0.0000	0.0000	0.0000	2.1213	0.0000
	0.0000	0.0000	0.0000	0.0000	0.0000	2.1213

C =	1.0000	-0.7071	0.0000	0.0000	0.0000	0.0000
	0.0000	0.7071	-0.9950	0.0000	0.0000	0.0000
	0.0000	0.0000	0.9950	-0.7071	0.0000	0.0000
	0.0000	0.0000	0.0000	-0.9950	-0.7071	0.0000
	0.0000	0.0000	0.0000	0.9950	0.7071	-1.0000

C.5 COUPLED TRUTH MODEL

Number of masses = 6

N = 11

M =	9.2500	0.3536	0.0000	0.0000	0.0000	0.0000	0.0000	0.0000	0.0000	0.0000	0.0000
	0.3536	1.0000	0.2500	0.0000	0.0000	0.0000	0.0000	0.0000	0.0000	0.0000	0.0000
	0.0000	0.2500	9.2500	0.2500	0.0000	0.0000	0.0000	0.0000	0.0000	0.0000	0.0000
	0.0000	0.0000	0.2500	1.0000	0.3518	0.0000	0.0000	0.0000	0.0000	0.0000	0.0000
	0.0000	0.0000	0.0000	0.3518	9.2500	0.0025	0.0000	0.0000	0.0000	0.0000	0.0000
	0.0000	0.0000	0.0000	0.0000	0.0025	1.0000	0.0025	0.0000	0.0000	0.0000	0.0000
	0.0000	0.0000	0.0000	0.0000	0.0000	0.0025	9.2500	0.3518	0.0000	0.0000	0.0000
	0.0000	0.0000	0.0000	0.0000	0.0000	0.0000	0.3518	1.0000	0.2500	0.0000	0.0000
	0.0000	0.0000	0.0000	0.0000	0.0000	0.0000	0.0000	0.2500	9.2500	0.2500	0.0000
	0.0000	0.0000	0.0000	0.0000	0.0000	0.0000	0.0000	0.0000	0.2500	1.0000	0.3536
	0.0000	0.0000	0.0000	0.0000	0.0000	0.0000	0.0000	0.0000	0.0000	0.3536	9.2500

K =	18.1244	-12.8159	0.0000	0.0000	0.0000	0.0000	0.0000	0.0000	0.0000	0.0000	0.0000
	-12.8159	18.1244	-9.0622	0.0000	0.0000	0.0000	0.0000	0.0000	0.0000	0.0000	0.0000
	0.0000	-9.0622	18.1244	-9.0622	0.0000	0.0000	0.0000	0.0000	0.0000	0.0000	0.0000
	0.0000	0.0000	-9.0622	18.1244	-12.7523	0.0000	0.0000	0.0000	0.0000	0.0000	0.0000
	0.0000	0.0000	0.0000	-12.7523	18.1244	-0.0906	0.0000	0.0000	0.0000	0.0000	0.0000
	0.0000	0.0000	0.0000	0.0000	-9.0906	18.1244	-0.0906	0.0000	0.0000	0.0000	0.0000
	0.0000	0.0000	0.0000	0.0000	0.0000	-12.7523	18.1244	-12.7523	0.0000	0.0000	0.0000
	0.0000	0.0000	0.0000	0.0000	0.0000	0.0000	-12.7523	18.1244	-9.0622	0.0000	0.0000
	0.0000	0.0000	0.0000	0.0000	0.0000	0.0000	0.0000	-9.0622	18.1244	-9.0622	0.0000
	0.0000	0.0000	0.0000	0.0000	0.0000	0.0000	0.0000	0.0000	-9.0622	18.1244	-12.8159
	0.0000	0.0000	0.0000	0.0000	0.0000	0.0000	0.0000	0.0000	0.0000	-12.8159	18.1244

D =	0.5550	0.0212	0.0000	0.0000	0.0000	0.0000	0.0000	0.0000	0.0000	0.0000	0.0000
	0.0212	0.0600	0.0150	0.0000	0.0000	0.0000	0.0000	0.0000	0.0000	0.0000	0.0000
	0.0000	0.0150	0.5550	0.0150	0.0000	0.0000	0.0000	0.0000	0.0000	0.0000	0.0000
	0.0000	0.0000	0.0150	0.0600	0.0211	0.0000	0.0000	0.0000	0.0000	0.0000	0.0000
	0.0000	0.0000	0.0000	0.0211	0.5550	0.0002	0.0000	0.0000	0.0000	0.0000	0.0000
	0.0000	0.0000	0.0000	0.0000	0.0002	0.0600	0.0002	0.0000	0.0000	0.0000	0.0000
	0.0000	0.0000	0.0000	0.0000	0.0002	0.5550	0.0211	0.0000	0.0000	0.0000	0.0000
	0.0000	0.0000	0.0000	0.0000	0.0000	0.0000	0.0211	0.0600	0.0150	0.0000	0.0000
	0.0000	0.0000	0.0000	0.0000	0.0000	0.0000	0.0000	0.0150	0.5550	0.0150	0.0000
	0.0000	0.0000	0.0000	0.0000	0.0000	0.0000	0.0000	0.0000	0.0150	0.0600	0.0212
	0.0000	0.0000	0.0000	0.0000	0.0000	0.0000	0.0000	0.0000	0.0000	0.0212	0.5550

B =	2.8723	0.0000	0.0000	0.0000	0.0000	0.0000
	0.0000	0.0000	0.0000	0.0000	0.0000	0.0000
	0.0000	2.8723	0.0000	0.0000	0.0000	0.0000
	0.0000	0.0000	0.0000	0.0000	0.0000	0.0000
	0.0000	0.0000	2.8723	0.0000	0.0000	0.0000
	0.0000	0.0000	0.0000	0.0000	0.0000	0.0000
	0.0000	0.0000	0.0000	2.8723	0.0000	0.0000
	0.0000	0.0000	0.0000	0.0000	0.0000	0.0000
	0.0000	0.0000	0.0000	0.0000	2.8723	0.0000
	0.0000	0.0000	0.0000	0.0000	0.0000	0.0000
	0.0000	0.0000	0.0000	0.0000	0.0000	2.8723

C =	1.0000	0.0000	-0.7071	0.0000	0.0000	0.0000	0.0000	0.0000	0.0000	0.0000	0.0000
	0.0000	0.0000	0.7071	0.0000	-0.9950	0.0000	0.0000	0.0000	0.0000	0.0000	0.0000
	0.0000	0.0000	0.0000	0.0000	0.9950	0.0000	-0.7071	0.0000	0.0000	0.0000	0.0000
	0.0000	0.0000	0.0000	0.0000	0.0000	0.0000	-0.9950	0.0000	-0.7071	0.0000	0.0000
	0.0000	0.0000	0.0000	0.0000	0.0000	0.0000	0.9950	0.0000	0.7071	0.0000	-1.0000